



ANALYSIS OF THE PERFORMANCE RATIO OF A PHOTOVOLTAIC POWER PLANT ACCORDING TO DEVELOPMENT AND OPERATION

RONNY DIAS RENKE BRANDÃO E SILVA

novembro de 2019

**ANALYSIS OF THE PERFORMANCE RATIO OF
PHOTOVOLTAIC POWER PLANTS ACCORDING TO
DEVELOPMENT AND OPERATION**

Ronny Dias Renke Brandão e Silva
1162205

2019

Instituto Superior de Engenharia do Porto
Departamento de Engenharia Mecânica – Mestrado em Energias Sustentáveis



POLITÉCNICO
DO PORTO

isep

ANALYSIS OF THE PERFORMANCE RATIO OF PHOTOVOLTAIC POWER PLANTS ACCORDING TO DEVELOPMENT AND OPERATION

Ronny Dias Renke Brandão e Silva
1162205

Dissertation presented in Instituto Superior de Engenharia do Porto to fulfil the requirements necessary to obtain a Master's degree in Sustainable Energies, under the guidance of Manuel Carlos Malheiro de Carvalho Felgueiras.

2019

Instituto Superior de Engenharia do Porto

Departamento de Engenharia Mecânica – Mestrado em Energias Sustentáveis



JURY

President

PhD Nidia Sá Caetano

Coordinator Professor - Department of Chemical Engineering, Instituto Superior de Engenharia do Porto - ISEP

Supervisor

PhD Manuel Carlos Malheiro de Carvalho Felgueiras

Adjunct Professor - Instituto Superior de Engenharia do Porto - ISEP

Co-supervisor

MSc Eric Herrmann

EPC Program Manager, IBC Solar Energy GmbH

Examiner

PhD Ana Isabel Palmero Marrero

Invited Auxiliary Professor - Instituto Superior de Engenharia do Porto - ISEP

ACKNOWLEDGEMENTS

Thank you.

To Instituto Superior de Engenharia do Porto, for opening its doors to all nations and fostering quality education above all.

To IBC Solar Team, for believing in my competence and for welcoming me in Germany.

To Prof. Carlos Felgueiras, for guiding and teaching me even on Sundays, demonstrating that there are no limits to knowledge dissemination.

To my family, for the incomprehensible help that has been given me in recent years outside Brazil.

To my bride, for always being by my side, for supporting me in the most difficult times and for pushing me, day after day, to achieve my goals.

KEYWORDS

Photovoltaic, yield forecasting, power plant, performance ratio

ABSTRACT

Photovoltaic plants are also evaluated according to their Performance Ratio. This indicator allows to compare solar plants, regardless of their location or capacity, and may vary between positive or negative values due to several factors. Based on the knowledge gained by the author during the curricular internship at IBC Solar Energy GmbH, this document shows the electrical calculations and energy losses involved during project development, and then analyses the development and operation of sixteen photovoltaic plants, seeking to determine, through a case study, the main factors that negatively impact the efficiency. Based on this study, the author shows a software he developed, that was designed to increase reliability and decrease time spent during Performance Ratio calculations.

PALAVRAS CHAVE

Fotovoltaico, previsão de rendimento, planta de energia, Performance Ratio

RESUMO

As usinas fotovoltaicas também são avaliadas de acordo com o *Performance Ratio* (razão de desempenho). Esse indicador, que permite comparar usinas solares, independentemente da sua localização ou capacidade, pode tomar valores positivos ou negativos, devido a diversos fatores. Com base no conhecimento obtido pelo autor durante o estágio curricular na empresa IBC Solar Energy GmbH, este documento demonstra os cálculos elétricos e as perdas energéticas envolvidas durante o desenvolvimento dos projetos, para então analisar o desenvolvimento e a operação de 16 usinas fotovoltaicas, buscando determinar, através de um estudo de caso, os principais fatores que impactam negativamente a eficiência. E, com base neste estudo, o autor demonstra um software criado por si, para aumentar a confiabilidade e diminuir o tempo gasto durante os cálculos do *Performance Ratio*.

LIST OF ABBREVIATIONS AND UNITS

List of Abbreviations

3D	Three Dimensional
AC	Alternating Current
CAT 7	CATegory 7 network cable
CO ²	Carbon dioxide
DC	Direct Current
DCCB	Direct Current Combiner Box
Eg	Energy gap
EPC	Engineering, Procurement and Contract
GHI	Global Horizontal Irradiance
GPM	Green Power Monitor
GTI	Global Tilted Irradiance
IAM	Incidence Angle Modifier
IEEE	Institute of Electrical and Electronics Engineers
I_{mp}	Current at maximum power
I_{sc}	Short-circuit current
KPI	Key Performance Indicator
MMS	Module Mounting Structure
MPP	Maximum Power Point
NASA	National Aeronautics and Space Administration
NOCT	Nominal Operating Cell Temperature
O&M	Operation and Maintenance
P.F.	Power Factor
P_{max}	Maximum power
PR	Performance Ratio
PV	Photovoltaic
RS485	Recommended Standard 485
SCADA	Supervisory Control And Data Acquisition
STC	Standard Test Condition
T_m	Module temperature
U_{oc}	Open circuit voltage
V_{mp}	Voltage at maximum power

List of Units

° C	Degree Celsius
A	Ampere
cm ²	Square centimetres
Hz	Hertz
kWh/y	Kilowatt hour per year
m	meter
V	Volt
VA	Volt-Amps
W	Watt
W/m ²	Watt per square meter
Wh/m ²	Watt hour per square meter
W _p	Watt peak
Ω	Ohm

GLOSSARY OF TERMS

Active Power	The actual amount of power being used, or dissipated, in a circuit. It is measured in Watt (W) and symbolized by the capital letter P.
Alternating Current	Electric current in which the direction of flow is reversed at frequent intervals-usually 100 or 120 times per second (50 or 60 cycles per second or 50-60 Hz for grids).
Amorphous Silicon	A thin-film, silicon photovoltaic cell having no crystalline structure. It is manufactured by depositing layers of doped silicon on a substrate.
Ampere	The unit for the electric current; the flow of electrons. One amp is 1 coulomb passing in one second. 1 A is produced by an electric force of 1 V acting across a resistance of 1 Ω .
Angle of incidence	Angle between the normal to a surface and the direction of incident radiation; applies to the aperture plane of a solar collector. Most modern solar panels have only minor reductions in power output within plus/minus 15 degrees. The loss is a function of the cosine, so at 45-degree angle, output drops off by about 30%.
Apparent Power	The combination of Reactive Power (Q) and Active Power (P) is called Apparent Power, and it is the product of a circuit's voltage and current, without reference to phase angle. Apparent Power is measured in the unit of Volt-Amps (VA) and is symbolized by the capital letter S.
Array	Any number of photovoltaic modules connected together to provide a single electrical output. Arrays are often designed to produce significant amounts of electricity.
Azimuth	Angle between the north direction and the projection of the surface normal into the horizontal plane measured clockwise from north. As applied to the PV array, 180-degrees azimuth means the array faces due south.
Bypass diode	A diode connected across one or more solar cells in a photovoltaic module such that the diode will conduct if the cell(s) become reverse biased. Alternatively, diode-connected anti-parallel across a part of the solar cells of a PV module. It protects these solar cells from thermal destruction in case of total or partial shading, broken cells, or cell string failures of individual solar cells while other cells are exposed to full light.

Circuit breaker	Switching device, which can be activated automatically, as well as manually, to control and protect an electrical power system respectively.
Czochralski process	A method of growing large size, high quality semiconductor crystal by slowly lifting a seed crystal from a molten bath of the material under careful cooling conditions.
Direct Current	Electric current in which electrons flow in one direction only. Opposite of alternating current.
Frequency	Number of repetitions per unit time of a complete waveform. Expressed in Hertz (Hz).
Inverters	Devices that convert DC electricity into AC electricity (single or multiphase), either for stand-alone systems (not connected to the grid) or for utility-interactive systems.
Maximum Power Point Tracker	A power conditioning unit that automatically operates the PV-generator at its maximum power point under all conditions. An MPP will typically increase power delivered to the system by 10% to 40%, depending on climate conditions and battery state of charge. You usually get more gain in winter and in colder weather due to the higher panel output. Most MPP tracking controllers are down converters - from a higher voltage to a lower one.
Module	Number of PV cells connected together, sealed with an encapsulant, and having a standard size and output power; the smallest building block of the power generating part of a PV array. Also called panel.
Parallel Connection	A way of joining two or more electricity-producing devices (i.e., PV cells or modules) by connecting positive leads together and negative leads together; such a configuration increases the current.
Photovoltaic efficiency	The ratio of electric power produced by a cell at any instant to the power of the sunlight striking the cell. At present, this value is typically between 9% and 14%, for commercially available cells.
Photovoltaic Watt peak	Maximum rated output of a cell, module, or system. Typical rating conditions are 0.645 watts per square inch (1000 watts per square meter) of sunlight, 20 degrees Celsius of ambient air temperature and 6.2×10^{-3} mi/s (1 m/s) wind speed.
Power Factor	The ratio of the Active Power and the Apparent Power. It is affected by the inductance and capacitance of the load. A pure resistance, such as an electric heater would have a power factor of 1.

Reactive Power	The power that moves back and forth between the load and source. It is measured in Volt-Ampere Reactive (VAR) and symbolized by the capital letter Q.
Reverse Bias	Condition where the current producing capability of a PV cell is significantly less than that of other cells in its series string. This can occur when a cell is shaded, cracked, or otherwise degraded or when it is electrically poorly matched with other cells in its string.
Solar Cell	The elementary unit of a PV panel that converts the energy of light directly into electricity by the photovoltaic effect.
Standard Test Conditions	Conditions under which a module is typically tested in a laboratory: Irradiance intensity of 1000 W/ m ² (0.645 watts per square inch), AM 1.5 solar reference spectrum, and a cell (module) temperature of 25 degrees Celsius, plus or minus 2 degrees Celsius.
String	A number of photovoltaic modules or panels interconnected electrically in series to produce the operating voltage required by the load.
Transformer	A transformer is a static device, which transfers electrical energy from one circuit to another through the process of electromagnetic induction. It is most commonly used to increase (step up), decrease (step down) and isolate AC voltage circuits.
Volt	Unit of measure for electromotive force (EMF), the electrical potential between two points. An electrical potential of 1V will push 1 A of current through a 1 Ω resistive load.
Watt	Rate of energy transfer equivalent to 1 A under an electrical pressure of one Volt. One Watt equals 1/746 horsepower, or one Joule per second. It is the product of voltage and current.

LIST OF FIGURES

FIGURE 1 - HEADQUARTER OF IBC SOLAR IN BAD STAFFELSTEIN, GERMANY [3].	2
FIGURE 2 - EFFICIENCY EVOLUTION OF CRYSTALLINE-SILICON PV CELLS. [24]	7
FIGURE 3 - GLOBAL INCREASE OF PV CAPACITY IN THE WORLD [7]	8
FIGURE 4 - PHOTOVOLTAIC POWER PLANT EQUIPMENT.	13
FIGURE 5 - ELECTROMAGNETIC SPECTRUM OF SOLAR RADIATION [9] .	14
FIGURE 6 - ENERGY DENSITY OF SOLAR SPECTRUM FOR DIFFERENT TEMPERATURES [7].	14
FIGURE 7 - YEAR CYCLE OF THE EARTH ORBIT AROUND THE SUN [7].	15
FIGURE 8 - SUMMARY OF THE SOLAR GEOMETRY ANGLES [8].	15
FIGURE 9 - SUN POSITION FOR THREE MONTHS AT LATITUDE 30° [8].	16
FIGURE 10 - SPECTRUM OF SOLAR RADIATION [9].	17
FIGURE 11 - ANGLE OF INCIDENCE IN THE SOLAR MODULE [23].	17
FIGURE 12 - ENERGY BANDS OF SEMICONDUCTOR MATERIAL [7].	18
FIGURE 13 - PV CELL STRUCTURE AND ITS LAYERS [8].	19
FIGURE 14 – MODEL EQUIVALENT ELECTRICAL CIRCUIT OF A PV CELL [2].	20
FIGURE 15 - PHOTOVOLTAIC CELL I-V CHARACTERISTIC CURVE [2].	20
FIGURE 16 - PHOTOVOLTAIC CELL EFFICIENCY ACCORDING TO SOLAR IRRADIANCE LEVELS.	21
FIGURE 17 - DECREASE OF PHOTOVOLTAIC CELL EFFICIENCY DUE TO TEMPERATURE.	22
FIGURE 18 - PHOTOVOLTAIC CELLS, MODULES, PANELS, AND ARRAYS.	24
FIGURE 19 - STRING OF MODULES - VOLTAGE GAIN WHILE CURRENT KEEPS THE SAME.	25
FIGURE 20 - ARRAY OF MODULES - VOLTAGE AND CURRENT GAIN.	25
FIGURE 21 - AC-TO-DC RATIO VS. OUTPUT GAIN.	30
FIGURE 22 - ENERGY GAIN DUE TO HIGHER AC-TO-DC RATIO [17] .	31
FIGURE 23 - TYPES OF STATIC MOUNTING STRUCTURE.	33
FIGURE 24 - SINGLE AND DUAL-AXIS TRACKER MOUNTING STRUCTURE.	33
FIGURE 25 - MPP TRACKING - PV GENERATOR ACHIEVES ITS MAXIMUM PERFORMANCE.	34
FIGURE 26 - CENTRAL INVERTER INTERCONNECTION WITH DC COMBINER BOXES [16] .	35
FIGURE 27 - STRING INVERTER INTERCONNECTION SCHEMATIC [16] .	36
FIGURE 28 - TRANSFORMER STATION NEXT TO SMARTGRID CENTRAL INVERTERS.	38
FIGURE 29 - DETAILING OF SOILING AND SHADING LOSSES IN THE PVSYS LOSS DIAGRAM – PART I	40
FIGURE 30 - DETAILING OF LOSSES IN THE PVSYS DIAGRAM - PART II	41
FIGURE 31 - RAMMING AND PULL-OUT TEST	47
FIGURE 32 - MODULES MOUNTING STRUCTURE SINKING DUE TO SOIL MOVEMENT.	48
FIGURE 33 - THERMAL CAMERA ANALYSIS TO IDENTIFY HOT SPOTS.	50
FIGURE 34 - TREES OUTSIDE THE POWER PLANT TERRAIN CAUSING SHADOW ON THE MODULES.	51
FIGURE 35 - IMPACT IN THE INVERTER’S ENERGY PRODUCTION DUE TO SHADING.	52
FIGURE 36 - ROW-TO-ROW SHADING	52
FIGURE 37 - STRINGS WITH INLINE INTERCONNECTION PATTERN.	53
FIGURE 38 - STRING WITH C INTERCONNECTION PATTERN.	53
FIGURE 39 - INCORRECT FORM TO INTERCONNECT C TYPES.	54

FIGURE 40 - STRINGS WITH S INTERCONNECTION PATTERN.	54
FIGURE 41 - STRING WITH <i>JUMP</i> AND <i>INLINE</i> INTERCONNECTIONS.	54
FIGURE 42 - STRING WITH MIXED PATTERNS INTERCONNECTIONS AND A JUMP.	55
FIGURE 43 - STRING CABLES RUNNING INSIDE THE MMS.	56
FIGURE 44 - TRENCH FOR CABLES BEING DUG BETWEEN THE MODULES MOUNTING STRUCTURES.	56
FIGURE 45 - BARE COPPER WIRE FOR EARTH GROUNDING.	57
FIGURE 46 - FROM LEFT TO RIGHT: HORIZONTAL PYRANOMETER, HORIZONTAL REFERENCE CELL, TILTED PYRANOMETER, TILTED REF. CELL.	59
FIGURE 47 - METEOCONTROL DATA STATION X SERIES FOR OUTDOOR APPLICATION.	60
FIGURE 48 - METEOCONTROL PORTAL FOR MONITORING AND ANALYSIS OF ALL DATA RETRIEVED BY THE POWER PLANTS.	60
FIGURE 49 - INVERTERS PRODUCTION CAPPING AT 50KW.	61
FIGURE 50 - SUN RISING AND FIRST REACHING THE IRRADIANCE SENSORS THAT ARE LOCATED IN THE TOP OF THE HILL.	62
FIGURE 51 - SUN REFLECTED BY THE MODULES DIRECTLY IMPACT THE IRRADIANCE SENSOR DATA.	62
FIGURE 52 - TRANSFORMER STATION PAINTED IN WHITE COLOR CREATING FALSE READING IN THE IRRADIANCE SENSOR.	63
FIGURE 53 - IRRADIANCE SENSOR WITH FALSE VALUES DURING THE MORNING.	63
FIGURE 54 - THIN LAYER OF ICE OVER MODULES AND ROW-TO-ROW SHADING.	64
FIGURE 55 - BIRDS RESTING ON THE IRRADIANCE SENSORS AND MODULES DURING WINTER.	64
FIGURE 56 - TEMPERATURE SENSOR ATTACHED BEHIND THE MODULE.	65
FIGURE 57 - HIGH GRASS COVERING LOWER MODULES.	65
FIGURE 58 – INVERTER LIMITING ITS POWER DUE TO VENTILATION ISSUE (BROWN LINE).	66
FIGURE 59 - MANUAL PERFORMANCE RATIO CALCULATION PROCESS.	69
FIGURE 60 - PROPOSED AUTOMATION IN THE PERFORMANCE RATIO CALCULATION PROCESS.	69
FIGURE 61 - FIRST VERSION OF THE AUTOMATIC PR CALCULATION.	71
FIGURE 62 - SECOND VERSION OF THE AUTOMATIC PR CALCULATION.	72
FIGURE 63 - THIRD VERSION OF THE AUTOMATIC PR CALCULATION	72
FIGURE 64 - RAW DATA TABLE FOR THE AUTOMATIC PR CALCULATION TOOL.	73
FIGURE 65 - AUTOMATIC PERFORMANCE RATIO CALCULATION FOR EVERY 5 MIN INTERVAL.	73
FIGURE 66 - REFERENCE PV CELL TEMPERATURE FOR AUTOMATIC CALCULATION OF THE PR.	73
FIGURE 67 - DAILY PR SPREADSHEET FOR THE AUTOMATIC CALCULATION OF THE PR.	74
FIGURE 68 - MONTHLY PR SPREADSHEET DATABASE.	75
FIGURE 69 - AUTOMATIC PR CALCULATION CONTROLLER.	75
FIGURE 70 - MONTHLY PR SPREADSHEET OVERVIEW OF ALL POWER PLANTS.	76
FIGURE 71 - RAW DATA TEMPERATURE SENSORS CORRELATION.	80
FIGURE 72 – FLOWCHART OF THE TOOL DEVELOPED TO PERFORM THE AUTOMATIC CALCULATION OF PR.	95

LIST OF TABLES

TABLE 1 - MONTHLY AND ANNUAL YIELD FORECAST EXAMPLE OF A PV POWER PLANT.	9
TABLE 2 - PV MODULE TECHNICAL DATA EXAMPLE [1].	23
TABLE 3 - EFFICIENCY RATING OF PV MODELS BY MANUFACTURER [11].	23
TABLE 4 - IBC POLYSOL 275 CS5 SOLAR MODULE TECHNICAL CHARACTERISTICS.	26
TABLE 5 - STRING INVERTER SUNGROW SG49K5J ELECTRICAL CHARACTERISTICS.	28
TABLE 6 - INVERTER SG49K5J MPP INPUTS OVERVIEW ACCORDING TO CALCULATED VALUES.	32
TABLE 7 - CENTRAL VS. STRING INVERTER CHARACTERISTICS.	37
TABLE 8 - REQUIREMENTS FOR THE AUTOMATIC CALCULATION SYSTEM.	70
TABLE 9 - RAW DATA FILTER OF THE AUTOMATIC PR CALCULATION.	77
TABLE 10 - AUTOMATIC PR CALCULATION WORK EFFORT.	79
TABLE 11 - PERFORMANCE RATIO AUTOMATIC CALCULATION ACHIEVEMENTS.	79

INDEX

1	INTRODUCTION	1
1.1	IBC SOLAR AND INTERNSHIP	2
1.2	CHAPTERS STRUCTURING.....	3
2	LITERATURE REVIEW.....	7
3	FUNDAMENTAL CONCEPTS.....	13
3.1	SOLAR RESOURCE.....	13
3.2	PHOTOVOLTAIC CELLS.....	18
3.2.1	Operation Principle	18
3.2.2	Electrical Characteristics.....	19
3.2.3	Performance.....	20
3.2.4	Cells Aggregation.....	22
3.3	PHOTOVOLTAIC MODULES.....	24
3.3.1	String Interconnection.....	24
3.3.2	Array Interconnection	25
3.3.3	Electrical Calculations.....	26
3.4	AC-TO-DC RATIO.....	30
3.5	MODULES MOUNTING STRUCTURE.....	32
3.6	INVERTERS.....	34
3.7	TRANSFORMER.....	37
3.8	CABLE LOSSES.....	38
3.9	YIELD FORECAST	40
3.10	PERFORMANCE RATIO.....	42
4	CASE STUDY.....	47
4.1	RAMMING AND PULL-OUT TEST	47
4.2	HOT SPOT HEATING.....	49

4.3	SHADING	50
4.4	MODULES INTERCONNECTION MISMATCH	52
4.5	CABLES ROUTING AND GROUNDING	55
4.6	MONITORING SYSTEM	58
4.7	INVERTERS CAPPING	61
4.8	SENSOR ERRORS AND FAULTS.....	61
4.9	MAINTENANCE.....	65
5	PERFORMANCE RATIO AUTOMATIC CALCULATION	69
5.1	OVERVIEW.....	69
5.2	SYSTEM REQUIREMENTS.....	70
5.3	CALCULATION STRUCTURE AND EVOLUTION	70
5.4	AUTOMATION MILESTONES.....	73
5.5	VALIDATION	77
5.6	WORK EFFORT	78
5.7	ACHIEVEMENTS.....	79
5.8	LONG-TERM ANALYSIS	80
6	CONCLUSION.....	83
6.1	FUTURE WORK	84
7	BIBLIOGRAPHY AND OTHER SOURCES OF INFORMATION.....	87
8	APPENDIX A - DATASHEETS.....	91
8.1	IBC PolySol 275 CS5 Module Datasheet.....	91
8.2	Sungrow SG49k5J String Inverter Datasheet	93
9	APPENDIX B – AUTOMATIC PR CALCULATION SOFTWARE	95

INTRODUCTION

1 INTRODUCTION

The world is changing. Our science is increasingly global, as we recognize the challenges of understanding interconnected Earth systems, meeting the rising global demand for natural resources, handling trade-offs regarding sustainable development, and reducing the risks of natural disasters [1]. All mainly related with the human life system, which is significantly based on electricity. Almost every process on the Earth nowadays depends or will depend of electrical energy, and this huge necessity started to face funnels on its production, mainly because all the power is still being produced in large part with fossil fuels, which are heating the planet and unbalancing biological systems.

Governments are effectively increasing their efforts in the form of policies and programs around the world, to push for faster and greater adoption of renewable energy. The sustainable future scenario of International Energy Agency projected that 57% of the world's electricity would be provided by renewable energy sources by 2050 [2]. In fact, by 2016, global investment in renewable energy outstripped investments in fossil fuels and more than half of the world's newly added power-generating capacity were renewable energy sources [7].

One promising solution for a clean and renewable energy production is the solar photovoltaic system. Been first used in 1958 by NASA to power the radios on the Vanguard I satellite, the technology faced a great evolution in the last decades, enabling not only the production of energy for machinery and equipment, but also for houses, industry and grid connected power plants. Despite been a simple electrical system, the solar power plants are almost never equal to each other, which demand attention to a lot of small and very important details during the project development. The lack of an accurate development can produce the reverse sustainable effect in which the system proposes, causing an environment impact with waste of raw material, lower energy production and also the depreciation of the PV market.

The engineering steps to design a PV power plant are analysed in this document. Starting with the Solar resource and how to explore it in the best way, all the aspects of the PV cells and modules operation, electrical calculations, modules interconnection, inverters types and applicability, cable losses, Yield Forecast and the Performance Ratio, which is analysed in a case study, demonstrating the key factors during the development and operation that negatively impact its value. In the end, the author demonstrates a software designed to increase the reliability and decrease the time spent with the PR calculations, which was created for IBC Solar Energy GmbH as part of its internship.

1.1 IBC SOLAR AND INTERNSHIP

IBC Solar is a company specialized in photovoltaic systems which provides products and services for sunlight-generated power in Germany and many other countries around the globe. The company was established in 1982 by Udo Möhrstedt in Bad Staffelstein and offer project management, consulting, planning and execution of photovoltaic installation from households to energy utilities. The Figure 1 shows the headquarter of the company in Germany.



Figure 1 - Headquarter of IBC Solar in Bad Staffelstein, Germany [3].

In 2009 the company generated over € 857 million in revenue and by 2016 IBC was able to achieve the mark of 3 GW in total power capacity installed. More than 100,000 ready-to-use photovoltaic systems all over the world. Today, IBC group contains more than 300 employees and has subsidiaries in the Netherlands, Spain, the Czech Republic, Turkey, Italy, Singapore, India and Japan. Although IBC is not responsible for producing any type of PV equipment. The enterprise work in cooperation with other manufactures to provide the necessary products for PV systems, like modules, inverters, storages unities and mounting structures. Every equipment that is sold by IBC has an excellent performance quality, assured by reputed testing laboratories.

A relevant area of activity of IBC is the development of solar power plants. The projects contemplate partially or fully EPC enterprises. This means that the company has the complete know-how to build a solar park, which include financial models, technical planning, project management, procurement and logistics, commissioning and monitoring. That's, from the sketch to the grid-connected fully functional power plant.

During the period that correspond from February 12th to August 9th 2019, the author of this document participated in the company daily tasks as an Intern in the technical sector of the international EPC department. The engineering activities were focused in the detailing of modules, string cable connections, trench patterns, inverters type and architecture, monitoring systems, combiner boxes, shading effects in different projects, mass calculation to minimize power losses, determination of cables specifications, preparation of data for yield calculations with PVSyst, daily PV plant monitoring using GPM and MeteoControl portals, creation of documents and As-built plans of power plants worldwide and site visits in photovoltaic power plants in Germany.

The projects in which the author participated in the development, have between 500 KW and 35 MW of total DC power capacity installed. The name and location of these projects are not detailed in this document as this data is mostly considered strategic and confidential by the company.

1.2 CHAPTERS STRUCTURING

The chapters of this document are arranged chronologically to facilitate reading and understanding of the subject.

The chapter Literature Review demonstrates the evolution of solar cells over the years and their efficiency, showing that is of little importance if the development of the plant does not have minimum quality standards. A didactic approach is made that fits the reader with the subject to be addressed in the case study.

The chapter Fundamental Concepts shows all concepts of the PV cells and modules with its electrical characteristics and calculations, string and array interconnections, inverter types, transformer characteristics, cable losses and calculations, Yield Forecast and the Performance Ratio, with all related concepts and how it is calculated.

The chapter Case Study analyses numerous possibilities and cases on which the Performance Ratio can be affected negatively. Are addressed situations both during the development as well as in the operation of the power plant.

The chapter Performance Ratio Automatic Calculation shows the software created by the author to increase the reliability and decrease the time spent with the PR calculations, which was part of the daily tasks as an intern at IBC Solar Energy GmbH.

The chapter Conclusion ends the subject proposed in this document by succinctly determining the problems that impact the PR and the possible solutions during the development and operation of PV power plants. The chapter is complemented by a Future Work section on possible improvements in the PR calculations.

LITERATURE REVIEW

2 LITERATURE REVIEW

In 1839 Alexandre E. Becquerel demonstrated for the first time in history the generation of electric energy through the incidence of light in a material. However, the first photovoltaic cell was produced only in 1883, by Charles Fritts. It was made with selenium and achieved an efficiency of 1%. Photovoltaic cells composed of crystalline silicon appeared only in 1941.

In the 1950s the industrial production of photovoltaic panels began, and at that time the efficiency hardly reached 6%, far from the current efficiency levels of the commercially most common PV modules utilized in the market. The expensive and performance-limited technology was used only by specific sectors such as telecommunications in order to power up systems installed in remote locations. In particular, space programs leveraged the development of photocells by the end of the 1970s. Another major boost was the oil crisis in 1973, which renewed interest in the photovoltaic sector, but still at an unaffordable cost for several applications [2].

The following decades were marked by global concern about climate change and the commitment of several nations to reduce CO₂ emissions, agreed in the Kyoto Protocol in 1997. In order to expand the use of renewable energy, governments (e.g. Germany and Japan) subsidized the production and application of photovoltaic systems. Nevertheless, the boom in the photovoltaic sector occurred with the rapid and massive rise of Chinese manufacturing. Since 2006, China has been among the largest manufacturers of photovoltaic modules, and currently leading market share with approximately 65% of all world production [7]. This enabled a great improvement in the technology of the commercially most common PV cells, increasing the efficiency in more than 5% in just 10 years, as shown in the Figure 2 .

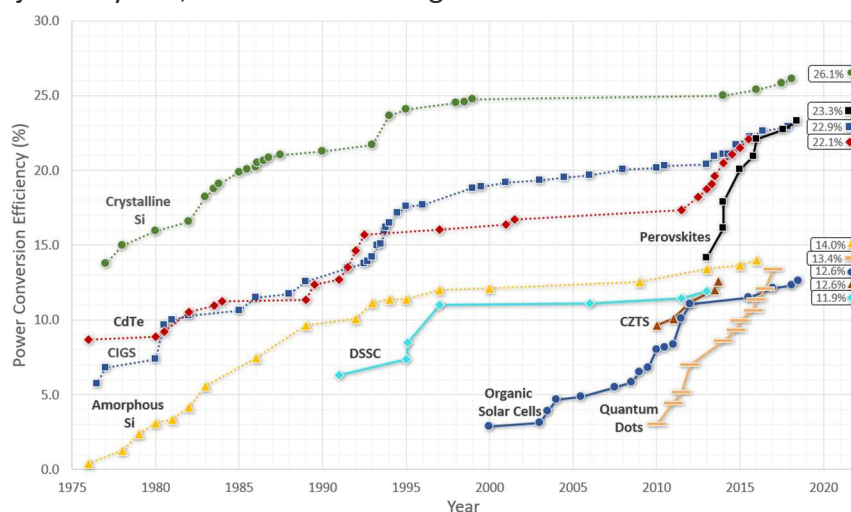


Figure 2 - Efficiency evolution of Crystalline-Silicon PV cells. [24]

The production of large-scale photovoltaic modules has significantly reduced the costs of PV solar energy, which has enabled the worldwide expansion of the use of this energy resource. As illustrated Figure 3, the countries with the largest photovoltaic capacity are China, Japan, the USA and Germany, which combined with the rest of the world exceeded in 2017 the installed power of 400 GW.

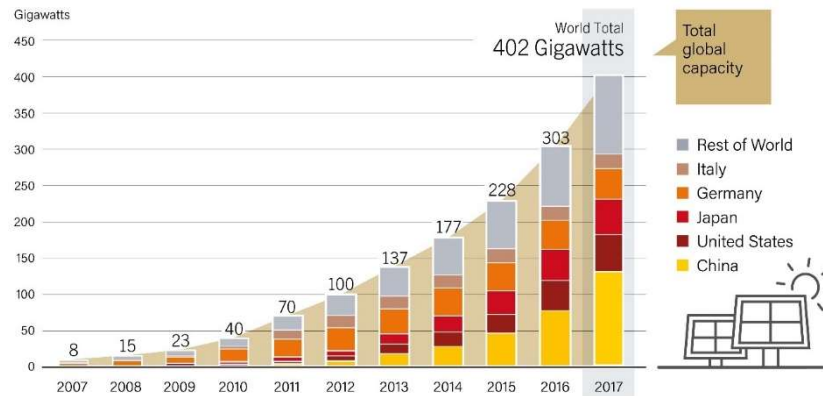


Figure 3 - Global increase of PV capacity in the world [7]

The increasing market and the search for new technologies are allowing the discovery of new materials and conducting research for the advancement of photovoltaic technology. Silicon is the main photovoltaic cell fabrication material and is used as the second most abundant chemical element on earth. It has been explored in several forms: crystalline, polycrystalline and amorphous [11].

While new technologies and materials are very important for the PV cells efficiency, it is also crucial to ensure that the system application is performed correctly. The efficiency of a single PV module is of no concern if the entire energy production system is not designed and built to the minimum standards of quality. Many losses are added until the real efficiency in energy production is obtained, and for this it's necessary to standardize a performance calculation that would allow the equalization of any solar plant, regardless of its capacity, location or technology employed.

The *Performance Ratio* (PR) is the ratio assessment that indicates the accurate production of the PV power plant and shows how energy efficient and reliable the plant is. The assessment enables to determine the real potential of a PV power plant and find hidden system failures in order to obtain relevant information, to maximise energy yield. Assessing the solar PV performance ratio is the only KPI that allows to compare the energy output of the plant with of other installations, thus making possible to match several plants regardless of their capacity, architecture or location. The PR also provides all parties and stakeholders with clarity about the efficiency and health of the plant and reduces financial uncertainty. Stakeholders can gain accurate and independent information for an evaluation of the return on investment.

$$PR = \frac{Y_f}{Y_r}$$

where:

Y_f is the System Yield [kWh/kWp] and Y_r is the Reference System Yield [kWh/kWp]

The PR is first calculated at the beginning of the project and takes into consideration real meteorological inputs like solar radiation, temperature, environmental factors (snow, dust, ice), losses involved during the power plant operation, which are mostly related with the energy conversion and transport, and objects around the plant that may cause shade on the modules during certain periods of the year. Based on this calculation is created the Yield Forecast of the PV power plant as shown in the Table 1 , which will determine both energy generation and PR for each month of the year.

Table 1 - Monthly and annual yield forecast example of a PV power plant.

Month	GHI (kWh/m ²)	GTI (kWh/m ²)	Ambient Temp. (°C)	Energy Generated (kWh)	PR (%)
January	170.3	199.3	24.3	877000	78.6
February	163.8	181.6	26.8	790000	77.7
March	199.4	208.3	29.7	896000	76.8
April	186.9	183.8	30.9	789000	76.7
May	182.5	172.3	30.7	746000	77.4
June	152.1	141.6	27.7	623000	78.6
July	146.8	138.0	27.2	610000	78.9
August	139.2	134.4	26.6	568000	75.5
September	151.3	153.5	26	677000	78.8
October	144.3	153.1	24.1	676000	78.9
November	143.6	162.3	23.3	706000	77.7
December	149.6	174.4	27	778000	79.7
Total	1929.8	2002.5	27	87360000	77.9

The losses accounted for the calculation of the Yield Forecast are fixed parameters, and during the daily operation of the power plant different issues may impact the energy production. If the structure that supports the PV modules sink modifying the irradiance angle of incidence, the vegetation height is too high that is covering the modules, a panel that is damaged and is creating a current bottleneck in the string and etc are a few examples of different situations that may occur. Thus, it is necessary to have the daily analysis and monitoring of the plant to find early signs of defect or malfunction, to provide a proper instruction for primary counter measures, reducing the unavailability period of the system and the associated financial losses.

The following chapters analyse the PV power plants in order to identify possible failures during development and operation that can affect its performance ratio, as well as a software created by the author of this document which allowed to increase reliability and decrease the time spent in the calculation of the daily PR of the power plants under the supervision of IBC Solar Energy GmbH.

FUNDAMENTAL CONCEPTS

3 FUNDAMENTAL CONCEPTS

This chapter explores the concepts of the solar resource, radiation, the earth's motion relative to the sun and the calculations involved, an overview of PV cells with its operation principle, performance, how they are aggregated to create a solar module and all equipment with its electrical characteristics used to build a photovoltaic power plant as shown in the Figure 4.

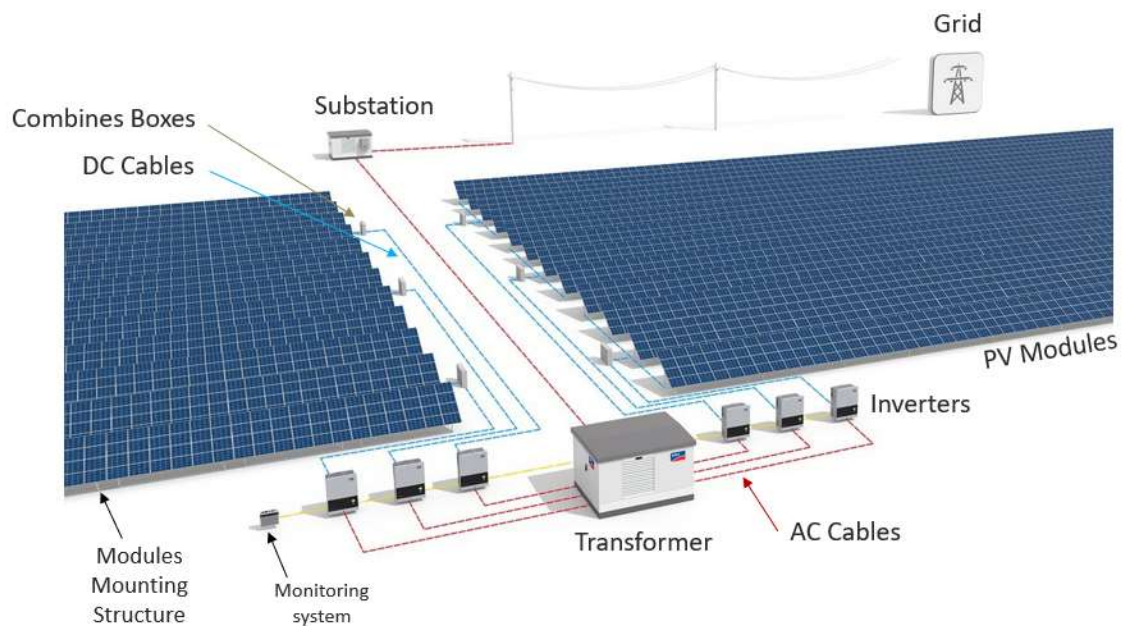


Figure 4 - Photovoltaic power plant equipment.

3.1 SOLAR RESOURCE

The Sun is the main source of energy of the Earth and it is responsible for sustain life in the planet. Its irradiation could be considered a limitless energy source at least for a few more billion years, as well as, constant to all extra-terrestrial space of the Earth which are reached by sunlight ($1,367 \text{ W/m}^2$). The amount of energy provided to the Earth by the solar irradiation is huge, approximately $1.03 \times 10^{18} \text{ kWh/y}$, which represents 10 thousand times the global energy necessity [8].

The solar radiation covers a wide range of the electromagnetic spectrum, which can be seen in the Figure 5. Most of the energy, that arrives at the earth atmosphere is within the visible bandwidth as shown in the following Figure 6. This energy feeds all thermic, dynamic and chemical process in the world, e.g. photosynthesis, hydrological cycle, dynamics of the atmosphere and oceans.

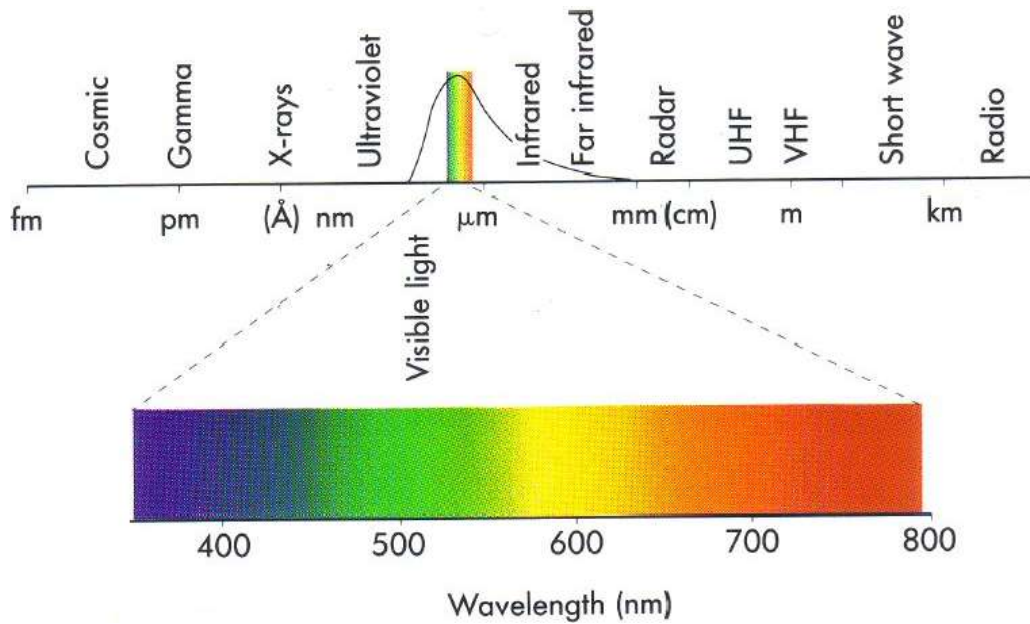


Figure 5 - Electromagnetic spectrum of solar radiation [9].

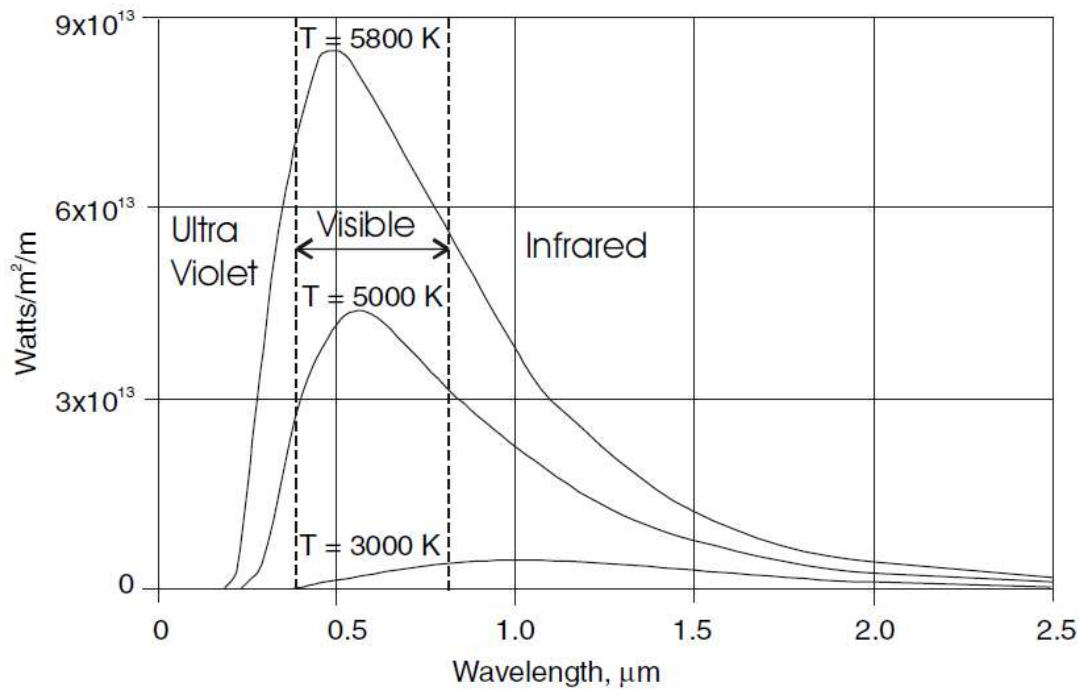


Figure 6 - Energy density of solar spectrum for different temperatures [7].

The availability of the solar energy resource and its spatial and temporal variability are intrinsically related to astronomical concepts. The first factor to be considered is the relative position between the Sun and the Earth. The Earth orbits the Sun at an average distance of about 150 million of kilometers, completing one cycle every 365.25 solar days. Throughout this period, the distance varies, as a result, the flow of irradiance ranges between 1,325 W/m² and 1,412 W/m². Although not strictly constant, the conventional value is the average, which is equal to 1,367 W/m² [9].

The duration and amount of sunlight exposure at a specific terrestrial surface is related by the annual and daily cycles. Different year seasons have longer or shorter sunlight hours, due to the polar axis of the Earth is inclined by an angle of 23.45 ° to the plane of the Earth’s orbit around the sun, as demonstrated in the Figure 7 . The angle of deviation of the sun from directly above the equator is called the declination (δ) and can be approximately expressed as:

$$\delta = 23.45^\circ \sin \left[\frac{360(n - 180)}{365} \right]$$

where n is the day of the year.

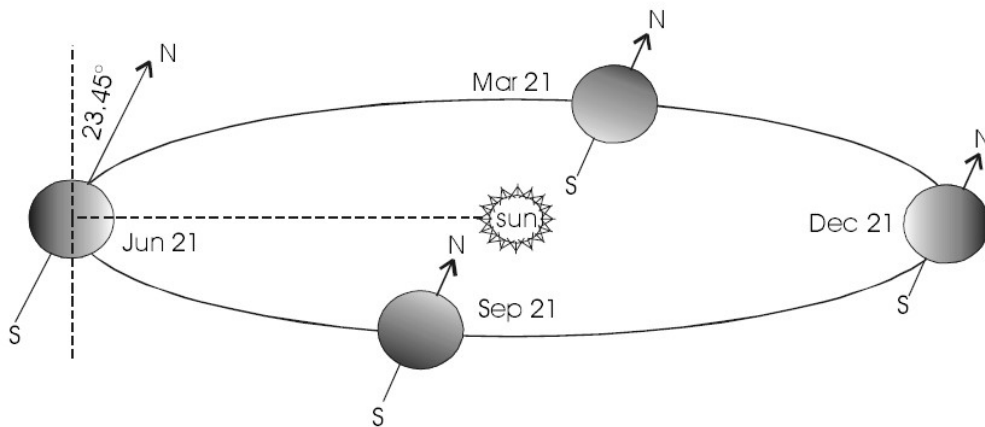


Figure 7 - Year cycle of the earth orbit around the sun [7].

In addition to the orbital movement, the Earth also rotates about its own polar axis once per day. The hour angle (ω) corresponds to the displacement of the Sun's apparent motion due to the rotation of the Earth and varies between -180° and + 180 °. Each hour corresponds to 15° of angle variation. By convention, during the morning is positive, the afternoon is negative and at noon zero. There are other important angles of solar geometry, which are illustrated in the Figure 8.

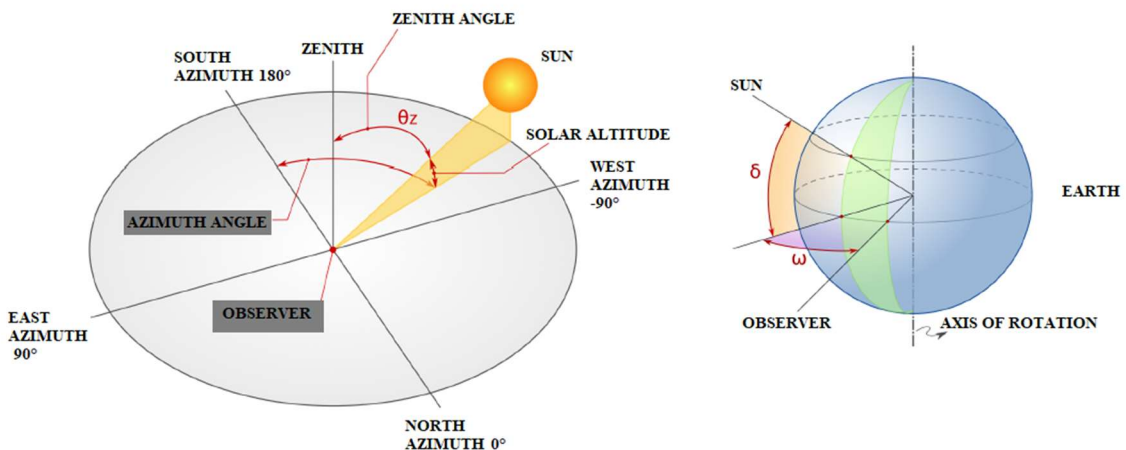


Figure 8 - Summary of the solar geometry angles [8].

The solar zenith angle (θ_z) represents the angle formed between the vertical at the observation point (straight up line perpendicular to the Earth) and the direction of the line which connects the same point on the surface of the Earth to the Sun. Complementary, the solar altitude angle (α) describes the angle between the incident solar beam and the projection of the horizontal plane. It can be expressed as

$$\theta_z + \alpha = 90^\circ,$$

$$\theta_z = \phi - \delta,$$

$$\cos(\theta_z) = \cos(\delta) \cos(\omega) \cos(\phi) + \sin(\delta) \sin(\phi)$$

where ϕ is the latitude angle.

Furthermore, the azimuth angle (ψ) is the angle formed between a north direction and a line from the observer to the sun projected on the same plane as the reference direction orthogonal to the zenith. The reference direction is typically north, but in some cases the reference could be south (i.e. South: $\psi = 0^\circ$, East: $\psi = -90^\circ$ North: $\psi = 180^\circ$ and West: $\psi = 90^\circ$).

Important relationships are described in the equations below. It expresses respectively the sunrise angle (ω_s), hours of daylight (DLH), position of the sun in terms of altitude and azimuth angle. The Figure 9 shows the position of the sun during three different months of the year at a location of latitude 30° north.

$$\omega_s = \cos^{-1}(-\tan(\phi)\tan(\delta)),$$

$$DLH = \frac{\cos^{-1}(-\tan\phi\tan\delta)}{7.5},$$

$$\sin(\alpha) = \sin(\delta)\sin(\phi) + \cos(\delta)\cos(\phi)\cos(\omega),$$

$$\cos(\psi) = \frac{\sin(\alpha) \sin(\phi) - \sin(\delta)}{\cos(\alpha) \cos(\phi)}.$$

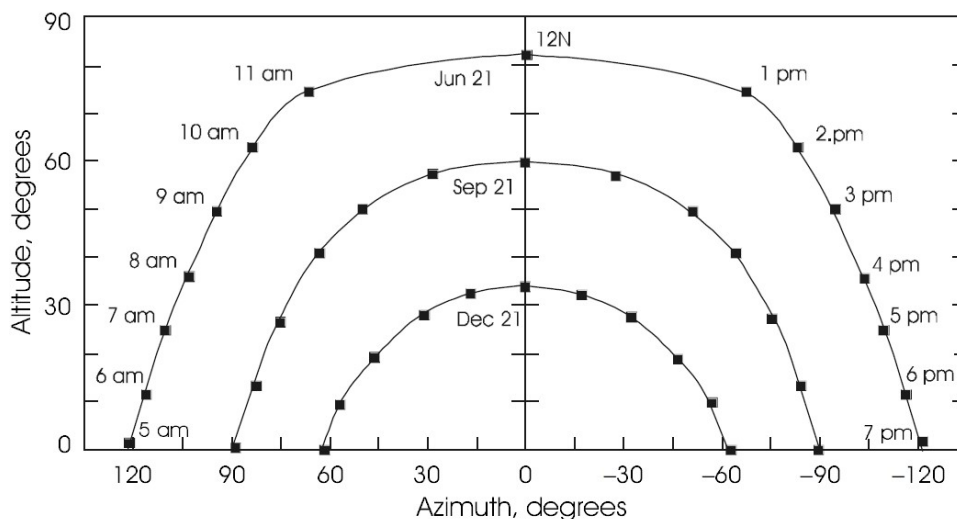


Figure 9 - Sun position for three months at latitude 30° [8].

Although the sun radiation can be considered uniform and constant at extra-terrestrial, it is not the same at the Earth’s surface. The sun beams are partly absorbed, reflected and diffused by the gases presented on the atmosphere. These effects combined with shadows of objects (e.g. clouds) attenuate and vary the intensity of solar radiation at ground level, as demonstrated in the Figure 10.

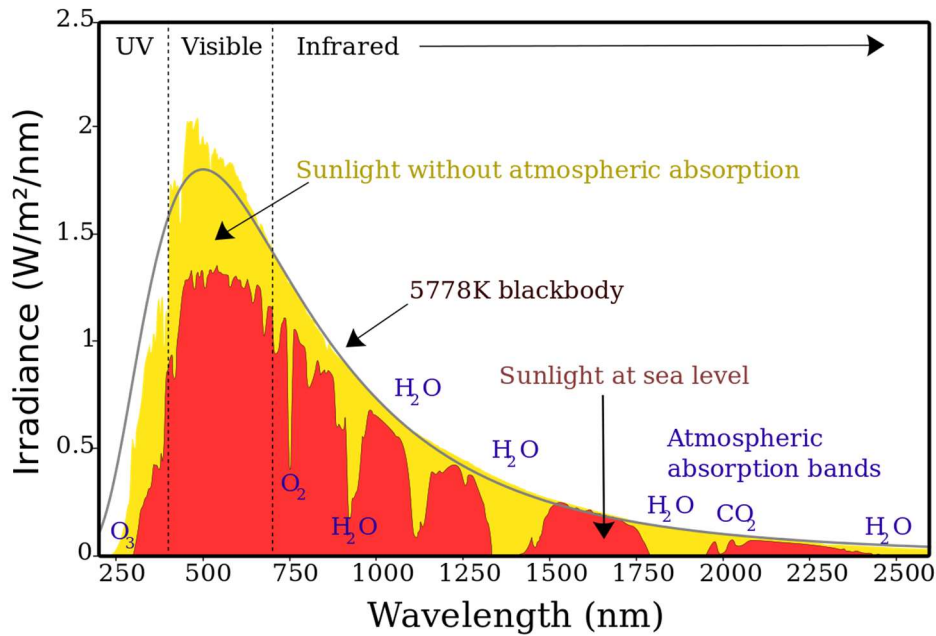


Figure 10 - Spectrum of solar radiation [9].

In order to estimate the sunlight incidence in a specific region, it is necessary the use of data based on measurements averaged over a long time. They take into account earth location and weather conditions (e.g. temperature, wind velocity and cloud formation). The angle at which the sun’s rays meet the surface of the solar panel determines how well the panel can convert the incoming light into electricity. This is known as the Angle of Incidence. As shown in the Figure 11, the narrower the angle of incidence q_i , the more energy a photovoltaic panel can produce [10].

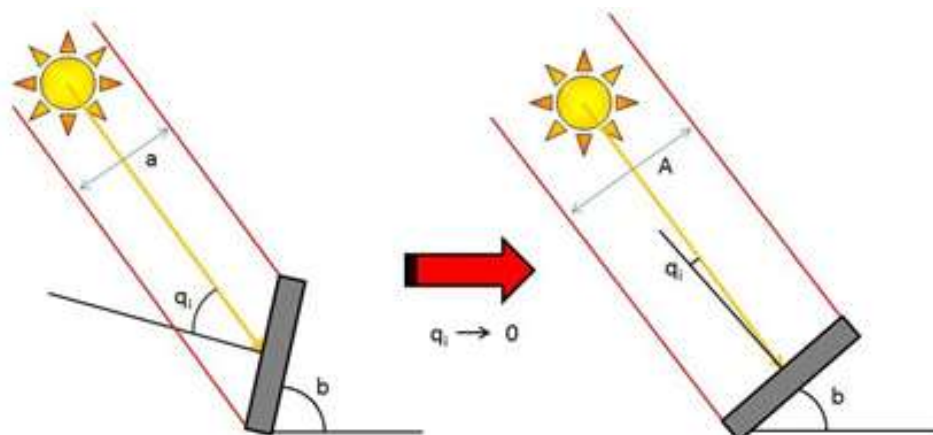


Figure 11 - Angle of incidence in the solar module [23].

3.2 PHOTOVOLTAIC CELLS

3.2.1 Operation Principle

The photovoltaic cells convert the energy of light into electricity through the photovoltaic effect. When light strikes on a material, it is reflected, transmitted or absorbed. The absorption of energy contained in the light is usually converted into heat, but there are materials with certain properties that can transform into electrical energy. The semiconductors have the necessary characteristics for the occurrence of the photovoltaic effect.

At the absolute zero temperature, all electrons of semiconductor materials fully fill the valence band, while the conduction band remains empty. Thus, at this temperature the semiconductors behave like an insulator, because of all electrons are attached to the atom, and there is no free electron that makes possible the conduction of electric energy.

As the temperature increases, enough energy is supplied to part of the electrons so that they move from the valence band to the conduction band. When an electron moves to the conduction band, its covalent bond is undone, leaving in the valence band a hole, which has a positive charge effect. This process can be observed in the Figure 12.

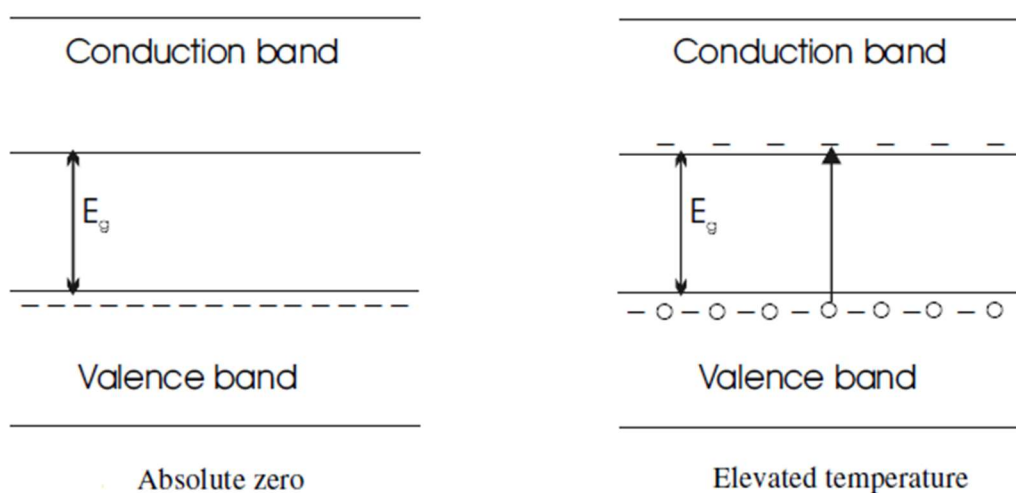


Figure 12 - Energy bands of semiconductor material [7].

Conduction and valence bands are separated by a band gap. An electron will only be excited to the other band when the Energy Gap (E_g) is reached, where it varies depending on the property of the material and temperature. This energy can be provided by photons, which are contained in the light that strikes the material. In the case of lower or higher values than E_g , the energy is dissipated as heat.

Visible light is part of the electromagnetic spectrum, which is quantized by photons. The energy is proportional to the frequency of the photon, and consequently its wavelength. Solar radiation includes wavelengths, whose photon energy corresponds

to E_g , and therefore can release the electrons from the valence band. In addition, the intensity of the radiation is related the number of photons.

After the change of state of the electron, it will quickly recombine with a hole in the valence band, releasing the acquired energy in the form of heat or light. In order to extract this charge, a potential difference is generated within the material, forcing the electrons and holes to move in the opposite direction to the usual.

The creation of an electric field in the material is made by the increment of other elements in the semiconductor, designating a PN junction. Type P is doped by elements (e.g. boron), which has one electron less in the outermost orbital compared to pure semiconductor (e.g., silicon). N-type is doped with one extra electron (e.g. phosphorus). Thus, the surplus electrons of the N region migrate to the P region, recombining with the holes present there and generating the potential barrier zone.

After the formation of the built-in potential, free electrons can move just in one direction (type P to type N), as the electrons are not able to cross the depletion layer back into the P-type material. When an external conductor path connects the two regions, the free electrons resulted of sunlight exposure can now flow, generating electrical current. This schema is demonstrated in the Figure 13.

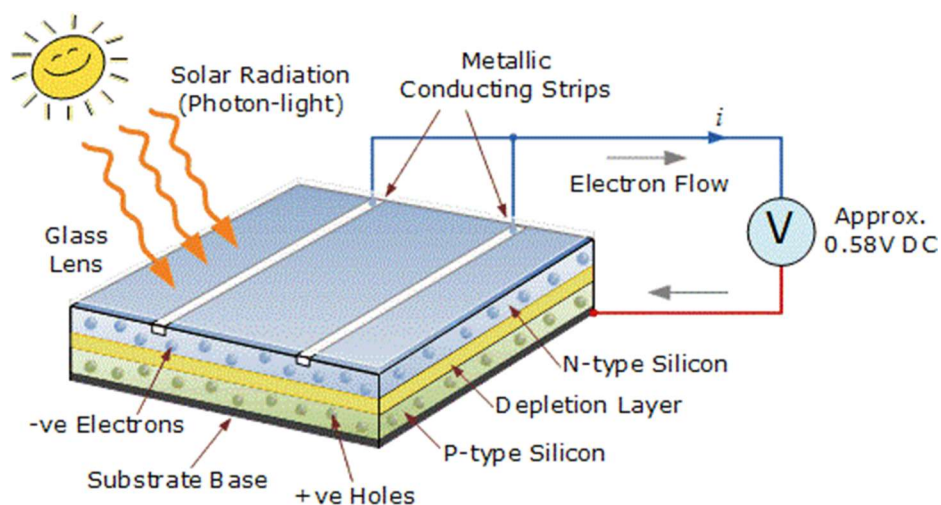


Figure 13 - PV cell structure and its layers [8].

3.2.2 Electrical Characteristics

The photovoltaic cell has similar behaviour and properties as a diode, however it has the capability of produce electrical current when the sunlight strikes on the surface of the cell. The Figure 14 shows a basic equivalent electrical circuit of a PV cell and the equation describes the output current.

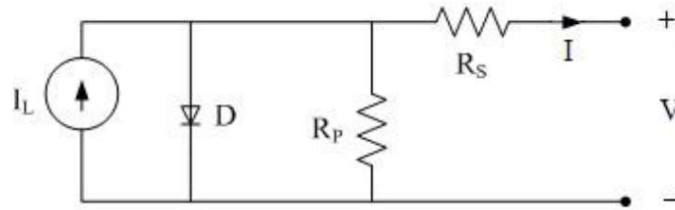


Figure 14 – Model equivalent electrical circuit of a PV cell [2].

$$I = I_L - I_0 \left[e^{\left(\frac{q(V+IR_S)}{nkT} \right)} - 1 \right] - \frac{V+IR_S}{R_P},$$

where I_L is the generated current due to photons with charge $q = 1.6 \times 10^{-19}$, considering the Boltzmann constant $k = 1.38 \times 10^{-23}$ and cell temperature T . I_0 is the reverse saturation current of the diode (D), n is the diode factor, V is the output voltage, R_S and R_P are respectively the series and parallel resistances.

The Figure 15 presents the I-V curve characteristic of a typical PC cell, which performance was taken under standard test condition (i.e. air mass 1.5, irradiance 1 kW/m² and cell temperature 25 °C). It should be noticed, that the current and voltage are limited by I_{SC} and V_{OC} . Additionally, the maximum power point P_{MPP} is reached when the current and voltage value are equal to I_{MPP} and V_{MPP} .

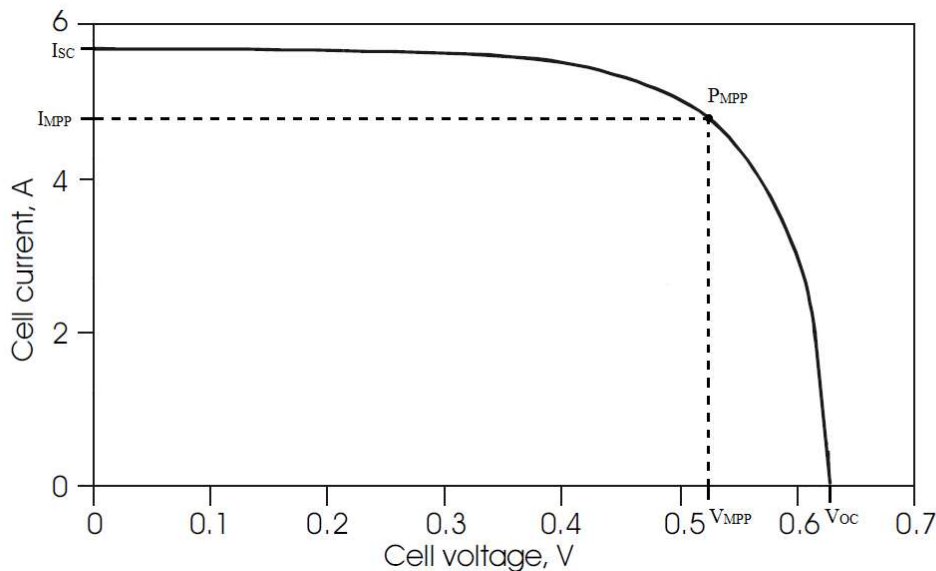


Figure 15 - Photovoltaic cell I-V characteristic curve [2].

3.2.3 Performance

There are some aspects that should be taken into account, in order to forecast the yield of electrical energy from PV cells. One of the most important criterions are the material technology. As explained in the operation principle section, the conversion of irradiance into electrical power is relative to the energy gap necessary to free the

electron from the valence band. This energy has different values depending on the semiconductor material. Hence, the energy production of a cell relies on its material. There are three technologies applied to the production of PV cells, classified in three studies according to their material and characteristics.

The first generation consists of crystalline silicon (c-Si), which is subdivided into monocrystalline silicon (m-Si) and polycrystalline silicon (p-Si), representing 85% of the market, as it is a better quality and a reliable technology [11]. The second generation, also called thin films, is divided into three chains: amorphous silicon (a-Si), copper indium gallium (CIGS) and cadmium telluride (CdTe). The third generation, defined by the IEEE such as:

Cells that use sunlight more efficiently than cells included in a single electronic band-gap. Generally speaking, a third generation should be highly efficient, low cost / watt and use abundant and low toxicity [11].

Another relevant influence in the cell performance is the solar irradiance. Without sun light, no energy is generated, and it reaches its maximum power output nearby 1000 W/m^2 . The current increases linearly with the irradiance and the voltage in a logarithm way, considering a stable temperature, as demonstrated in the Figure 16 .

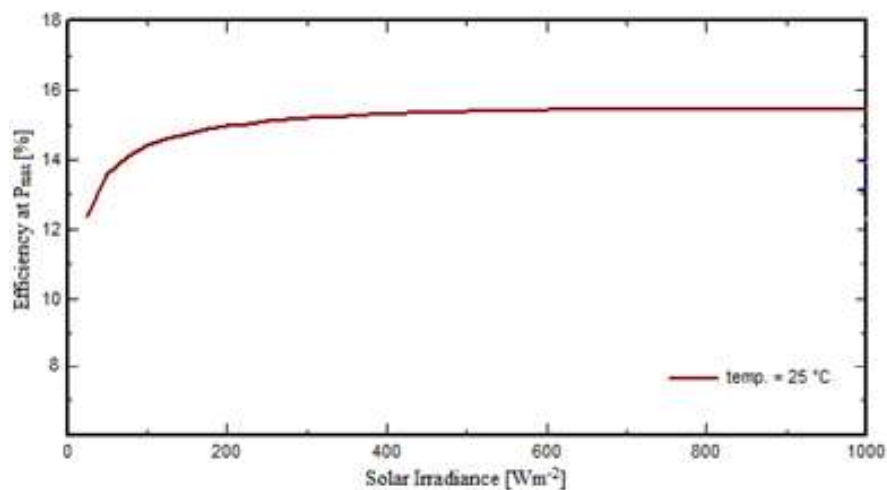


Figure 16 - Photovoltaic cell efficiency according to solar irradiance levels.

The last aspect that should be considered is the temperature. Higher temperatures decrease the efficiency of the PV cell, by reducing the operation voltage, while the current keeps unchanged, as shown in the Figure 17. Therefore, the weather and consequently the location, plays an important role in the photovoltaic energy production.

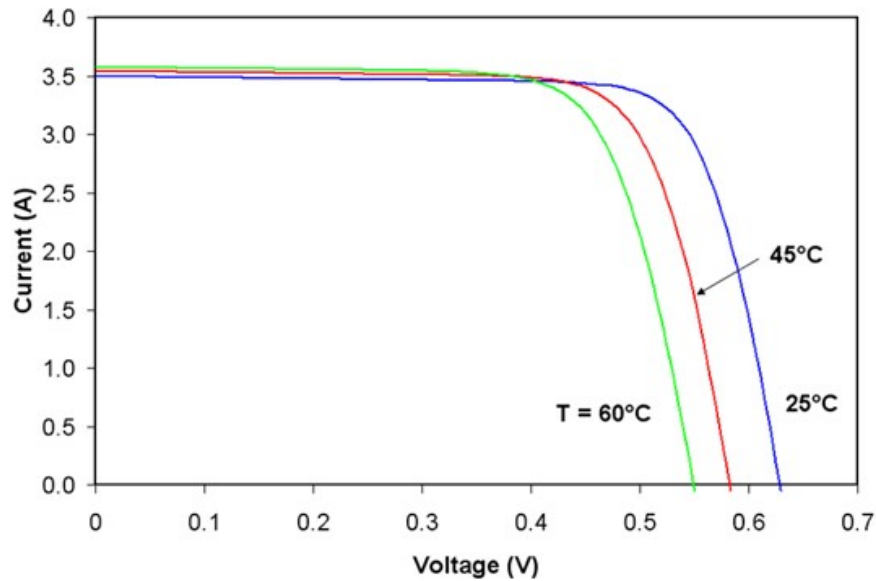


Figure 17 - Decrease of photovoltaic cell efficiency due to temperature.

Due to power plants has thousands of solar modules, and in each of these modules a few dozen cells, the efficiency loss related with the temperature of the modules is a parameter that great impact the energy production. As the efficiency of the modules is indicated by the equipment manufacturer, it is possible to predict the loss due to temperature and consequently design the system to compensate it. The assessment of electrical losses and the compensation of these losses are discussed more fully in the following chapters.

3.2.4 Cells Aggregation

The PV cell is the smallest single unit of a photovoltaic system, which for cells made of Silicon, typically at STC the values are around 250 cm^2 , 0.6 V and 4 W . They can be combined in order to obtain higher and desired electrical output parameters, while a series connection will increment the voltage, a parallel will rise the current. The PV module, which consist of a set of wired PV cells encapsulated with tempered glass (or some other transparent material) on the front surface, and with a protective and waterproof material on the back and edges surfaces. In addition, an aluminium frame holds everything together in a mountable unit and in the back of the module there is a junction box, or wire leads, providing electrical connections.

Typical power ranges of PV modules go from 100 W to 365 W . They also present an average efficiency of 16.8% , according to the major solar panel manufactures. The module efficiency indicates how much of irradiance is converted to usable electrical energy. The Table 2 shows a technical data example of a PV module and the following Table 3 the efficiency ratio of PV modules per manufacturer.

Table 2 - PV module technical data example [1].

Electrical data (STC)	Value
STC Power Pmax (Wp)	275
STC Nominal Voltage Umpp (V)	31.8
STC Nominal Current Impp (A)	8.67
STC Open Circuit Voltage Uoc (V)	39.0
STC Short Circuit Current Isc (A)	9.23
Module Efficiency (%)	16.8
Power Tolerance (Wp)	- 0 / + 5
Temperature Coefficient	Value
NOCT (°C)	44.1
Tempcoeff Isc (% / °C)	+ 0.041
Tempcoeff Voc (mV / °C)	- 121
Tempcoeff Pmpp (% / °C)	- 0.411

Table 3 - Efficiency rating of PV models by manufacturer [11].

Solar Panel Manufacturer	Minimum Efficiency (%)	Maximum Efficiency (%)	Average Efficiency (%)
Amerisolar	14.8	17	16
Axitec	15.4	17.9	16.5
Canadian Solar	15.8	18.6	17
China Sunergy	15	16.5	15.8
ET Solar	15.4	17.5	16.5
Grape Solar	16.2	17.6	16.8
Green Brilliance	14.2	15.6	15
Hanwha Q CELLS	14.7	19.6	17.1
Hanwha SolarOne	14.7	16.2	15.5
Hyundai	14.2	18.4	16
Itek Energy	16.5	18.9	18
Kyocera	14.8	16.1	15.4
LG	16.8	21.1	18.7
Mitsubishi Electric	16.3	16.9	16.6
Panasonic	19	21.6	20.3
ReneSola	14.9	16.9	15.9
Renogy Solar	15.3	18.5	17.3
Seraphim	15.7	17.5	16.6
SunPower	16	22.2	19.9
SunSpark Technology	15.2	18.2	16.7
Trina Solar Energy	15	18.6	16.4

If higher electrical output parameters are required for a photovoltaic system, it is possible to stack the PV cells even further than a module. While PV panels are the combination of one or more modules assembled as pre-wired and field-installable unit, a photovoltaic array is the complete power generating unit, consisting of any number of PV components as shown in the Figure 18.

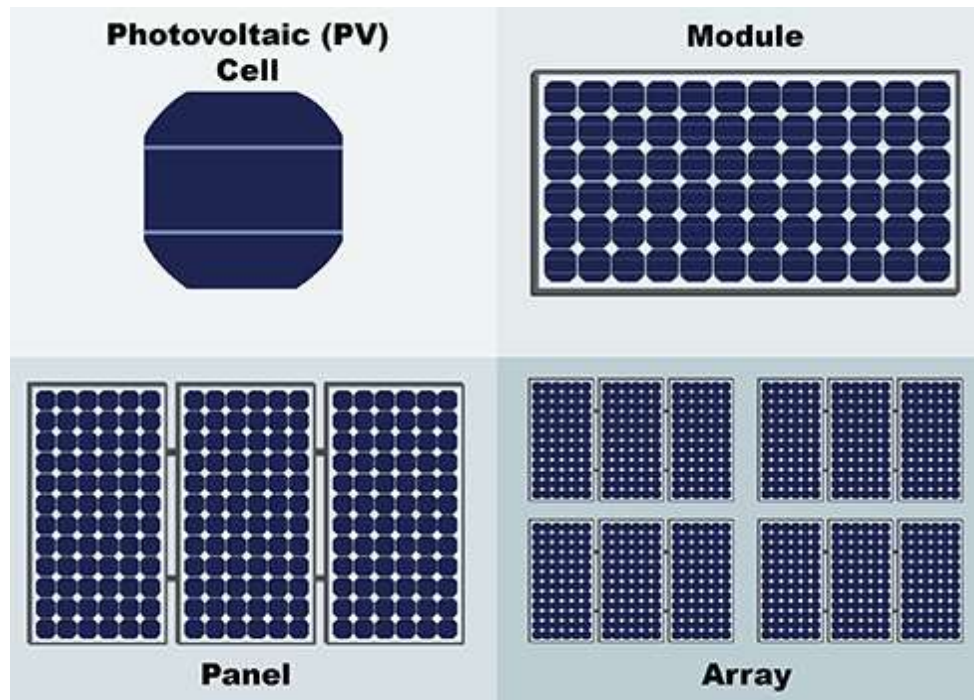


Figure 18 - Photovoltaic cells, modules, panels, and arrays.

3.3 PHOTOVOLTAIC MODULES

The solar module is the simplest electrical equipment in a solar park. Alone each module has no use for the system, but when interconnected in strings and then in arrays, the panels are able to deliver the exactly predicted power, with voltage and current within a specific range [8]. A module is in fact the aggregation of numerous PV cells in one equipment, making it ready to be installed outdoor.

The modules can be arranged in series and in parallel, according to the electrical needs of the system.

3.3.1 String Interconnection

The string interconnection aims to raise the output voltage of the panels until the desired operating voltage of the inverter is reached [10]. The current in this case goes through every module in the circuit. Therefore, all the modules in a series connection carry the same current, as shown in the Figure 19.

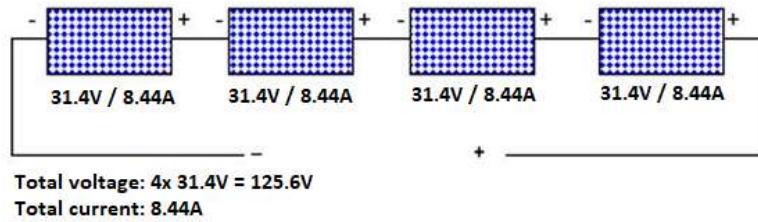


Figure 19 - String of modules - voltage gain while current keeps the same.

The circuit has only one path in which its current can flow. Opening or breaking a series interconnection at any point causes the entire circuit to stop operating. For example, if one module is removed or become damaged, the entire string will stop producing. The equations to obtain the total voltage and current of strings are expressed as:

$$U_{string} = n^{\circ}_{modules} \times U_{module}$$

$$I_{string} = I_{module}$$

3.3.2 Array Interconnection

The array interconnection is the junction of several strings to increase the current output. If two or more modules are connected in parallel, they have the same difference of potential across their ends. The potential differences across the panels are the same in magnitude, and they also have identical polarities. The same voltage is applied to all circuit components connected in parallel. The total current is the sum of the currents through the panels strings, in accordance with Kirchhoff’s current law, as shown in the Figure 20.

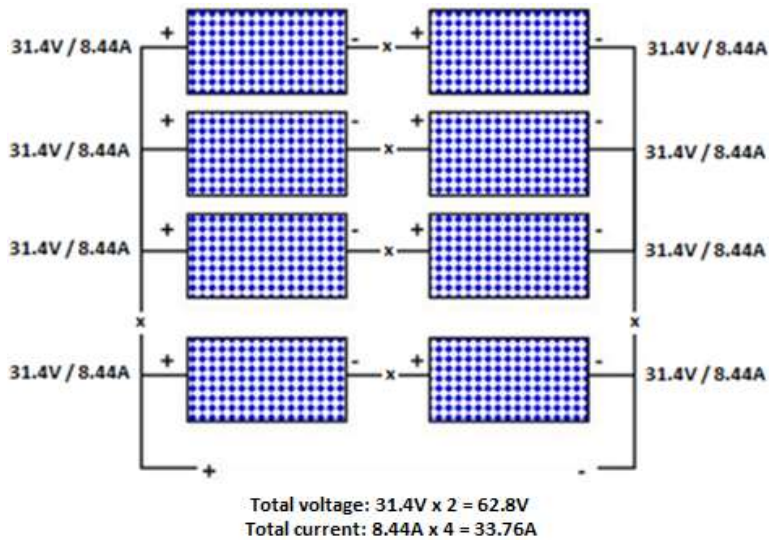


Figure 20 - Array of modules - voltage and current gain.

The equations to obtain the total voltage and current of arrays are expressed as:

$$U_{array} = n^{\circ}_{modules_{pe\ string}} \times U_{module}$$

$$I_{array} = n^{\circ}_{strings} \times I_{module}$$

3.3.3 Electrical Calculations

In a solar park they are used to obtain a voltage and current range according to the inverters to which they will be connected, that will subsequently convert the energy to AC. Thus, the PV modules must have the size of its strings and the number of interconnected arrays according to the technical characteristics of the inverters. This chapter follows a chronological order in the electrical calculations to determine these parameters and uses technical data from commercially available equipment to illustrate the results.

Taking the IBC PolySol 275 CS5 as the example PV module, the important data to be assumed during the development are the P_{MAX}, that shows the nominal power output of the module in watts, the U_{mpp} and I_{mpp} that indicate respectively the nominal voltage and current of the panel during loaded operation, as shown in the Table 4 .

Table 4 - IBC PolySol 275 CS5 Solar module technical characteristics.

IBC PolySol	275 CS5
STC Power P _{max} (Wp)	275
STC Nominal Voltage U _{mpp} (V)	31.8
STC Nominal Current I _{mp} (A)	8.67
STC Open Circuit Voltage U _{oc} (V)	39.0
STC Short Circuit Current I _{sc} (A)	9.23
Module Efficiency (%)	16.8
Power Tolerance (Wp)	- 0/+5
NOCT (°C)	44.1
Tempcoeff I _{sc} (% / °C)	+0.0041
Tempcoeff Voc (mV / °C)	-122
Tempcoeff P _{mpp} (% / °C)	-0.411

The U_{oc} and I_{sc} are both also important and phrase the values on which the panel output when in operation and not connected to the inverters. But these data are expressed in STC, and are generated during laboratory tests assuming an irradiation of 1000 W/m², air mass of 1.5 and PV cell temperature of 25 °C. On the field, the conditions are not constant and are subject to change every second. To predict the panel behaviour, at least on the electrical point of view, is necessary to calculate the voltage range of the panel. The V_{oc} value shows the temperature coefficient of the voltage, an determine that minus 122 millivolts is produced by the panel cell for each degree above 44.1 °C, or 122 millivolts more for each degree below. This way, the voltage range calculation can be expressed as:

$$V_{adj} = U_{oc} \frac{(T_{mod} - NOCT)(T_{coeff})}{^{\circ}C}$$

As an example, assuming $-10\text{ }^{\circ}\text{C}$ as the lowest possibly panel temperature:

$$V_{adj} = 31.8 + (-10 - 44.1)(-0.120) = 37.89\text{ V}$$

And $70\text{ }^{\circ}\text{C}$ as the highest panel temperature:

$$V_{adj} = 31.8 + (70 - 44.1)(-0.120) = 28.29\text{ V}$$

The voltage range of the IBC PolySol 275 CS5 solar panel would be between 28,29 V and 37,89 V. As with voltage, the current produced by the panels will also vary with the temperature of the modules by an additional 0.041%.

$$I_{adj} = I_{sc} \frac{(T_{mod} - NOCT)(T_{coeff})}{^{\circ}\text{C}}$$

Also assuming $-10\text{ }^{\circ}\text{C}$ as the lowest possibly panel temperature:

$$I_{adj} = 8.44 + (-10\text{ }^{\circ}\text{C} - 44.1\text{ }^{\circ}\text{C})(0.041) = 6.22\text{ A}$$

And $70\text{ }^{\circ}\text{C}$ as the highest panel temperature:

$$I_{adj} = 8.44 + (70\text{ }^{\circ}\text{C} - 44.1\text{ }^{\circ}\text{C})(0.041) = 8.96\text{ A}$$

This means that the current may vary with temperature contrary to voltage, with lower temperatures having lower current output as 6.2 A, and higher temperature having higher output as 8.96 A. After determining the panels voltage and current limits, is necessary to create the system architecture, which can be two different types of operating model based on the inverter type.

As explained in section 3.2 PHOTOVOLTAIC CELLS, in order to obtain the amount of current and voltage required by the inverters, is necessary to interconnect many PV cells into a single unit, which is termed as a PV module. These modules are then connected in series and parallel to form respectively a photovoltaic string and array. The length of the strings and the arrangement of the arrays are very important for the operation of the inverter's MPP tracking. It is mandatory that every MPP input receives the most equal amount of voltage and current as possible.

Since the solar panels output DC, is very simple to calculate and to conceive the pattern on which the modules should be interconnected. The strings are directly related with the voltage, and the number of modules connected in series dictates the total voltage output. These values should always be in conformity with the inverter electrical characteristics, as demonstrated in the Table 5.

Table 5 - String inverter Sungrow SG49K5J electrical characteristics.

Type Designation	SG49K5J
INPUT	
Max. PV input voltage	1000 V
Min. PV input voltage	200 V / 250 V
Nominal input voltage	660 V
MPP voltage range	200 – 950 V
MPP voltage range for nominal power	490 – 850 V
No. of independent MPP inputs	4
Max. number of PV strings per MPP	3
Max. PV input current	112 A (28 A / 28 A / 28 A / 28 A)
Max. current for input connector	12 A
Max. DC short-circuit current	140 A (35 A / 35 A / 35 A / 35 A)
OUTPUT	
AC output power	49.5 kVA @ 50 °C / 55 kVA @ 50 °C (settable)
Max. AC output current	80 A
Nominal AC voltage	3 / PE, 420 V / 440 V
AC voltage range	374 – 506 V
Nominal grid frequency / Grid frequency range	50 Hz / 45 – 55 Hz, 60 Hz / 55 - 65 Hz
THD	< 3% (at nominal power)
DC current injection	< 0.5% in
Power factor at nominal power / Adjustable power factor	> 0.99 / 0.8 leading – 0.8 lagging
Feed-in phases / Connection phases	3/3
EFFICIENCY	
Max. efficiency	98.9 %
Euro. efficiency	98.5 %

The SG49k5J is a 3-phase string inverter of 49.5 kVA manufactured by Sungrow. Taking its electrical characteristics as an example, the best operating point at 98.9 % of efficiency can be reached when the nominal input voltage is at 660 V. Based on this value, if the nominal voltage of each IBC PolySol panel is 31.8 V, the quantity of modules per string needed to satisfy the inverter ideal input would be:

$$V_{dc_{nominal}} = U_{mpp_{module}} \times n^{\circ} \text{ of panels}$$

$$n^{\circ} \text{ of panels} = \frac{660}{31.8} \cong 21$$

Therefore, connecting 21 modules in series would deliver the correct inverter operating voltage, achieving its best performance. However, the solar panels output is affected by several factors, for instance solar irradiance, module rating, operating temperature, soiling, changing of solar spectrum and angle of incidence. As expressed and calculated previously, the maximum voltage output of the IBC PolySol 275W CS5 panels at -10° is 37.89 V and the minimum voltage at 70°C is 28.29 V. Extending these limits to 21 panels:

$$V_{dc_{max}} = 37.89 \times 21 \quad \therefore \quad V_{dc_{max}} = 795.69 \text{ V}$$

$$V_{dc_{min}} = 28.29 \times 21 \quad \therefore \quad V_{dc_{min}} = 594.09 \text{ V}$$

That way, the maximum and minimum values produced by the series of panels under normal weather condition are within the range of the inverter, which are 1000 V for maximum and 250 V for minimum.

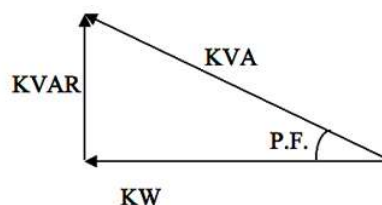
With the length of each string determined, is then necessary to calculate the quantity of strings that will be connect to the inverter input in parallel, which allows to increase the current [8] .

The SG49k5J electrical characteristics shows that these inverter model has 4 independent MPP tracking inputs, that enables to connect up to 3 strings per MPP with a maximum current of 28 A. In that way is possible to obtain the current range output of each string as follows:

$$I_{max} = 8.96 \times 3 \text{ strings} \quad \therefore \quad I_{max} = 26.88 \text{ A}$$

$$I_{min} = 6.22 \times 3 \text{ strings} \quad \therefore \quad I_{min} = 18.66 \text{ A}$$

This means that each array of 3 strings conforms to the 28 A limit of the SG49k5J. Inverters are by factory configured with a power factor of 0.99 at nominal power. At this rate the inverter output 99% of active power and 1% of reactive power, but despite the P.F. of 0.99 occurs in some situation, in almost all countries where the public grid is closely monitored and kept within a restrict range, power factor is actually configured between 0.8 and 0.9, according to the local authority [8] . Thus, converting the 49.5 kVA nominal power of the SG49k5J inverter into kilowatt:



$$P.F. = \frac{P}{S} = \frac{\text{Inverter}_{kW}}{\text{Inverter}_{kVA}}$$

$$0.9 = \frac{\text{Inverter}_{kW}}{49.5 \text{ kVA}}$$

$$Inverter_{kW} = 44.1 \text{ kW}$$

So, the maximum nominal power on which the inverter configured with a P.F. of 0.9 is able to deliver in kilowatt is 44.91 kW. Having this value, in conjunction with modules nominal power output, it's possible to know the total number of modules interconnect to each inverter.

$$P_{Inverter \text{ P.F.}} = n^{\circ} \text{ of panels} \times \text{panel power}$$

$$44.91 \text{ kW} = n^{\circ} \text{ of panels} \times 0.275 \text{ kWp}$$

$$n^{\circ} \text{ of panels} = 163 \text{ units}$$

3.4 AC-TO-DC RATIO

When designing a solar installation and selecting an inverter, it's important to consider how much DC power the array will produce and how much AC power the inverter can output, that is also known as its power rating. The ratio of the quantity and wattage of solar panels is installed to the inverter's AC power rating is called the DC-to-AC ratio. Taking a 120 kW DC array connected to a 100 kW AC inverter has a DC-to-AC ratio of 1.2. It often makes sense to oversize a solar array, such that the DC-to-AC ratio is greater than 1 [17]. In other words, adjust the number of solar panels so the DC capacity divided by the AC output is greater than one. This allows for a greater energy harvest when production is below the inverter's rating, which it is typically for most of the days. The idea is for the inverter to run at full power when energy is the most valuable. However, oversizing only improves project economics up to a certain point at which energy losses and costs outweigh the economic benefit from the additional modules [17]. The Figure 21 shows the AC-to-DC ratio in relation with the power output gain factor.

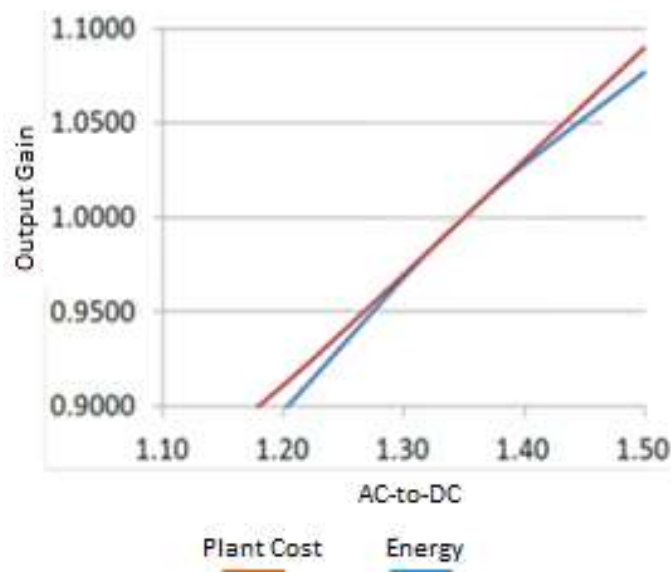


Figure 21 - AC-to-DC ratio vs. Output gain.

The optimal DC-to-AC ratio depended on the design goal. For example, regardless of site conditions, sizing a system to maximize specific yield allows for an ideal DC-to-AC ratio at or slightly below 1.2. However, sizing a system to target the best financial output could lead to higher DC-to-AC ratios, between 1.3 and 1.6. This means that an inverter that could manage a DC-to-AC ratio up to 1.6 would be the most ideal, because then the project could achieve the best economic benefit of increasing the DC capacity, without adding to the fixed cost of the system. The Figure 22 shows the energy production gain due to an AC-to-DC ratio higher than 1.

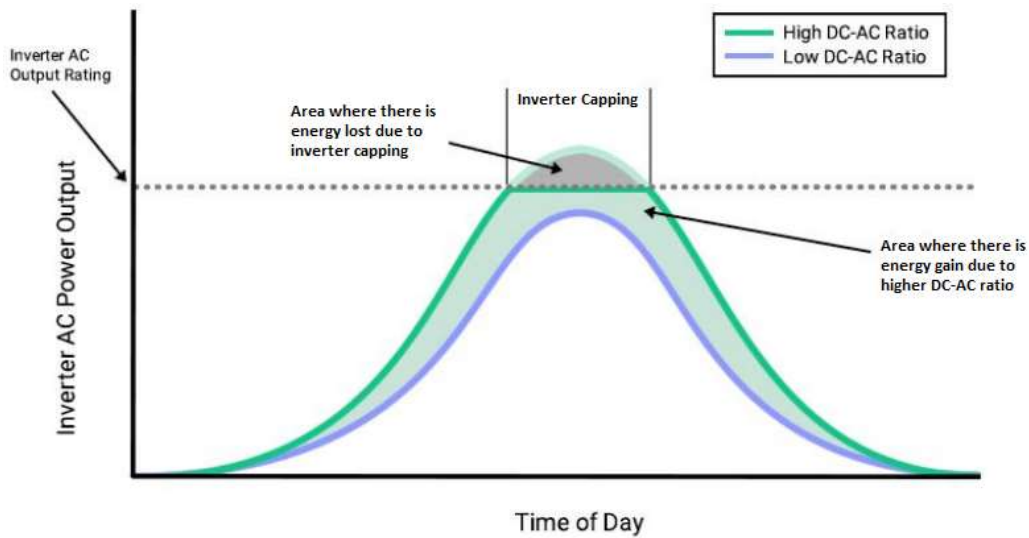


Figure 22 - Energy gain due to higher AC-to-DC ratio [17] .

One way to determine the ratio is analysing the maximum capacity of the inverter. Usually, the equipment is already developed with a number of inputs vs. output capacity to enable a specific DC-to-AC ratio.

The inverter SG49K5J has 4 MPP tracking analysers, which are able to care up to 3 arrays. This means that 12 arrays can be connected to the inverter:

$$n^{\circ} \text{ of panels} = \text{panels per string} \times \text{arrays per MPP} \times n^{\circ} \text{ of MPP inputs}$$

$$n^{\circ} \text{ of panels} = 21 \times 3 \times 4$$

$$n^{\circ} \text{ of panels} = 252 \text{ units}$$

Obtaining the nominal power output of the panels:

$$P_{nominal_{total}} = n^{\circ} \text{ of panels} \times P_{nominal_{panel}}$$

$$P_{nominal_{total}} = 252 \times 0.275 \text{ kWp}$$

$$P_{nominal_{total}} = 69.3 \text{ kWp}$$

With this, the DC-to-AC ratio can be obtained as:

$$ratio = \frac{DC_{power}}{AC_{power}} = \frac{P_{nominal_{total}}}{Inverter_{kW}}$$

$$ratio = \frac{69.3 \text{ kW}}{44.91 \text{ kW}} = 1.54$$

With a ratio of 1.54 the panels can produce 54% more than the inverter capacity, which means that the system is able to operate in full power during more hours and days than those previously forecasted. While that is good on one hand, on the other it is bad from the point of view of the performance analysis, which will be greatly altered due to the power limitation in the inverter. This production capping and how it impacts the power plant performance is outlined in the chapter 4.7 INVERTERS CAPPING. The Table 6 outline how the inputs of each inverter would be after adopting the 1.54 DC-to-AC ratio and according to the voltage and current values obtained in the previous chapter.

Table 6 - Inverter SG49K5J MPP inputs overview according to calculated values.

INPUT	MPP 1	MPP 2	MPP 3	MPP 4
Strings	1, 2 and 3	4, 5 and 6	7, 8 and 9	10, 11 and 12
n° of panels per string	21	21	21	21
n° of strings per MPP	3	3	3	3
Nom. Current	25.32 A	25.32 A	25.32 A	25.32 A
Nom. Voltage	659.40 V	659.40 V	659.40 V	659.40 V
Max. Current	26.88 A	26.88 A	26.88 A	26.88 A
Max. Voltage	795.69 V	795.69 V	795.69 V	795.69 V

3.5 MODULES MOUNTING STRUCTURE

The modules mounting structure is a metal frame that holds all panels aligned to the desired irradiance angle of incidence. Recent power plant installations have adopted various MMS designs, which include structures made of galvanized iron as well as aluminium. Some also combine both materials in order to reduce costs and increase the service lifetime, thereby enhancing it from corrosion. These structures can be divided in two main types, the statics and the trackers.

The statics are the most common used and place the panels' arrays in one fixed angle that will not change. Depending on the number of the panels placed in each array and the soil characteristics, the structure can be of a single pole or double pole, as showed in the Figure 23 .

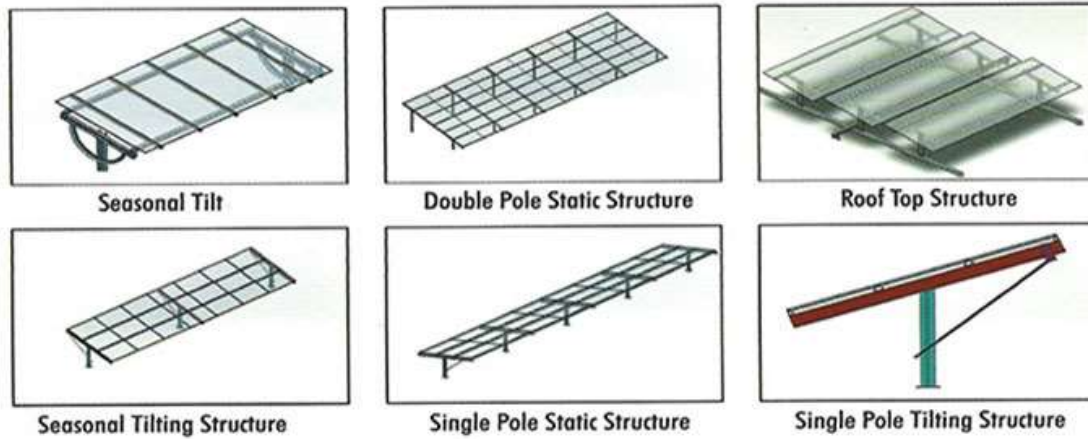


Figure 23 - Types of static mounting structure.

Source: <http://www.gangesintl.com/solar-structure-design.html>

In addition, the statics can also present a seasonal tilt option that allow the structure to change its Azimuth angle during periods of the year. This solution is only indicated for small power plants, since it is necessary to manually correct the panels' angle.

The trackers are motorized mechanical tracking systems that orient the solar panels towards the sun. A tracker optimizes the angle at which panels receive solar radiation thereby maximizing electricity production of a solar plant [10]. There are primarily two types of solar tracking systems, namely single-axis and dual-axis, as shown in the Figure 24 .

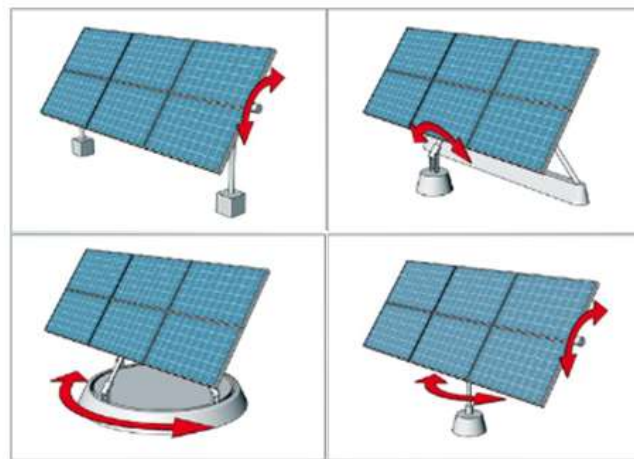


Figure 24 - Single and dual-axis tracker mounting structure.

A single-axis tracker moves the solar panels on one axis of movement, which allows the panels to arc from east to west and track the sun as it moves through the sky. A dual-axis tracker allows panel movement on two axes, aligned for both north-south and east-west. This kind of a system is designed to further maximize solar energy collection throughout the year as it not only tracks the daily east-west motion of the sun but also adjusts for seasonal variation in the path of the sun [6]. Despite increasing the efficiency of the power plant, the tracker system boosts the construction cost, naturally

increases maintenance costs, and also can cause shading problems during periods of the year.

Several factors must be considered when determining the use of trackers. Some of these include the solar technology being used, the amount of direct solar irradiation, feed-in tariffs in the region where the system is deployed, and the cost to install and maintain the trackers [10] .

3.6 INVERTERS

An inverter basic function is to convert the direct current outputted by the PV panels into alternating current, which is the standard used by all commercial appliances [12]. Its technologies have advanced significantly, such that in addition to converting DC to AC, they provide a number of other capabilities and services to ensure that the inverter can operate at an optimal performance level, such as data monitoring, advanced utility controls, applications and system design engineering.

A photovoltaic system is only rarely operated under constant ambient conditions because the sun's radiation values are subject to changes related to the weather and the time of day. Since the solar inverter is responsible for managing the output of the entire PV system, it must react dynamically to these changes. This is the only way to constantly always achieve the best possible energy yield from the solar modules. The dynamic reaction of the inverter is significantly determined by the Maximum Power Point tracking, as shown in the Figure 25.

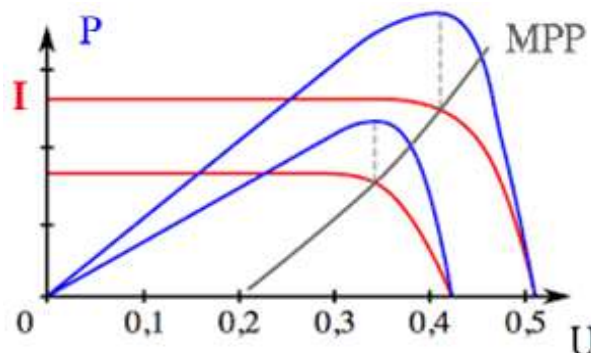


Figure 25 - MPP tracking - PV generator achieves its maximum performance.

This function is defined as the process of continually determining the operating point at which the PV generator achieves its maximum performance [14] . This means that the inverter is able to play with the inputted voltage and current to output the maximum power possible at that instant moment. However, for the MPP tracking work properly, all feed in cables connected to the inverter must have the same voltage range.

Solar parks mainly use Central or Strings inverters. They nothing differ from each other in the mode of operation but are very differently applied in the system architecture.

The Central inverter will centralize all DC power produced by the panels into one place. They are physically much larger than String inverters, use longer wires and can convert more power per unit. The equipment doesn't have enough inputs to connect thousands of DC cables coming from the panels. To solve this issue DC Combiner Boxes (DCCB) are used to decrease the amount of cables that will feed into the Central inverter. These combiner boxes can be simple cable splitters or intelligent monitoring systems, that will analyse the voltage and the current of the panels connected to it, as shown in the Figure 26 .

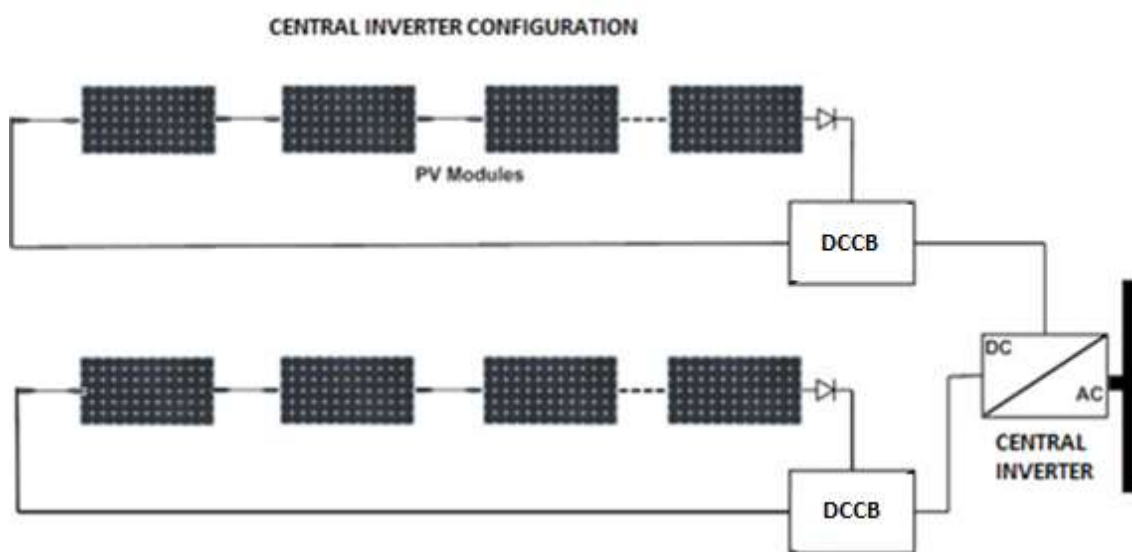


Figure 26 - Central inverter interconnection with DC combiner boxes [16] .

Central inverters are much larger than string inverters. Sizes may range from 125 kW to 2.5 MW, with even the smallest variants are much larger than the biggest string inverters. Weights can reach many tons at the high end. The 2.5 MW variants can be ordered with or without transformers. Whereas string inverters are mainstays of both commercial and residential solar projects, central inverters are exclusive to utility-scale applications. Common environments for central inverter utilization are industrial facilities, large buildings and field arrays.

String inverters are a distributed architecture for solar plants. They are small, and each unit converts a much smaller amount of power than a central inverter. There's an inverter sited at each row of panels, so the input strings leading from the panels to the inverters can be much shorter. When using string inverters, there are multiple smaller inverters for several strings, so the DC power from a few strings runs directly into a string inverter rather than a combiner box and is converted to AC, as show in the Figure 27.

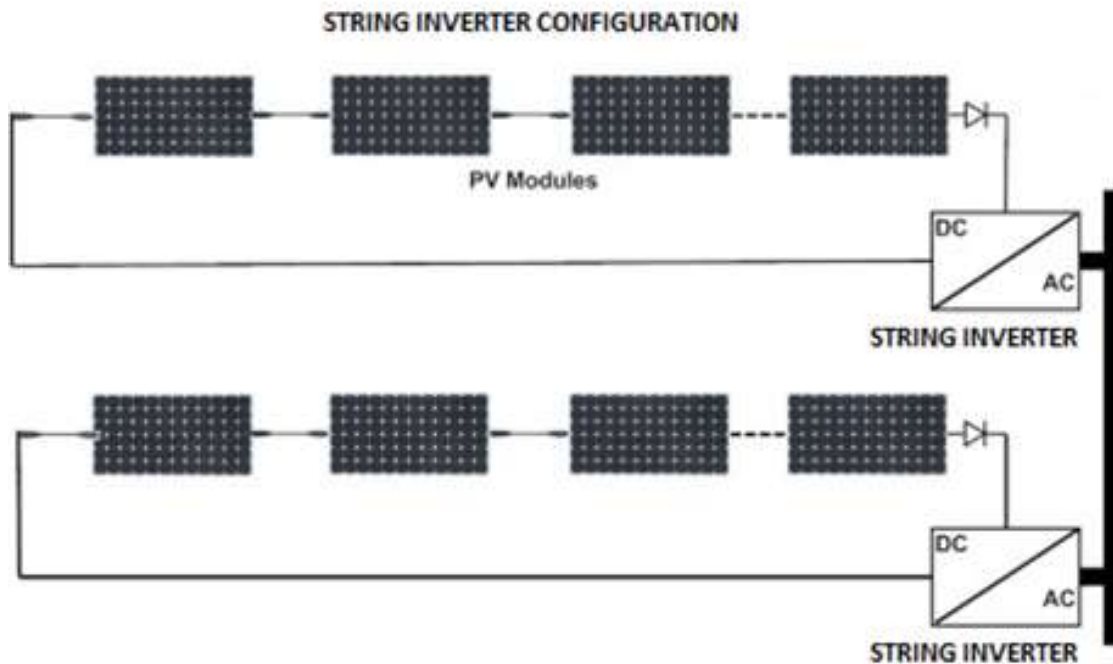


Figure 27 - String inverter interconnection schematic [16] .

From the perspective of a plant owner, there are three major areas string inverters excel. The acquisition cost per MW is much less than central inverters. If an inverter faults, the generation loss is significantly smaller than a central inverter. Because 33 string inverters are equal to one central inverter, losing one string inverter (vs. one central inverter) is less impactful to revenue. If you lose one string inverter, it is not an emergency, but if you lose one central inverter, it's all hands-on deck to get it repaired. String inverters produce common, off-the-shelf 480 V AC, whereas central inverter output is more uncommon 315 V AC [16] . Often the transformer and other infrastructure is more readily available, and often a little less expensive.

With string inverters there's no need of maintenance contract with manufacturer. The owner does not have to pay to ensure an availability, because it is known that it will always be fulfilled. Those are big costs within the life of the installation. Furthermore, no preventive maintenance is mandatory, the only operation to be done is cleaning the fans with compressed air when needed. Even if some maintenance is performed, the time of technical stop is lower with string inverters, because with central inverters is necessary to stop all the installation during at least some hours.

The decision on whether to use a central inverter or string inverters needs to be made on a case-by-case basis taking into account primarily the total system cost (including space constraints) and total energy production. Table 7 shows the positive and negative characteristics of each inverter type.

Table 7 - Central vs. string inverter characteristics.

Inverter Type	Advantageous	Disadvantageous
Central Inverters	<ul style="list-style-type: none"> • Lower DC watt unit cost. • Fewer component connections. • Optimal for large systems where production is consistent across arrays. • Proven field reliability. 	<ul style="list-style-type: none"> • Higher installation cost (e.g., inverter pad work). • Higher DC wiring and combiner costs. • Larger inverter pad footprint • Specialized manpower maintenance.
String Inverters	<ul style="list-style-type: none"> • Lower balance of systems costs. • Lower ongoing maintenance costs (e.g., no fans or air filters). • Simpler design and modularity; ideal for limited inverter pad spaces. • Modularity of string inverters is better for systems with different array angles and/or orientations. • Fewer arrays are impacted with one inverter failure. 	<ul style="list-style-type: none"> • Higher DC watt unit cost. • More inverter connections. • Requires more distributed space to mount inverters.

3.7 TRANSFORMER

The transformer connects the PV power plant into the grid, enabling the generated electricity to be transmitted to the areas of consumption. As the conditions of solar power plants can vary greatly and become severe, these transformers must withstand high temperatures due to the harsh climate conditions [21] .

Sizing these transformers is a crucial factor when planning a PV plant. A very large rated power can lead to instability and economic problems disadvantages, while very small transformers may not exploit the full capacity of the plant. These transformers are special design for three-phase and single-phase, with multiple windings that allows the interconnection of several AC combiner boxes or multiple small transformers.

The vast majority of string inverters produce at a standard rate of 480 V, while the central inverters can produce from 315 V to 600 V. Therefore, Medium Power

Transformers are used to increase the voltage level of the generated electricity to usually about 6 kV or 30 kV. The precise requirements vary from device to device, from site to site and from country to country, because the transmission lines voltage rate is not standard, and each country has its own. That is why each transformer must be - almost as unique as a fingerprint when it comes to voltage, power, climate efficiency, network topology, permissible noise level, and other factors [21] .

Basically, to calculate the capacity of the transformer in VA it is necessary to sum the total capacity of inverters installed in the solar plant. For instance, a plant with 11 inverters of 55 kVA each, the maximum total output is 605 kVA. Thus, it can be determined that a 605 kVA transformer is required or two transformers, one of 330 kVA and other of 275 kVA is required. Possibly the closest models of transformers for such values available on the market would be respectively 650 kVA, 350 kVA and 300 kVA. The idea of having two transformers enables the plant to keep the energy production even if one of the transformers get damage. The Figure 28 shows two Smartgrid central inverters with 2 independent transformers.



Figure 28 - Transformer station next to Smartgrid central inverters.

The transformers for PV power plants are generally delivered as a ready system, with the transformer inside a container that simply require the construction of a concrete base and the connection of the cables.

3.8 CABLE LOSSES

The PV power plants can have thousands of meters of different cables that transport the energy from the modules to the inverters, and from the inverters to the transformers. The power losses related with these cables are one of the most important aspects of the energy production system due to its natural ohmic resistance. Each cable

needs to be measure, and based on its electrical characteristics, it is necessary to calculate the power losses. The cables have an ohmic resistance that causes a voltage drop according to Ohm's law:

$$U = R \times I$$

The resistance R of the cable depends on the cable length, the longer the cable, the more the resistance is, the cable cross-section area, the larger this area, the smaller the resistance is, and the material used and its specific resistance - copper or aluminium. At higher temperatures, the resistance of the material increases and the conductivity decreases. The calculation that determines all losses due to cabling is called Mass Calculation [18]. To accomplish this, it is necessary to know the length of all cable types, one by one, and then multiply each length by its resistance. The power loss P at an ohmic resistance is:

$$P = U \times I = R \times I^2$$

Taking a string with 21 IBC PolySol 275 W CS5 modules, and assuming an ideal 1% of power loss per string:

$$P_{string} = n^{\circ} \text{ of panels} \times P_{nominal_{panel}} \times Losses$$

$$P_{string} = 21 \times 275 \text{ Wp} \times 1\% = 57.75 \text{ Wp}$$

At a current of 8.44 Ampere, the maximal cable resistance should be:

$$P = R \times I^2$$

$$57.57 = R \times 8.44^2 = 0.811 \Omega$$

The ohmic resistance of the cable is calculated according to the formula:

$$R = \frac{\rho L}{A}$$

where:

A - is the cable cross-section

ρ - is the resistivity of conductor, i.e cooper $1.68 \times 10^{-8} \Omega \cdot m$ at $20^{\circ}C$

L - is the cable length

R - is the cable resistance

Rewriting the expression to obtain the cable cross-section of a cable with 100m:

$$A = \frac{\rho L}{R}$$

$$A = \frac{1.68 \times 10^{-8} \times 100}{0.811} = 2.07 \text{ mm}^2$$

In this case, an industry standard cable cross-section of 2.5 mm^2 is enough to maintain the losses below 1%.

3.9 YIELD FORECAST

The yield forecast is the determination of the power plant production capacity and its efficiency. It is the first step in the engineering process of developing a solar park and is based on the geographic location of the land where intends to install the power plant.

The process to obtain the yield forecast deals with a lot of different stages, calculations and meteorological data from the past years to predict the possible production. These data, usually the hourly average of the ambient temperature and irradiance incidence from the past 10 to 20 years, are the only values that do not change during the many stages of the calculation. It is initiated from the annual radiation available at the site where the plant will be built, then each existing loss is debited, until the actual energy that can be produced is obtained.

In addition to determining the possible capacity of the plant, the simulation informs one of the most important variables for evaluating the efficiency of a PV plant, the Performance Ratio. The PR is stated as percent and describes the relationship between the actual and theoretical energy outputs of the PV plant [19]. It thus shows the proportion of the energy that is available for export to the grid after deduction of energy loss and of energy consumption for operation. From the contractual point of view, the company that develops the plant uses the PR as one of the key drivers in selling the asset to the customer. The details in the calculation of the PR are detailed in section 3.10 PERFORMANCE RATIO.

To perform the yield forecast calculation is used the *PVSyst*, which is a PC software package for the study, sizing and data analysis of complete PV systems. The program outputs the Loss Diagram, which is a schematic draw that illustrate every possible loss over the year in a photovoltaic energy system. It follows a specific order and starts detailing the losses due to shading and soiling, as shown in the Figure 29.

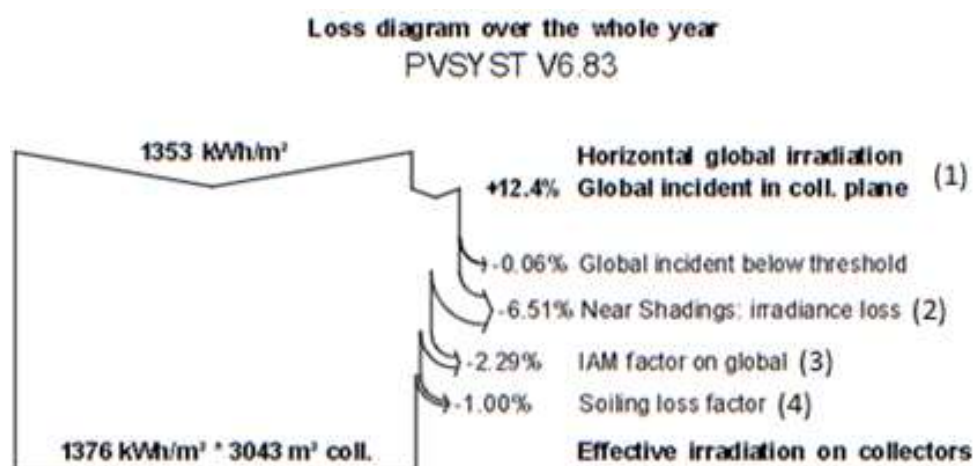


Figure 29 - Detailing of soiling and shading losses in the PVSyst Loss Diagram – Part I

The first reductions are related specifically with the behaviour of the solar panel together with the azimuth angles that were chosen during the simulation. For each location on the globe a different azimuth angle is used to increase radiance uptake. It also take in consideration any possible shading object around, that may partially or completely obstruct the panels. To obtain the shading debit during the simulation is necessary to upload a 3D plan map in the software, that will demonstrate every building, tree or tall objects in the surrounding area. The higher the percentage, the greater the shading. Shading is a very difficult variable to predict because many factors can change around the place where the solar plant is installed. As plants have a useful life of approximately 20 years, this is a very long period to stipulate how demographic growth will be in the region, which may result in the construction of new buildings, in addition to the natural growth of trees and so on. Added to that, are the IAM and the Soiling factor. The IAM is based on the panel angle in relation with the sun path during different periods of the year. The Soiling factor is also crucial for the panel performance, especially in areas next to arid regions or deserts [11]. Dust clouds and airborne sediments may accumulate over the modules, especially affecting the current produced by the PV module, while the voltage remains the same. Following the diagram order, the next reductions are called Array Nominal Energy, and summarize the losses related with the DC energy produced by the solar panels, as shown in the Figure 30 .

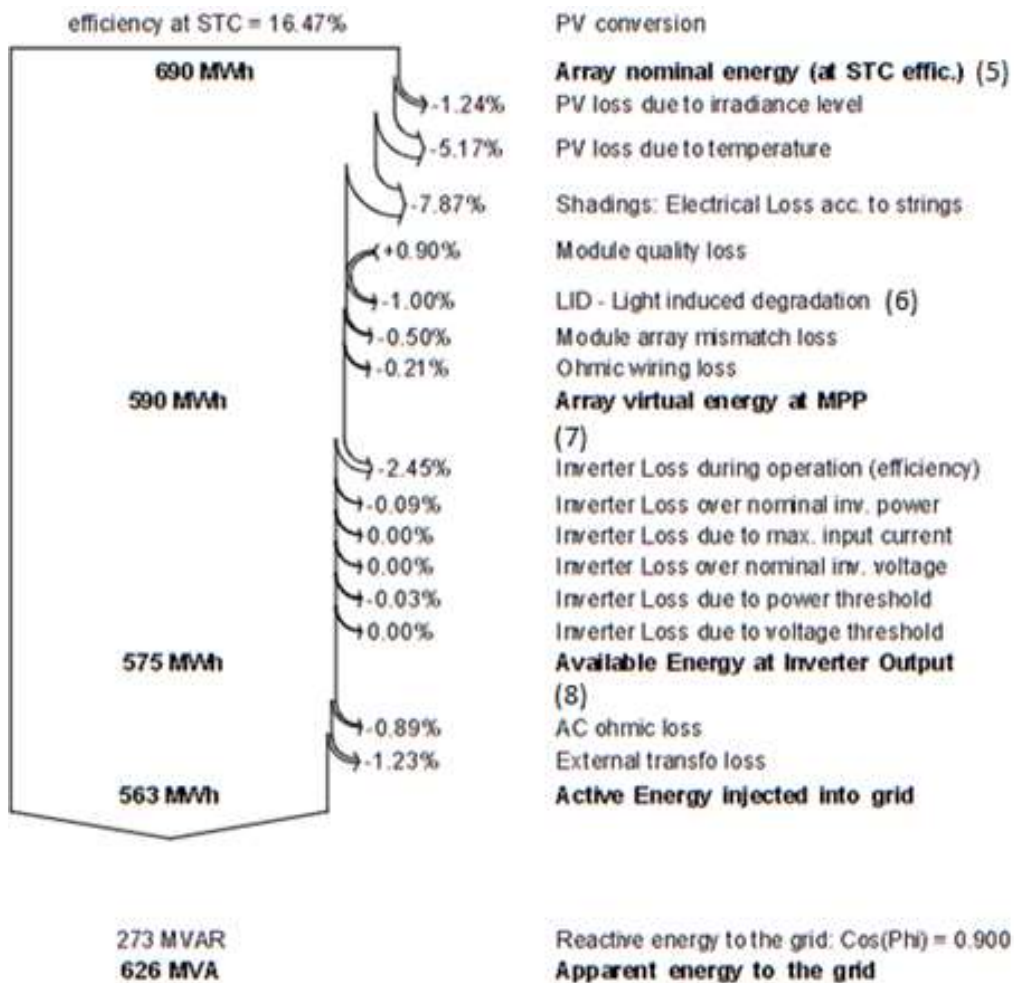


Figure 30 - Detailing of losses in the PVsyst Diagram - Part II

The DC produced by the PV modules can be affected by the cell temperature, irradiance level, shadows caused by other modules, electrical resistance in the interconnection wires and the Light Induced Degradation, which only occur with Crystalline modules and is a loss of performances arising in the very first hours of exposition to the sun. The LID is related to the quality of the wafer manufacturing, is informed by the producer and may be in the order of 1% to 3% [12]. It happens due to traces of Oxygen included in the molten Silicon during the Czochralski process.

Posteriorly the losses in the inverters are accounted for. The rated values are defined by the manufacturer and matches with the chosen voltage and current values that the system will operate. The AC energy outputted is also altered by the electrical resistance of the wires and by the Iron Losses, caused by the alternating flux in the core of the transformer.

The Loss Diagram is very important from a contractual point of view and playing with input values is a frequent occurrence among developers. These losses are intertwined with the performance of the solar plant, and it is interesting having the results of the report exaggerated, so the system performance is always higher than the one sold to the customer. Having low KPIs often means paying a fine by the project developer [13].

3.10 PERFORMANCE RATIO

The performance ratio (PR) calculates the efficiency of a photovoltaic power plant [15]. It uses measurements made on site of module and ambient temperature, solar irradiance and energy exported to the grid. Therefore, it is possible to estimate the theoretical energy production of the modules, based on the real weather data. The PR relates the theoretical energy with the exported energy. This maximum value is one, however it does not achieve this mark, because of the losses of all system. Losses can be found on PV module, cable, inverter, transformer, hence the typical efficiency is more than 75% for good facilities [15]. The PR is an important indicator of productivity and could be compared between other solar parks in the whole world, independent from the weather and location factor. Normally is an index utilized in contracts between client and EPC companies. Due to the energy production is not well predicted and could vary a lot depending on the weather condition, the PR is one of the most critical factors of PV power plant quality.

The calculation starts as soon as the power plant begins its operation. The data is collected by the sensors in field and transmitted to a monitoring portal that can be remotely accessed. The PR is determined every day and for all facilities in operation. The data is exported is the average of a five minutes interval.

The PR calculation according to IEC standard 61724-1 [19] is expressed as:

$$PR = \frac{Y_f}{Y_r} = \frac{\frac{E_{feed-in}}{P_0}}{\frac{H_{POA} C_k}{G_{STC}}} = \frac{E_{specific}}{H_{specific} C_k}$$

where:

$E_{feed-in}$ is the energy fed into the grid

$E_{specific}$ is the specific energy yield

P_0 is the rated DC power of PV array

H_{POA} is the plane-of-array irradiation

$H_{specific}$ is the specific irradiation sum (time integral of irradiance)

G_{STC} is the irradiance under STC conditions (1000 W/m²)

C_k is the temperature correction factor

The C_k is the temperature correction factor and will correct the calculation according to PV module specification and temperature onsite. This correction allows for a more reliable PR, but there are cases where it is set aside for contractual reasons, because removing this compensation the result of the PR tends to be higher. The temperature correction factor can be expressed as:

$$C_k = 1 + \gamma (T_{mod} - T_{ref})$$

where:

γ is the relative temperature coefficient at maximum performance level

T_{mod} is the PV module temperature

T_{ref} is the reference temperature (the same used in the Yield Forecast simulation).

While the modules temperature data are reported by monitoring system of the power plant every 5 min, the reference temperature values change only per month, and are based in the accumulated real weather data from 20 years.

According to the IEC standard 61724-1 [19], when the irradiation values are below 20 W/m², the calculation of PR should be discarded. Many companies extend this value up to 60 W/m² depending on the type of solar plant and location. This is due to the low efficiency of solar modules under such low radiation conditions, which usually occur during dawn and dusk. Each module has its own specification, but usually the efficiency drops around 2% when the radiation is less than 100 W/m². This also occurs with the inverters, as the panels do not produce enough power for the device to enter in the nominal rated operating range.

CASE STUDY

4 CASE STUDY

The development and operation of a PV power plant can diverse a lot due to the geographic position, production capacity desired, financial investment available, size of useful plant terrain, grid connection capacity and local laws for energy exploration. Based on the fundamental concepts previously outlined in this document, this chapter analyses different conditions during the development and operation of power plants that can directly affect the energy production and consequently the Performance Ratio.

4.1 RAMMING AND PULL-OUT TEST

The Module Mounting Structure, thoroughly addressed in chapter 3.5, is responsible for holding and positioning the solar panels on the correct arrangement and angle defined by the Yield Forecast. The beginning of the construction of the structure is marked by the realization of the *Ramming and Pull-out Test*, which analyses the soil characteristics and enables the determination of the best option between cost and structural resistance, as shown in the Figure 31 .



Figure 31 - Ramming and Pull-out Test

The modules have a considerable flat area, which can be highly resistant to winds and snow precipitation. To avoid the structure from moving or sinking due to the modules weight, snow or wind, a *Ramming and Pull-out Test* should be performed on the local soil. These tests show the vertical and lateral resistance of the soil when removing poles on different locations of the terrain, and allows to determine what depth the poles should be buried. In some situations when the soil is very unstable, concrete bases are added to the posts to improve their resistance. Since the structure is designed to endure for at least 25 years, it is also essential to analyse the soil corrosivity. This test also reports the soil chemical characteristics and indicate the potential corrosion in the galvanized steel poles. After determining the power plant terrain aspects, the engineers are able to choose the best structure design that match with the panels mounting arrangement and the lower cost.

In a situation where the terrain conditions are not favourable for installing the posts directly into the ground, concrete is commonly added at the base to increase its contact area and strength.

But despite all these tricks to stabilize the MMS, there are situations that may evade the rule. For instance, in countries where rainfall is higher, soil runoff and displacement occur both on the surface and in deeper layers. This can cause the supports to weaken, causing the posts to sink into the ground. When this happens, the modules naturally move with the structure, and often have their irradiance angle of incidence changed, as shown in the Figure 32 .



Figure 32 - Modules Mounting Structure sinking due to soil movement.

When this event occurs, the production of the panels eventually decreases compared to what was previously stipulated in the Yield Forecast. Thus, the PR of the power plant decreases, as the panels are no longer at their optimum angle. It is impossible to determine how much the PR is affected without recalculating the Yield Forecast and taking into account the new angle of the panels hit by the sinking.

This type of problem is considered serious because it implies the shutdown of part of the solar plant to correct the structure, which must be completely dismantled and have the soil of the site thoroughly analysed. The action to be taken to solve the problem must be considered on a case-by-case basis, as it is often less expensive to maintain the incorrect angle of the modules and create devices to strengthen the structure, than stopping part of the plant to rebuild the affected section.

4.2 HOT SPOT HEATING

Hot spots are high temperature areas that can significantly affect solar panel efficiency during power generation. They are rarely stable and generally intensify to full failure of the panel in terms of production and electrical insulation. There are multiple factors that can generate hot spots, that can be divided in functional or operational.

Functional hot spots happen due to manufacturing problems. Cell incompatibility is one these problems and occurs when cells with different characteristics are connected in series and occur due to difference in the quality of materials used in module manufacturing. Cellular damage is also an issue that can occur during the production process. The silicon cell undergoes various mechanical procedures during its manufacture, handling and transportation. These problems often appear in the module manufacturing process, so using a supplier that meets quality requirements is critical to the proper functioning of the solar system.

Operating reasons for hot spots are related to the design and operation of the solar generator unit, and may include partial shading, connecting different types of modules in series and abnormal mechanical pressures on the panels, which may occur with repeated snowfall over the years.

Shading should be avoided as much as possible for greater durability and production for the system. When cells in a module are partially shaded, the result is an increase in temperature in shaded cells that will degrade the panel, and in extreme cases may render the panel unusable. Connecting different types of modules is a problem similar to cell incompatibility, which occurs when cells with different characteristics are connected in series. However, in this case, there is the connection of some different modules (of different brands or power), which can cause damage to the whole system. The panels may also have been dirty due to dust, leaves and other contaminants during use. The generating unit should also identify situations that require cleaning whose frequency is strongly dependent on the climate around the unit.

Hot spots are initially identified through the MPP tracking of the inverters, which enables the analysis of the production of each array. Since all strings of these arrays have the same arrangement and size, the output is nearly equal. When an array starts to show a low throughput compared to the others, a module-by-module analyse using a thermal camera, as shown in the Figure 33, may be necessary to identify the defective module.

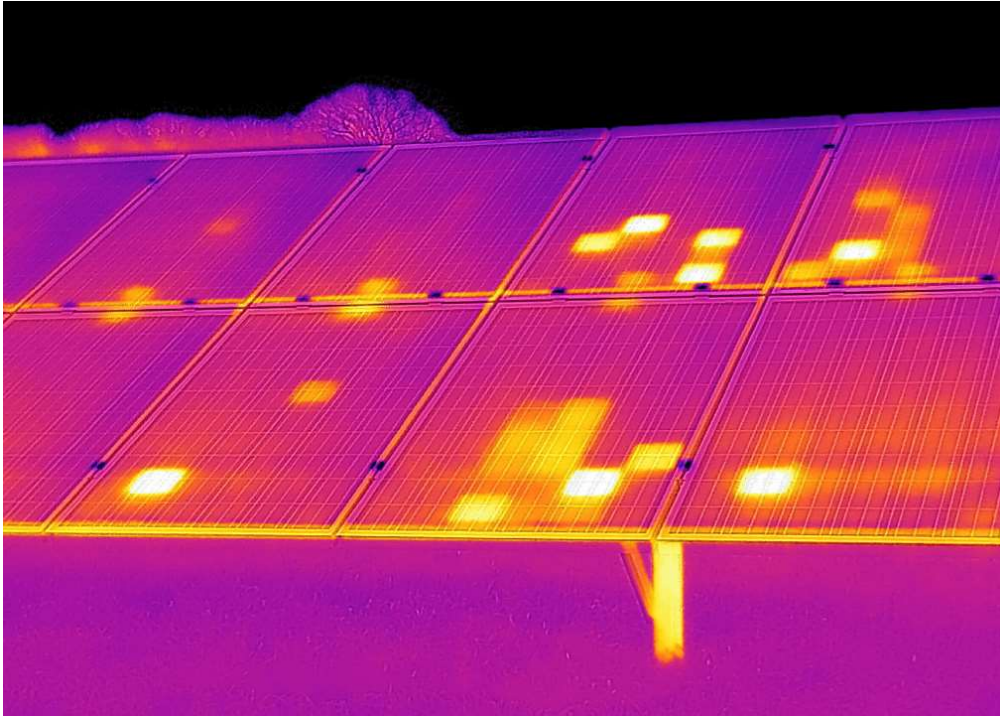


Figure 33 - Thermal camera analysis to identify Hot Spots.

When the hot spots occur in only a few cells scattered throughout the modules, the string production is very little affected due to the bypass diode, which allows the current to flow unobstructed. When this situation happens, the impact caused by hot spots in the power output is very small compared to the total production of the string, which consequently is not noticeable in PR calculation. But hot spots are phenomena that tend to increase over time, and eventually affect adjacent cells with the high temperature and the overload in the diodes.

Thus, when a set of cells are eventually damaged, and together they result in a power drop similar to, for instance, three entire modules or 825 W, then the PR starts to fall by 1% in a 69.3 kW DC capacity installation with 275 W modules.

4.3 SHADING

A photovoltaic plant can contain several thousand of modules. They can be arranged in many ways throughout the plant, in order to maximize the total area covered with modules. The larger the area covered by panels the better, but this means that possibly some areas may be affected by shadow caused by objects adjacent to the site, such as trees and buildings, as shown in the Figure 34.



Figure 34 - Trees outside the power plant terrain causing shadow on the modules.

Under normal unshaded operation, each cell in the module will operate in forward bias. When a typical module is exposed to shading conditions, regardless of module orientation, complete rows of cells may be partially or fully shaded. This condition creates a mismatch in current between cells, and shaded cells may become reverse biased. Left unprotected, this reverse bias condition could create cell or module damage due to the hotspot heating effect [16]. Bypass diodes used in the modules will limit current in reverse bias conditions and will therefore protect the module against hotspot heating. Only a small amount of shading is enough to activate the bypass diode and isolate the illuminated cells from the rest of the module. This reduces the module's power output disproportionately and annual energy loss due to shading will be greater than simply the loss due to the physical shading event.

Shading is a phenomenon that is taken into account in the Yield Forecast calculation. And the PR of the solar plant already reflects the losses due to this situation. But what often happens is the change over the years of the land surrounding the plant. Trees can grow, further increasing the shadows previously taken into consideration, and also houses and building can be built, which ultimately creates shadows that had not been previously stipulated. When this occurs, the PR is greatly affected, being proportional to the number of modules that are shaded.

Figure 35 shows the result of shading in part of the PV modules. It is possible to notice the AC power of some inverters with a low production during the morning in comparison with others.

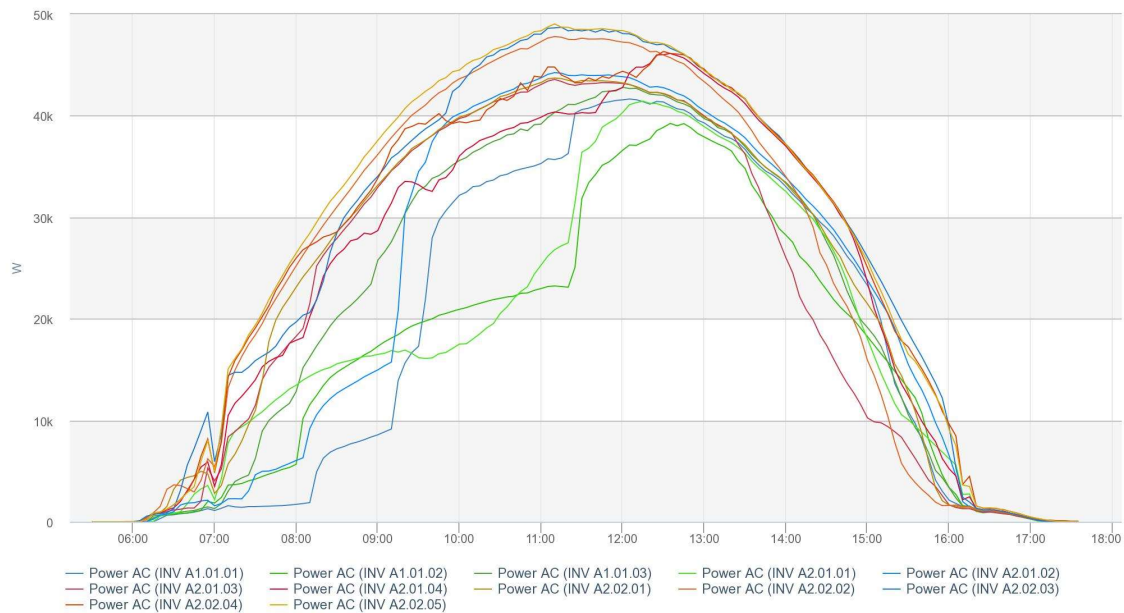


Figure 35 - Impact in the inverter's energy production due to shading.

In many cases, building solar plants in remote regions becomes a good option due to the low likelihood of changes around the plant. What turns out to be the opposite in heavily populated regions.

4.4 MODULES INTERCONNECTION MISMATCH

The interconnection of the modules is very important for the operation of the inverters and the MPP tracking that needs the voltage and the current of all arrays producing at same range. In addition, besides that, the way these modules are interconnected also greatly influences the efficiency of the power plant during operation.

The row-to-row shading is an event that typically occurs during dawn or dusk, at low irradiation conditions, as shown in the Figure 36 .

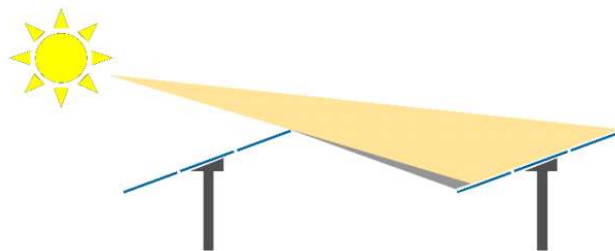


Figure 36 - Row-to-row shading

The modules situated in the highest part of the MMS can produce a shade in the lower modules of the MMS right behind it. This shading may occur in the entire solar

park and in different periods of the year. Therefore, during the plant development this condition should be taken into account to avoid the modules located at the bottom of the MMS, which can receive the row-to-row shading, from being interconnected with the modules at the top, which do not suffer from this kind of shading. This would not allow entire arrays to have a power bottleneck due to a few modules that might be in the shadow.

However, even trying to avoid mixing upper and lower modules, there are situations where there are not enough modules to be connected in a straight line, to keep the same MMS height. To resolve this problem or decrease the influence of shading in the energy production, the modules interconnection plan should adopt patterns according to these shades, which will inevitably occur in any solar park. These patterns can be classified in 3 types: *inline*, *C* and *S*.

The inline interconnections are those in which panels of the same string are always connected forming a straight line. The strings that are at the bottom of the row are the ones that are most prone to row-to-row shading. Strings connected in parallel to a single MPP tracking should always keep the same height. As shown in the Figure 37, strings in higher 4th position should only be connected to other strings that are also in the 4th row.

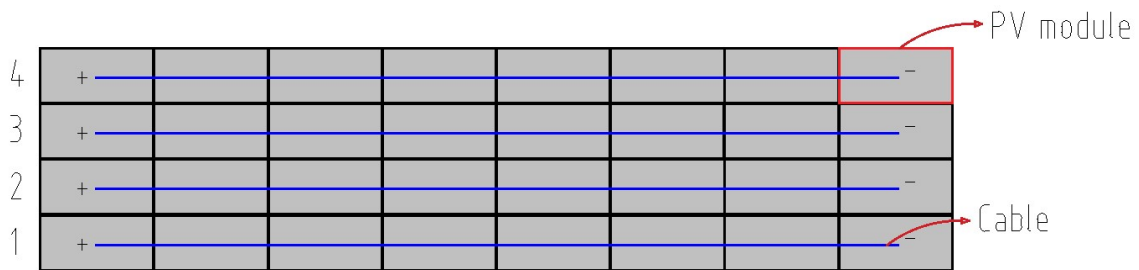


Figure 37 - Strings with inline interconnection pattern.

The *C* type interconnections are very similar to inline and connect the panels in a straight line, but also allows the joining of other directly adjacent panels, as demonstrated in the Figure 38. As with the inline, the strings in *C* pattern that are connected in parallel to a single MPP tracking should keep the same height to avoid current mismatch.

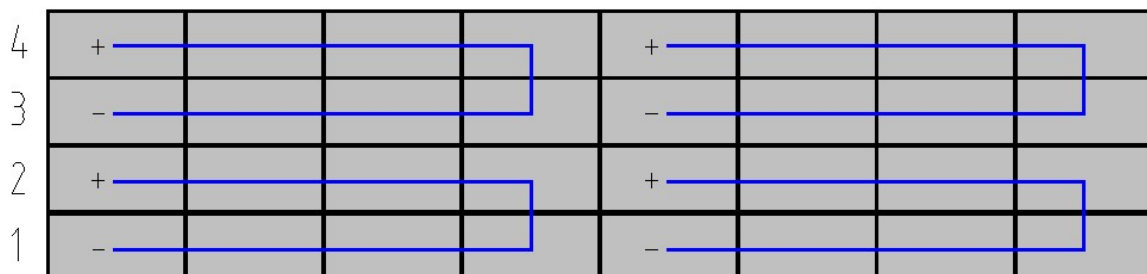


Figure 38 - String with C interconnection pattern.

The incorrect C type interconnection demonstrated in the Figure 39 should always be avoided.

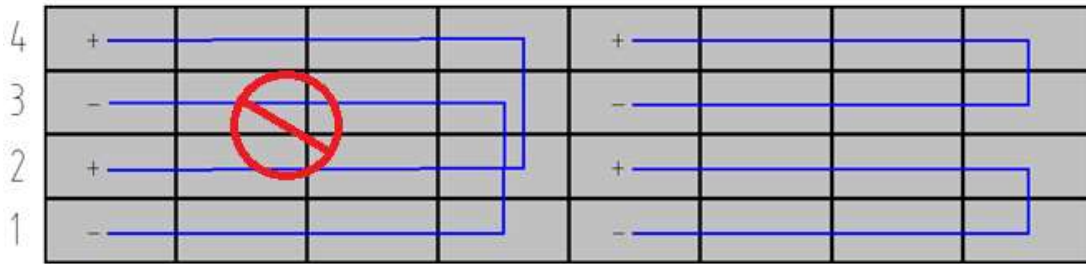


Figure 39 - Incorrect form to interconnect C types.

The type S is also a very common interconnection method and is widely used at the end of the MMS, where usually just a few panels are mounted and there is no possibility to employ inline or C types, as shown in the Figure 40.

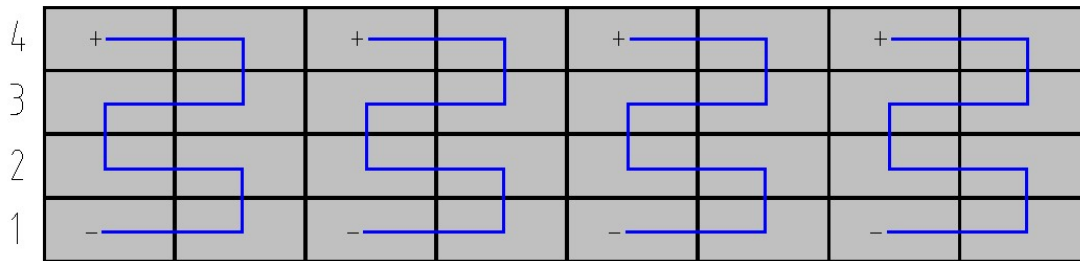


Figure 40 - Strings with S interconnection pattern.

Despite the three standard types of interconnection, it usually occurs that a structure containing a given number of panels is not sufficient to create a complete string of, for example, 8 panels. When this occurs, it is necessary to create a *Jump*. This gimmick should be avoided whenever possible, as it can add problems related to row-to-row shading of different mounting structures, besides entails a considerable increase in the length of the string cables, since the cabling must cross from one structure to another through trenches. Even in these situations, an interconnection type must be maintained to avoid an even bigger loss in the energy production. The Figure 41 below shows an example of Jump.

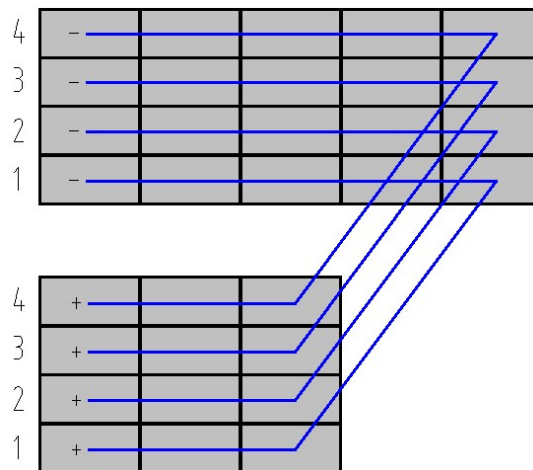


Figure 41 - String with Jump and inline interconnections.

The Figure 42 shows an interconnection of modules with several mixed patterns and a *Jump*, which should never be reproduced in any project.

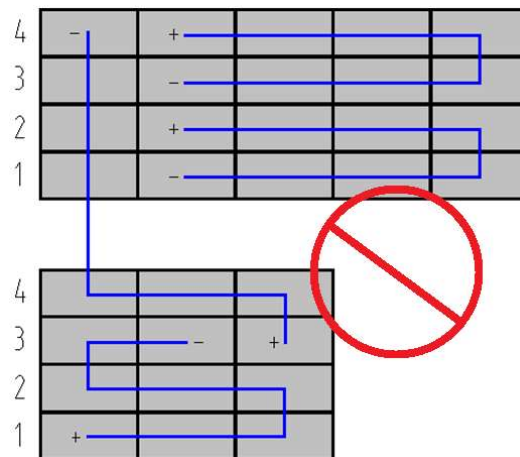


Figure 42 - String with mixed patterns interconnections and a Jump.

The three typologies have positive and negative points, while Jump has only negative. Both the *inline* and *C* types are great standards and can be freely used, while the *S* can compromise the production of the string and can be avoided when developing the mounting structure of the panels according to strings sizes. The correct connection of the modules allows the energy production to be constant and predictable, reducing negative impacts in the power plant's PR.

4.5 CABLES ROUTING AND GROUNDING

A photovoltaic power plant can have thousands of meters of different types of cables. They have enormous importance during the development and should have their measurements estimated as accurately as possible to avoid losses. A solar plant can basically contain 2 types of cabling; the active lines, which are those energized with high voltage and are related to the energy production, and the passive lines, which are not related to energy production, but may be energized with low voltage.

Active lines are all cables that are related to power production. They are responsible for transporting the DC produced by the modules to the inverter, and the AC from the inverter to the transformer or from the transformer to the substation. Normally the total cable losses for a well-designed installation should be less than 1% and this proportion should not rise over time [18]. The cause of some of the losses occurring in the cables is corrosion and overheating. The so-called Solar Cables are specific designed to connect the PV modules to the inverter, carrying DC, while the standard AC cables are responsible for carrying the energy produced by the inverters and by the transformer. Both are in fact ordinary cables, but the Solar Cables are developed to work with a maximum of 1500 V, resist to UV, all possible weather conditions and have a service life of 25 years, as they are placed under the modules and are not buried in trenches as the AC cables, as shown in the Figure 43.



Figure 43 - String cables running inside the MMS.

The sizes, or cross sections, of the cables are determined by the power on which they must carry. The losses are related with the resistance of the conductor and is inversely proportional to the cross-sectional area. If the cross-sectional area is increased, the resistance of the conductor is decreased. Thus, the Solar cables generally vary between 2.5 and 6 mm², while the AC cables between 20 to 240 mm².

Unlike the PV modules, the inverters should be mounted as close to the feed-in counter as possible, because the losses caused by the length of cable are higher on the AC side than on the DC side [18]. The direct current generated from the solar panels should reach as far as possible without losses to the solar power inverter. The AC cables carry a high potential, and therefore are usually buried in trenches, as shown in the Figure 44.



Figure 44 - Trench for cables being dug between the modules mounting structures.

On the opposite way, the passive lines are all other cables that are not connected to the energy production. In this group are all cables of the monitoring system and the earth grounding. The monitoring system cabling is based on RS485 protocol and use a CAT 7 cable, that basically interconnect inverters, DC combiner boxes, transformer and the monitoring cabinet. The maximum recommended length between two devices is 1,200 meters and allows to connect up to 32 devices before a repeater is needed. The details of the monitoring system are exposed in section 4.6. The monitoring cables also have great importance for the performance of the power plant, even not being directly linked to the energy production. This cable is responsible for monitoring and transmission of real-time data collected by all inverters and sensors. A failure in this wiring means the loss of very important information, and consequently a possible failure in the calculation of the PR.

When installing a solar system, it is extremely important that all equipment are earth grounded correctly. Failure to ground the entire system, can be devastating, especially in an area that experiences lightning on a regular basis. Even if seldom have electrical storms, all it takes is one lightning strike and a single loose wire and all the equipment can be destroyed. Worse yet, it can start a fire and cause even more damage. Electricity follows the path of least resistance [20], and while it is almost impossible to know its exact path, it is necessary to take reasonable steps to direct the electricity some place safe when a surge occurs, otherwise the power plant can stop producing for a short or long period of time, what would impact its performance. The Figure 45 shows a bare cooper wire that is commonly used for earth grounding.



Figure 45 - Bare cooper wire for earth grounding.

4.6 MONITORING SYSTEM

The monitoring system is a tool that allows to optimize the power generation system, enabling management and measurement of the system to achieve more effective performance levels and control over its production [15].

In order to keep an eye over the production the power plant rely on a SCADA system, which is a type of software application program for process control. It consist of a central control system that includes controllers, network interfaces, input/output, communication equipment and a software [15]. They are used specifically to monitor and control all sensors, energy meters, circuit breakers, inverters, combiner boxes, transformer, UPS and the onsite camera. All these equipment are connected to the monitoring cabinet of the plant, which will then make the data available to external servers via internet.

The inverter is not only an equipment that converts DC into AC, it also allows to analyse in detail the voltage, current, power and insulation resistance of each DC array connected to its inputs. The same occurs with the exported AC, with addition of active and reactive power, power factor, frequency and phase-by-phase analysis. The instrument can be configured to keep on track over the production and produce specific alarms related with the current operating condition. It can also include hours of operation, internal temperature and communication status. The inverters are daisy-chained with a CAT 7 cable, having a master-slave arrangement operation in half-duplex bidirectional communication using RS485 protocol, where the monitoring cabinet act as master and all inverters as slaves.

The transformer also count with sensors to monitor its operation, such as the Energy Meter, which is a set of 3 network analyser, a pulse generator and a temperature sensor, that analyses the energy imported and exported by the plant in the external grid, giving high accuracy information on voltage, current, power, frequency and power factor. A temperature sensor is also used to monitor possible overheating in the system. The Grid Connection Cubicle, where the transformer is located, has several circuit breakers that operate independently to protect the entire power plant and the grid of ground faults, lightning dischargers, grid overvoltage and frequency disturb. They are connected to the monitoring cabinet and has its condition (triggered or not) supervised. In some countries, where the electrical regulations allows, it's possible to remotely modify its open-closed state, reconnecting the plant into the grid in case of fault. The Energy Meter is connected to the monitoring cabinet as the inverters, using a daisy-chained CAT 7 cable with RS485 protocol, while the circuit breakers also use the CAT 7 cable without any communication protocol, barely being monitored or triggered by digital inputs and outputs of the monitoring cabinet.

Irradiance and temperature sensors are part of the monitoring system and are very important for the calculation of the power plant performance ratio. For irradiance, a total of 4 sensors are used, being 2 Pyranometers and 2 Reference Cells. They all indeed measure irradiance, but in different positions. A set of one Pyranometer and one

Reference cell are placed horizontally, while the other two are placed at the same azimuth angle in which the modules are. This makes possible the analysis of incidence of both global and module plane irradiance. Having two different sensors in the same angle enables to compare the data for a more accurate result. Temperature sensors are not employed in a fixed quantity but should measure the module temperature of each height in a row and the ambient temperature of the site. Figure 46 shows two Pyranometers and two reference cells in horizontal and tilted plane, from the Kepp&Zonen brand.



Figure 46 - From left to right: Horizontal Pyranometer, horizontal reference cell, tilted Pyranometer, tilted ref. cell.

All data produced by the inverters, sensors, transformer and circuit breakers are managed by the Monitoring Cabinet. This IP65 protected station is a centralized measuring equipment for recording and processing all system data in the PV power plant. Internally, it has a 24 V power supply for the peripherals, a battery-powered UPS system to keep the connection always active even in a power outage, various circuit breakers to protect the electrical equipment, cable terminals for easy interconnection of the internal and external peripherals, an automatic heating and cooling system that works with Peltier elements, an internet modem that typically uses optical fiber and the datalogger, which is electronic programmable device that records data over time from all external peripherals and sensors connected to it.

One of the primary benefits of using dataloggers is the ability to automatically collect data on a 24-hour 7-days basis. Upon activation, dataloggers are typically deployed and left unattended to measure and record information. Figure 47 shows a monitoring cabinet with its components of the company Meteocontrol.



Figure 47 - Metecontrol Data Station X Series for outdoor application.

This allows for a comprehensive, accurate picture of the power plant conditions being monitored, such as energy production, string-by-string DC output, modules and ambient temperature, irradiance and state of electrical protection devices.

The PR calculation depends entirely on the monitoring system. According to IEC 61724 - Photovoltaic system performance series of standards, data retrieved from the power plant must be collected by the dataloggers in a minute-by-minute period, for later evaluation and calculation based on the average of 5 minutes values. This means that the monitoring system should not fail under any circumstance, and if so, it should have a backup and an alarm to inform the O&M team of the failures.

The monitoring cabinet, where all monitoring equipment are located, is a cage assembled and installed by third parties. Usually these companies have a complete package of services, which includes not only the SCADA system in the power plant, but also the web portal for tracking the all data in real time, as shown in the Figure 48 .



Figure 48 - Metecontrol Portal for monitoring and analysis of all data retrieved by the power plants.

In some cases, the company itself providing this service also performs the operation and maintenance of the plant, which shortens the response time in case of emergencies, reducing impacts on production and performance.

4.7 INVERTERS CAPPING

Despite the PR calculation have a high accuracy, there are several factors that may affect the outcome. One of the main factors is called Capping and is related to the power plant's DC-to-AC ratio. Having for instance, a ratio of 1.54 means that the DC capacity is 54% above the AC capacity of the inverters. This way, the inverters will work for several days at their maximum, making the PR result very low, while in fact the solar plant is working on its limit. As shown in the Figure 49, it is possible to notice the inverters capping at 50kW and limiting energy production.

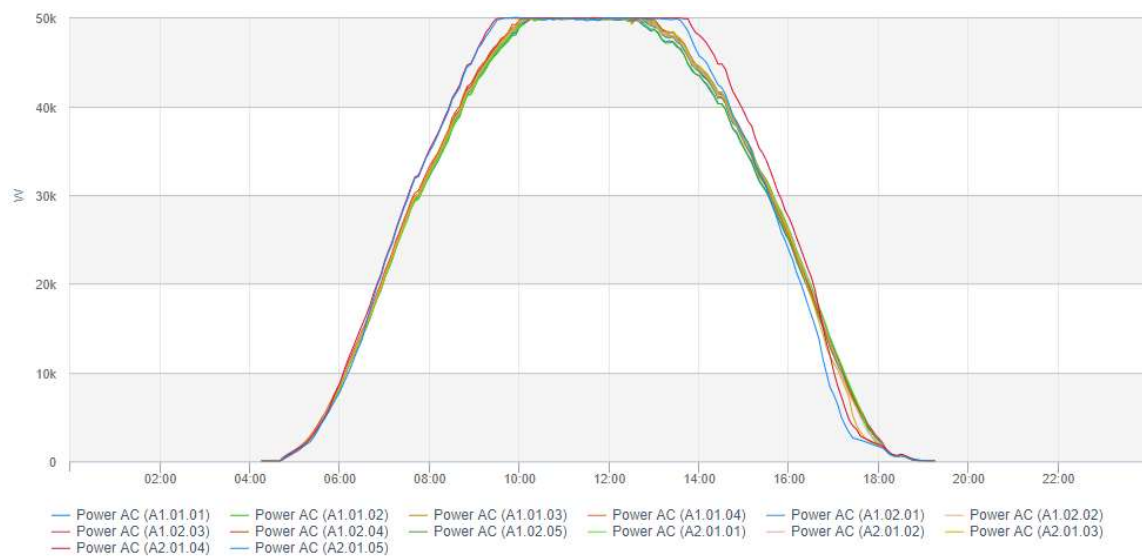


Figure 49 - Inverters production capping at 50kW.

For the PR calculation it means that, irradiance levels are high, enabling a much greater production of energy by the solar panels. However, that ends up being limited by the capacity of the inverters, thus creating a huge impact in the performance result.

4.8 SENSOR ERRORS AND FAULTS

There are situations where the whole system works perfectly, but specific conditions occurs that impact the sensors reading onsite. The solar modules themselves may reflect the sun directly on the radiance sensors during morning and afternoon periods, when the sun is lower on the horizon, as shown in Figure 51.



Figure 51 - Sun reflected by the modules directly impact the irradiance sensor data.

Power plants that are placed on hills can also have the PR affected due to the sun first reaching the radiance sensors and lately the modules. As shown in the Figure 50.



Figure 50 - Sun rising and first reaching the irradiance sensors that are located in the top of the hill.

In addition, large and light-coloured objects can also affect irradiance if they are too close to the sensor. As shown in the Figure 52 , the transformer station is painted in white and stand only 2 meters far away from the irradiance sensors, creating false reading during certain periods of the day.



Figure 52 - Transformer station painted in white color creating false reading in the irradiance sensor.

The three situations mentioned above negatively impacts the PR, as it does not reflect the actual irradiance incidence at that time. Figure 53 shows the result of these conditions with the daily irradiance available in relation to the power. It is clearly noticeable the increase of irradiance during the morning, while the energy does not change.

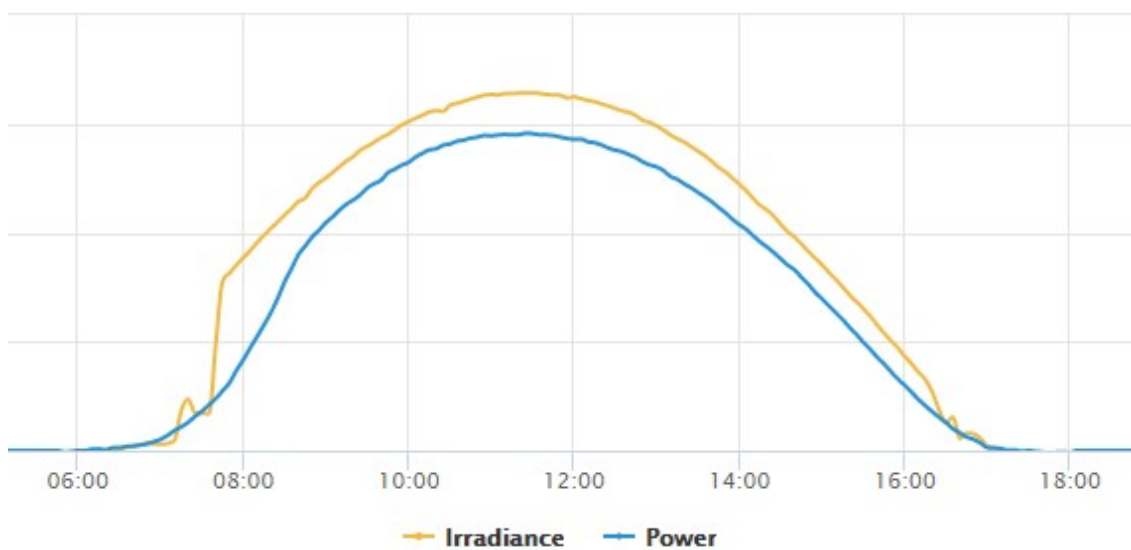


Figure 53 - Irradiance sensor with false values during the morning.

Birds can also distort the reading of the sensors for short periods of time if they land over it. The situation can get worse if the animal leaves scambles on the sensor, which is common. This occurs mainly during cold winter mornings, when the sun warms the panels and creates a very attractive place for the animals, as shown on the Figure 55



Figure 55 - Birds resting on the irradiance sensors and modules during winter.

Another frequently recurring situation during winter is the formation of a thin layer of ice on the panels and on the irradiance sensors at night, which melt during the early hours of the day [19], as shown in Figure 54. However, the area of the layer over the sensors is much smaller than on the panels, making in many cases the values retrieved by the sensors larger than those produced by the panels, creating a discrepancy in the PR.



Figure 54 - Thin layer of ice over modules and row-to-row shading.

Performance and efficiency of a solar cell depend, amongst others, on the temperature of the PV module. At lower temperatures, a PV module is especially efficient. If under these conditions, full solar irradiation is incident on the cold PV module, then it operates very efficiently. This can generate a high PR value briefly. After a certain time, the PV module heats up and the efficiency falls again. Since the calculation of PR is closely linked to the temperature values of the modules, close

attention should be paid to the temperature sensors attached under the modules, as shown in the Figure 56. If the sensor is not correctly fixed to the panel, inaccurate values can be read, impacting the result.



Figure 56 - Temperature sensor attached behind the module.

4.9 MAINTENANCE

Despite the Yield Forecast take into consideration losses that may occur due to shading, situations that were not previously anticipated may occur, such as shading due to high vegetation. Accelerated growth of grass, especially in spring and summer, inside or around the solar park, often cause partial or complete coverage of the modules. It is up to the O&M team to carry out ordinary surveys in order to cut the vegetation, to avoid such situations as shown in Figure 57.



Figure 57 - High grass covering lower modules.

Excessive vegetation near the inverters can also hinder proper ventilation, causing abnormal heating in the equipment. When this occurs, the inverter automatically decreases its output to avoid overheating, immediately impacting production and consequently the PR. Figure 58 shows one inverter (brown line) during the afternoon that is limiting its power production due to problems on the ventilation system caused by high grass.

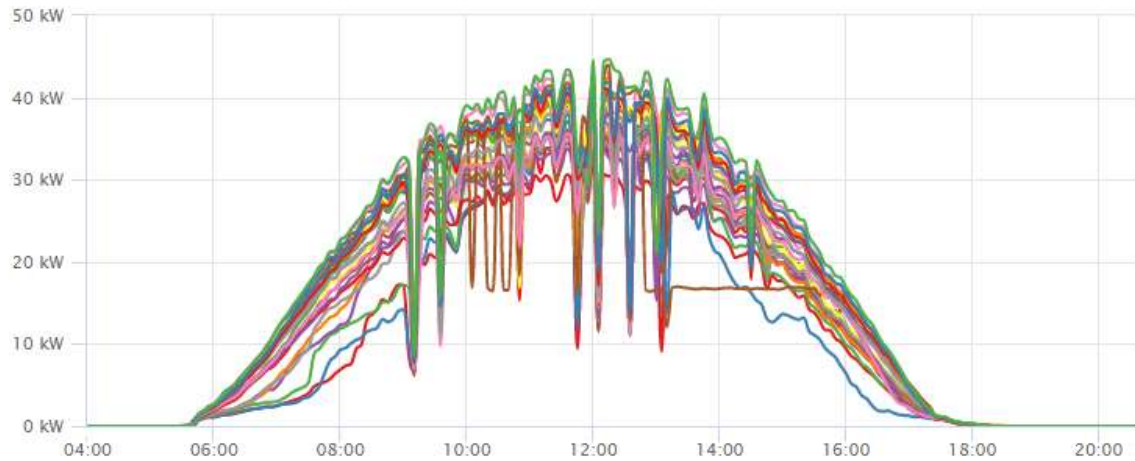


Figure 58 – Inverter limiting its power due to ventilation issue (brown line).

**PERFORMANCE RATIO
AUTOMATIC CALCULATION**

5 PERFORMANCE RATIO AUTOMATIC CALCULATION

During the internship at IBC Solar Energy GmbH, the author of this document developed a software to automatically calculate the Performance Ratio of power plants which the company monitors daily. What the tool does, what it improves and how it was developed is detailed in this chapter.

5.1 OVERVIEW

Every power plant developed by IBC Solar Energy that is in the first 2 years of operation must have its efficiency evaluated, and for that, it was originally required to perform the entire process of calculating the Performance Ratio manually. This meant downloading the raw data from the sensors on the monitoring website of the companies GPM and Meteocontrol, and then copy all the values for an Excel document that calculated the daily PR and the monthly accumulated, through formulas contained in the file. This entire process was completely manual and took on average four hours per day for the calculation of approximately 16 plants, as shown in Figure 59. Many errors ended up not being identified in this repetition, as there was not a gimmick to check if all data range was correct and in order. This caused the errors to ultimately alter the actual performance of the power plants.



Figure 59 - Manual performance ratio calculation process.

Thus, a program was developed that automated the processes that were previously manual as shown in the Figure 60, but also sought to be as simple as possible, enabling anyone without programming knowledge to correct and adapt the program in the future as needed.



Figure 60 - Proposed automation in the performance ratio calculation process.

5.2 SYSTEM REQUIREMENTS

The proposed system to perform the automatic calculation took into account the requirements described in Table 8.

Table 8 - Requirements for the automatic calculation system.

System requirements
Employ Microsoft Excel as database.
Employ VBA as programming software.
Employ C/C++ as programming language.
Eliminate human errors.
Decrease time spent with calculation.
Allow updates and evolution in source code.
Have simple and user-friendly interface.
Allow analysis of results at each step of calculation and automation.
Allow the calculation of the Performance Ratio on several different power plants, regardless of DC capacity.
Allow to use numerous temperature sensors.
Inform system user of possible errors in raw data.
Allow the analysis of the Performance Ratio from all power plants together.
Flag with colour if plant Performance Ratio is below or above stipulated.

5.3 CALCULATION STRUCTURE AND EVOLUTION

The calculation of the Performance Ratio in the company has always been done manually. A task that took many hours every day and was usually employed by the company's interns. The initial version of the PR calculation process was rudimentary and did not perform any automatic validation on data that was downloaded from power plants monitoring system. These data, which include radiation, AC energy output and temperature of the photovoltaic modules, are retrieved by the power plant dataloggers at 5-minute intervals. From then on, the PR is calculated manually using the software MS Excel. Therefore, it is extremely important to analyse the integrity of this data to ensure a reliable result.

The verification of the data was done visually on all raw data files of each plant during the calculation process. It started by downloading the original datalogger files from the monitoring sites. The document was checked one by one to determine if all intervals were in order and went from midnight of the previous day until 23:55 of the current day. It was also analysed if all fields were filled, without blank gaps.

After the normalization of all raw data, the values were copied to an Excel spreadsheet to calculate the PR using formulas contained in the file. All this process took on average 15 minutes per power plant, which resulted in almost 2 hours per day with the 16 plants in operation. As shown in Figure 61, the first version of the automatic PR calculation was almost a manually process.

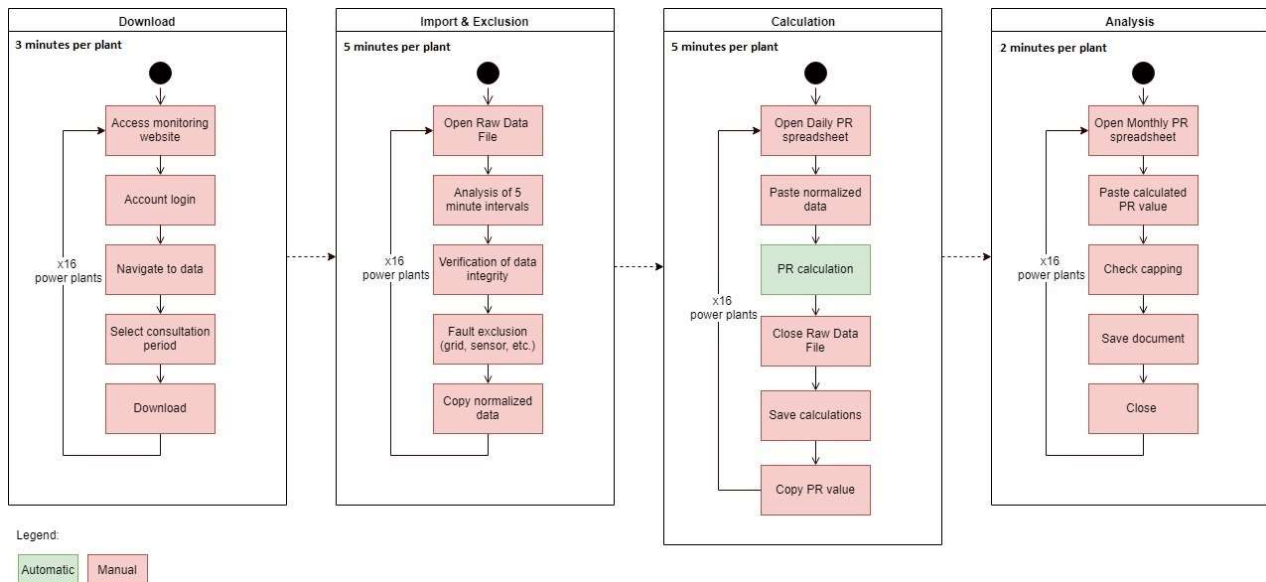


Figure 61 - First version of the automatic PR calculation.

Considering the existing first version of the PR document and the process established by the company to perform the calculation, a second version of the calculation was developed, which focused on the automatic validation of raw data. The system automatically checks whether all five-minute intervals are contained in the document, and all fields are filled in with actual values within a predetermined range. This process allowed to clear errors related to faults from the monitoring system, as it alerts the user about the corrupted data. This automation also decreased the time spent, from 15 to 7 minutes per power plant.

While the second version improve a lot in the calculation, the task was still taking around 1 hour to be accomplished. The manual repetition of opening and closing each website to download the raw data, and opening and closing each Daily PR Excel file, comprised with 90% of the time spent on the calculation, while the rest was spent on data analysis. Figure 62 shows the aggregation of the import process of the raw data in the automatic calculation, making it a bit faster and reliable.

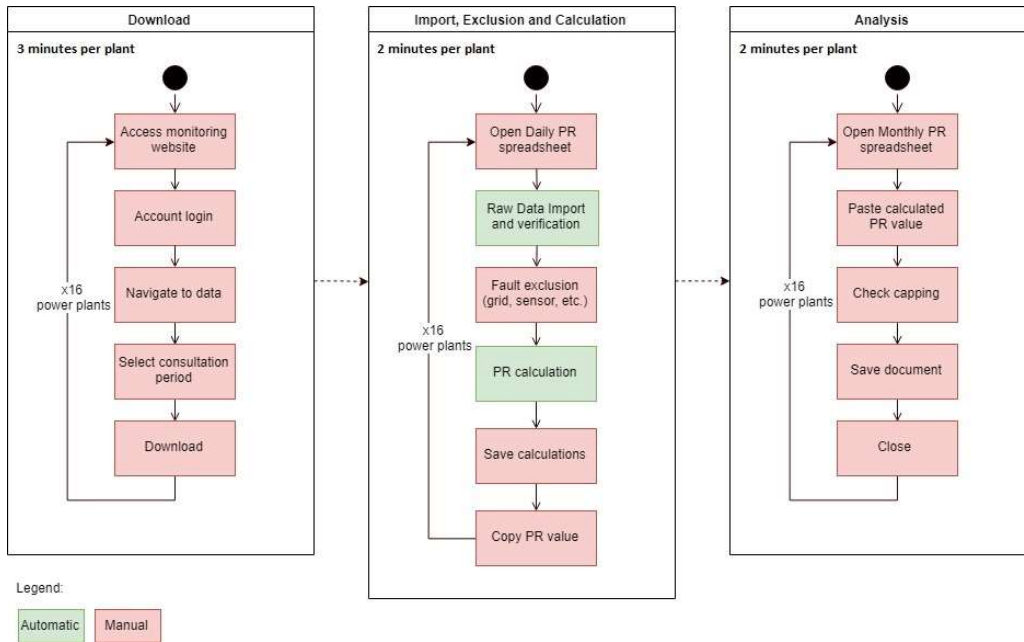


Figure 62 - Second version of the automatic PR calculation.

In the third version of the software a central controller was created in a file called Monthly PR. This file had all the data calculated by each Daily PR spreadsheet, and allowed to download, import the raw data and to calculate the PR of each plant automatically. In the end, the user should only monitor the machine's operation, while it produces the results and records errors found in the calculations. The Figure 63 shows how the process of calculating the PR is currently taking place, which for all 16 power plants takes an average of 13 minutes to download, import and analyse the raw data, calculate the PR and export it to a central spreadsheet called Monthly PR.

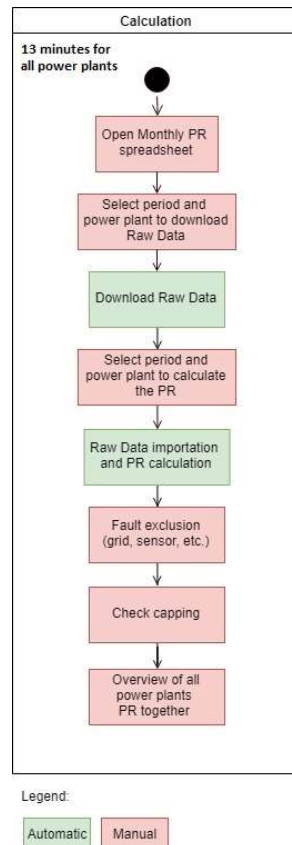


Figure 63 - Third version of the automatic PR calculation

5.4 AUTOMATION MILESTONES

The first step in the development of the automatic calculation was the analysis of the raw data from the sensors, and from them build a standardized table that would work for all projects. Specific columns were created for dates, time intervals, exported energy, irradiance and module temperature sensors, which varied in quantity according to plant. Figure 64 shows a sample of the raw data table created to archive all data from the sensors.

Calculated Performance Ratio for every time step

time / date	01/10/2019	02/10/2019	03/10/2019	04/10/2019	05/10/2019	06/10/2019	07/10/2019	08/10/2019	09/10/2019	10/10/2019	11/10/2019
12:00	89%	88%	89%	91%	87%	96%	89%	96%	86%	88%	92%
12:05	89%	90%	95%	91%	88%	76%	94%	80%	85%	88%	94%
12:10	88%	88%	92%	89%	90%	76%	82%	93%	87%	88%	94%
12:15	89%	91%	93%	86%	89%	88%	80%	89%	87%	88%	92%
12:20	88%	92%	90%	89%	91%	94%	89%	89%	87%	88%	95%
12:25	87%	89%	81%	79%	90%	87%	89%	92%	87%	88%	92%
12:30	88%	87%	92%	70%	89%	95%	83%	90%	86%	80%	94%
12:35	88%	87%	89%	95%	89%	93%	93%	94%	87%	89%	91%
12:40	85%	86%	92%	87%	90%	93%	93%	89%	79%	88%	92%
12:45	82%	88%	90%	80%	79%	90%	93%	94%	88%	88%	83%
12:50	89%	83%	91%	93%	90%	91%	96%	95%	87%	89%	92%
12:55	80%	87%	91%	91%	90%	91%	95%	91%	87%	89%	92%
13:00	89%	91%	85%	87%	89%	80%	91%	91%	87%	89%	93%

Figure 64 - Raw data table for the automatic PR calculation tool.

With the normalized sensors data, it became possible to calculate the PR for each 5-minute interval using the MS Excel formulas, as shown in Figure 65 .

Date	Time	PC-11B PULSE METER - EXPORTED ACTIVE ENERGY (PULSES) (kWh)	PYRANOMETER (TILTED) - IRRADIANCE (W/m2)	TEMPERATURE SENSORS - PANEL TEMPERATURE (SENSOR 1) (°C)	TEMPERATURE SENSORS - PANEL TEMPERATURE (SENSOR 2) (°C)	TEMPERATURE SENSORS - PANEL TEMPERATURE (SENSOR 3) (°C)	TEMPERATURE SENSORS - PANEL TEMPERATURE (SENSOR 4) (°C)
07/10/2019	12:00	68.00	664.83	45.71	44.30	43.97	44.37
07/10/2019	12:05	70.00	641.10	43.57	42.35	41.96	41.99
07/10/2019	12:10	89.00	936.60	44.57	43.43	43.11	43.28
07/10/2019	12:15	98.00	1078.50	47.77	46.78	46.34	46.73
07/10/2019	12:20	69.00	689.52	50.06	49.10	48.55	49.15
07/10/2019	12:25	47.00	460.20	46.97	45.99	45.55	45.96
07/10/2019	12:30	30.00	305.17	40.68	39.66	39.21	39.25
07/10/2019	12:35	29.00	259.10	35.60	34.85	34.48	34.40
07/10/2019	12:40	36.00	318.43	32.40	31.84	31.53	31.55
07/10/2019	12:45	34.00	297.53	31.39	30.83	30.64	30.71
07/10/2019	12:50	42.00	355.03	30.81	30.31	30.12	30.33
07/10/2019	12:55	74.00	635.62	32.21	31.80	31.73	32.18
07/10/2019	13:00	52.00	472.70	35.51	34.87	34.77	35.32

Figure 65 - Automatic performance ratio calculation for every 5 min interval.

However, according to the PR’s equation, it is necessary to know the temperature of the reference PV cell for each month, to then calculate the losses or gains due to temperature variation. Thus, a table, as the sample shown in the Figure 66, was created in the same document that is filled with the reference temperatures used in the Yield Forecast, which also determined the PR that the plant must meet.

month	T _{cell-avg.-monthly} [°C]	PR _{guaranteed} monthly [%]	PR _{minimum} monthly [%]
1	3	73	63.5
2	4	77	66.5
3	7	84	73.5
4	12	83	72.5
5	16	81	70.5
6	17	79	68.5
7	20	79	67.5
8	20	78	67.5
9	15	80	68.5
10	11	82	70.5
11	7	82	71.5
12	4	80	71.5

Figure 66 - Reference PV cell temperature for automatic calculation of the PR.

Then the Daily PR spreadsheet was created, which concentrates all the results and parameters of each power plant, such as the name, capacity, temperature correction coefficient of the modules (1), daily (3) and monthly PR values (4), and the buttons to control the automation process (5), respectively numbered in Figure 67 .

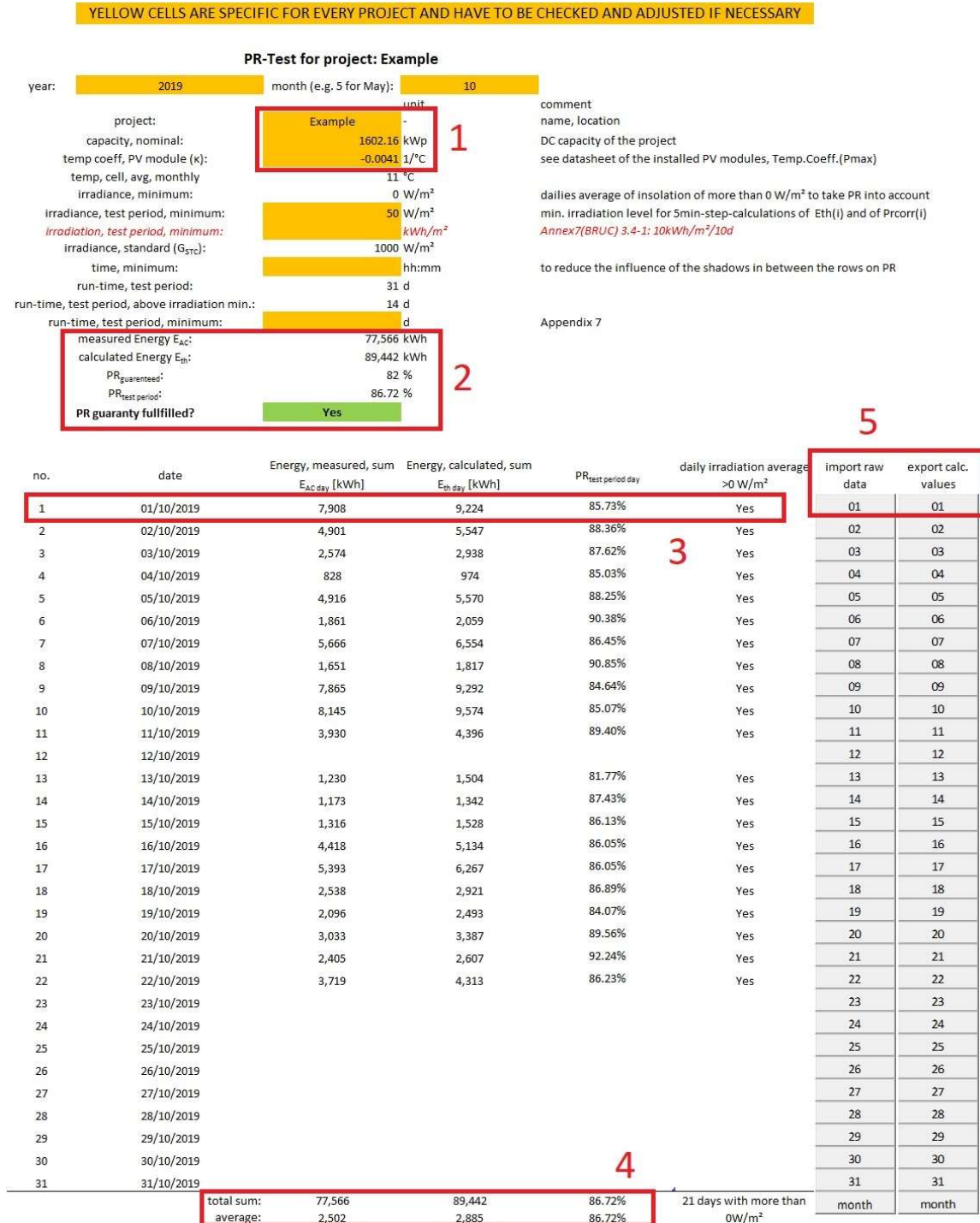


Figure 67 - Daily PR spreadsheet for the automatic calculation of the PR.

The Daily PR spreadsheet also had an internal algorithm that parsed every interval of the raw data that was imported, informing when an error or failure was found in the file. However, this document was single, and a copy was created for each of the

power plants. Happened to be at the end of the calculations, the need to analyse all the PR calculated in a single spreadsheet. This gave rise to the idea of creating the Monthly PR spreadsheet, which would encompass all PRs in a single spreadsheet, which ultimately facilitated the analysis of other departments of the company that needed to track the performance.

Similar to the Daily PR spreadsheet, which had the database created with the raw data from the sensors, the Monthly PR spreadsheet also use a database to record all PRs previously calculated. The process of uploading these values into this spreadsheet is fully automated, and the algorithm automatically opens Daily PR files, copies the values, and pastes in the exact power plant and day. Figure 68 shows the structure of the Monthly PR spreadsheet database.

Toyama			Gifu			Hiki		
Date	Emeter [kWh]	Ecalc [kWh]	Date	Emeter [kWh]	Ecalc [kWh]	Date	Emeter [kWh]	Ecalc [kWh]
01/02/2019	0	0	01/02/2019	1835	2848.784418	01/02/2019	7313	9009.226384
02/02/2019	0	0	02/02/2019	1923	2659.931375	02/02/2019	7026	8714.575741
03/02/2019	2203	2900.435832	03/02/2019	511	910.0206388	03/02/2019	6016	7311.039433
04/02/2019	2016	2555.184774	04/02/2019	1865	2511.758897	04/02/2019	7317	8881.897606
05/02/2019	6634	8325.934135	05/02/2019	1942	2617.637064	05/02/2019	3916	4608.111114
06/02/2019	2735	3225.659146	06/02/2019	481	579.3390625	06/02/2019	609	758.802781
07/02/2019	4058	5009.703709	07/02/2019	672	977.2748156	07/02/2019	5831	6845.430938
08/02/2019	21	1531.675417	08/02/2019	1546	2035.646184	08/02/2019	3522	4070.677345
09/02/2019	53	1548.563891	09/02/2019	75	79.05098228	09/02/2019	351	399.3794867
10/02/2019	58	5097.015941	10/02/2019	1874	2535.570004	10/02/2019	6350	8612.825426
11/02/2019	1299	3756.765926	11/02/2019	540	640.3829694	11/02/2019	1584	1793.579971
12/02/2019	1680	1984.67153	12/02/2019	2165	2820.163969	12/02/2019	7942	9618.667149
13/02/2019	192	1047.912668	13/02/2019	1946	2454.485494	13/02/2019	5275	6201.864798
14/02/2019	87	4376.615146	14/02/2019	1615	2079.600565	14/02/2019	7156	8803.052474
15/02/2019	598	3665.187086	15/02/2019	594	855.9604991	15/02/2019	5038	6001.794166
16/02/2019	790	1106.843958	16/02/2019	1937	2458.941635	16/02/2019	7132	8576.026437
17/02/2019	3094	6189.273453	17/02/2019	2307	2963.578303	17/02/2019	8255	10049.01217
18/02/2019	6773	8595.071675	18/02/2019	2275	2887.438484	18/02/2019	8122	9926.901778
19/02/2019	935	996.7075785	19/02/2019	167	184.0531734	19/02/2019	1796	1920.130108
20/02/2019	1144	1253.034461	20/02/2019	1701	2102.746242	20/02/2019	6004	7037.482274
21/02/2019	2193	2413.311973	21/02/2019	2219	2752.239197	21/02/2019	7778	9209.734772
22/02/2019	7643	9258.049262	22/02/2019	1855	2248.25462	22/02/2019	6930	8272.919452
23/02/2019	4068	5028.015382	23/02/2019	2256	2790.228609	23/02/2019	8296	9781.470309
24/02/2019	8621	10754.25875	24/02/2019	1553	1959.456559	24/02/2019	7724	9109.401502
25/02/2019	6885	8282.281585	25/02/2019	2114	2475.136965	25/02/2019	5780	6665.196778
26/02/2019	4678	5777.508617	26/02/2019	2363	2892.992241	26/02/2019	4855	5702.859077
27/02/2019	4079	4492.709869	27/02/2019	1258	1414.482609	27/02/2019	3085	3327.691758
28/02/2019	1040	1143.018081	28/02/2019	114	123.6126009	28/02/2019	460	503.352747

Figure 68 - Monthly PR spreadsheet database.

The Monthly PR spreadsheet eventually improved over time and started to automatically download the raw data from the monitoring websites. This was made possible by creating a VBA controller that navigates to each website and downloads the file on its own, as shown in Figure 69 .

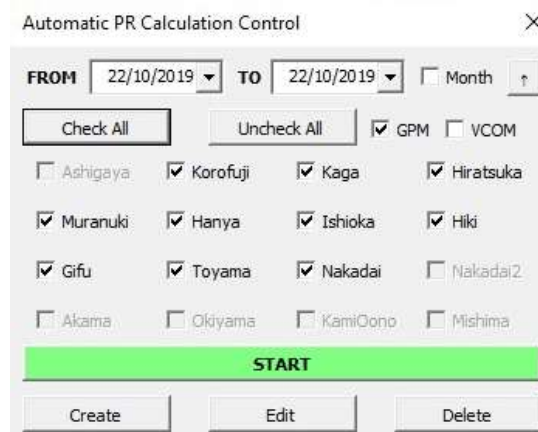


Figure 69 - Automatic PR Calculation Controller.

The Monthly PR spreadsheet has become a tool that currently controls the entire calculation of PR in the company. It is possible to download the sensor files from the Portals, calculate the daily PR of each power plant and import the calculated values into the Monthly PR database automatically, from the beginning until the end of the process. To view the result of all this huge data processing, the user should only access the overview, to have a monthly view of the power plants PR progress, with colour indicative according to the current yield, being red for when it is below 1.5% of the stipulated PR, yellow when between 1.5% and 0.1% below the stipulated, and green for the PR as stipulated or above. It is also possible to see the amount of capping that have already occurred during the month, which strongly impacts the monthly PRs, as marked in the red circles in Figure 70.

MONTH: 9		YEAR: 2019		PR						
Project	Goal	Boundary	Real-Goal	Capping		01/09/2019	02/09/2019	03/09/2019	04/09/2019	05/09/2019
Toyama	80.00%	78.50%	6.24%		PR (Day)	90.70%	87.74%	88.24%	89.95%	88.58%
					PR (Month)	90.70%	89.93%	89.59%	89.70%	89.31%
					Capping					
Gifu	78.00%	76.50%	0.69%		PR (Day)	82.32%	77.83%	78.62%	81.80%	82.05%
					PR (Cummul.)	82.32%	80.00%	79.48%	80.05%	80.44%
					Capping					
Hiki	81.00%	79.50%	-4.10%	9	PR (Day)	76.17%	70.16%	74.94%	76.33%	73.76%
					PR (Cummul.)	76.17%	72.30%	72.65%	73.30%	73.40%
					Capping	Yes	Yes			
Ishioka	79.00%	77.50%	1.62%	13	PR (Day)	82.67%	80.56%	80.66%	82.72%	80.19%
					PR (Cummul.)	82.67%	81.56%	81.40%	81.59%	81.31%
					Capping		Yes			
Hanya	79.00%	77.50%	-4.44%	21	PR (Day)	74.91%	74.50%	74.59%	75.96%	74.97%
					PR (Cummul.)	74.91%	74.68%	74.67%	74.83%	74.86%
					Capping	Yes	Yes			
Muranuki	82.60%	81.10%	-3.79%	20	PR (Day)	74.85%	72.72%	74.86%	75.80%	74.95%
					PR (Cummul.)	74.85%	73.64%	73.83%	74.07%	74.28%
					Capping	Yes	Yes			
Hiratsuka	82.40%	80.90%	-9.45%	17	PR (Day)	75.02%	75.76%	74.61%	76.24%	75.26%
					PR (Cummul.)	75.02%	75.42%	75.30%	75.42%	75.38%
					Capping		Yes			
Kaga	81.10%	79.60%	0.11%	11	PR (Day)	85.89%	79.46%	83.35%	82.34%	82.28%
					PR (Cummul.)	85.89%	83.08%	83.22%	82.99%	82.81%
					Capping		Yes	Yes		
Korofuji	79.50%	78.00%	-3.23%	17	PR (Day)	69.37%	68.51%	69.41%	68.80%	67.93%
					PR (Cummul.)	69.37%	68.94%	69.02%	68.97%	68.71%
					Capping	Yes	Yes			Yes
Ashigaya	82.50%	81.00%	1.88%	12	PR (Day)	90.06%	84.37%	91.94%	93.87%	88.61%
					PR (Cummul.)	90.06%	86.90%	87.73%	88.44%	88.48%
					Capping		Yes			
Nakadai	82.70%	81.20%	0.59%	20	PR (Day)	82.85%	83.60%	82.20%	82.81%	80.48%
					PR (Cummul.)	82.85%	83.23%	83.04%	82.99%	82.50%
					Capping	Yes	Yes			Yes
Nakadai2	82.60%	81.10%	5.20%	9	PR (Day)	90.12%	87.79%	91.02%	91.31%	89.47%
					PR (Cummul.)	90.12%	88.92%	89.31%	89.73%	89.68%
					Capping		Yes			
Akama	82.60%	81.10%	4.25%	18	PR (Day)	90.38%	89.18%	90.02%	90.00%	88.09%
					PR (Cummul.)	90.38%	89.65%	89.70%	89.75%	89.29%
					Capping		Yes			Yes
Okiyama	83.10%	81.60%	7.77%	15	PR (Day)	90.18%	87.73%	85.08%	93.45%	93.26%
					PR (Cummul.)	90.18%	88.95%	88.12%	89.19%	90.09%
					Capping	Yes	Yes			Yes
KamiOono	80.90%	79.40%	2.85%	7	PR (Day)	86.00%	84.89%	86.15%	86.93%	84.58%
					PR (Cummul.)	86.00%	85.42%	85.55%	85.83%	85.59%
					Capping					
Mishima	73.10%	71.60%	10.11%	11	PR (Day)	86.00%	84.89%	86.15%	86.93%	84.58%
					PR (Cummul.)	86.00%	85.42%	85.55%	85.83%	85.59%
					Capping	Yes	Yes			

Means: no data or PR < (Monthly PR goal - 1.5%)
 Means: (Monthly PR goal - 1.5%) < PR < Monthly PR goal
 Means: PR > Monthly PR goal

Figure 70 - Monthly PR spreadsheet overview of all power plants.

5.5 VALIDATION

After the automation of all the calculation process, it was necessary to validate if the obtained results were really the expected. In the first version of the PR calculation, which was done completely manually, the result was validated by a second person on the last day of the month. This validation basically consisted in checking the daily PRs of each power plant, and if the value was below the stipulated, an analysis was done on the raw data and in the calculations. Thus, even if the PR calculation was satisfactory compared to what was stipulated in the Yield Forecast, this did not mean that the result obtained was reliable.

The second version of the calculation process was developed exactly to filter and inform the user about possible errors in raw data. The data integrity check is made to verify that the file has all 288 intervals of 5 minutes that are expected to be in 24 hours. The irradiance exported energy and temperature values were also analysed one by one according to Table 9 .

Table 9 - Raw data filter of the automatic PR calculation.

Sensor	Minimum value	Maximum value
Irradiance [W/m ²]	0	1400
Exported Energy [kWh]	0	Not limited
Module Temperature 1 [°C]	- 15	85
Module Temperature 2 [°C]	- 15	85
Module Temperature 3 [°C]	- 15	85
Module Temperature 4 [°C]	- 15	85
Module Temperature <i>n</i> [°C]	- 15	85

The third and final version of the calculation, which automated 100% of the process, focused on eliminating simples' human errors. When the PR was calculated for each of the plants, it was still necessary to manually copy the values from the Daily PR to the Monthly PR spreadsheet. This repetition in some cases caused values of one plant to be erroneously copied to another plant. The creation of the algorithm to export the calculated values allowed to definitively solve this problem.

While all these improvements to validate the raw data and to copy the results correctly, it was still needed to validate if the algorithm created for the software contained no errors. For 2 months, the automatic and manual processes were made in parallel, allowing the comparison of the results obtained. Thus, it was possible to determine that every 10 days an error occurred in the manual calculation process.

According to Luiz Bueno, Electrical Engineer at IBC Solar, the result obtained with automation reached the proposed requirements:

Ronny worked as a trainee at IBC Solar in Bad Staffelstein from February to August 2019, and one of his tasks was to optimize the monitoring control of solar energy plants designed and built by the company. Upon completion of each project, IBC Solar will guarantee the minimum monthly energy production performance for a period of two years. This control is given by the calculation of parameters measured in the photovoltaic station, such as energy, irradiance and temperature. The values should be calculated at a five-minute interval, which represented a total of approximately 1728 separate data per day and per solar plant. Due to the large amount of information, several data control spreadsheets were used. However, the data management system was very rudimentary. Data should be manually exported by the user from the monitoring storage portal to the control spreadsheets. This process was time consuming (on average 2 hours per day) and susceptible to many errors. In addition, poorly structured calculation management made analysis and control very complicated.

He has developed various methods for optimizing and automating data management. First an automatic tool for downloading database information was added. Then the process for importing the data into the spreadsheet was automated. The spreadsheet has been restructured, improving the user interface and making it more dynamic and efficient. Additionally, new features were implemented which made the spreadsheet aspect clearer and simpler. Subsequent corrections and analysis increased in effectiveness and robustness. Finally, a general control worksheet was developed which interconnected with the individual worksheets. Solar plant monitoring task has become very practical reducing daily work to 15 minutes (increasing efficiency by 8x).

Luiz Bueno – EPC Electrical Engineer

5.6 WORK EFFORT

The automation system was developed in three different stages, producing three different versions of the program, and consumed approximately two and a half months of working time and more two months of validation, divided according to the Table 10 below.

Table 10 - Automatic PR calculation work effort.

Stage	Assignment	Duration (h)
Version 1	Performance Ratio system analysis and formula	20
	Requirement gathering for the system	80
	Discussions and suggestions with work team	40
Version 2	Raw data import algorithm	8
	Development of source code for import process	20
	Data normalization algorithm	8
	Development of source code for data normalizer	20
	Data checker algorithm	8
	Development of source code for data checker	20
	Prototype tests	40
Version 3	Raw data automatic downloader algorithm	20
	Development of source code for downloader	80
	System controller algorithm	8
	Development of source code for system controller	80
	Prototype tests	40
Validation	Result analysis and error correction	320

5.7 ACHIEVEMENTS

The developed software was able to close the PR calculation chain process, making it completely automatic, eliminating 95% of errors during the raw data analysis and 90% of improvement in the time spent with the daily calculation, as shown in the Table 11.

Table 11 - Performance Ratio automatic calculation achievements.

Before	After
Manual download of raw data	Download completely automatic
Manual copy and paste of raw data	Automatic import of raw data to spreadsheet
Visual check of raw data integrity	Automatic raw data check
Absence of sensors data range analyzer	Automatic sensors data range analyzer according to configurable parameters
PR calculation taking around 2 hours per day + analysis of results	PR calculation taking 13 minutes per day + analysis of results (90% improvement)
Absence of calculation controller or dashboard	Full control of calculation with one controller and one dashboard for all power plants
Absence of PR goals analyzer	Power plants PR flagged by colour according to yield forecast (below or above)

5.8 LONG-TERM ANALYSIS

After 5 months of use, it was possible to detect a failure in the analysis of temperature sensors that had not been considered at the beginning of the automation project. The temperature sensors that over the years eventually detaches from the back of the PV modules, start to send erroneous readings. As power plants always have at least 4 temperature sensors, it is possible to make a correlation of the values of all these sensors as shown in Figure 71.

Same sensor type

Date	Time	PC-11B PULSE METER- EXPORTED ACTIVE ENERGY (PULSES) (kWh)	PYRANOMETER (TILTED) - IRRADIANCE- IRRADIANCE (W/m ²)	TEMPERATURE SENSORS - PANEL TEMPERATURE (SENSOR 1) (°C)	TEMPERATURE SENSORS - PANEL TEMPERATURE (SENSOR 2) (°C)	TEMPERATURE SENSORS - PANEL TEMPERATURE (SENSOR 3) (°C)	TEMPERATURE SENSORS - PANEL TEMPERATURE (SENSOR 4) (°C)
07/10/2019	12:00	68.00	664.83	45.71	44.30	43.97	44.37
07/10/2019	12:05	70.00	641.10	43.57	42.35	41.96	41.99
07/10/2019	12:10	89.00	936.60	44.57	43.43	43.11	43.28
07/10/2019	12:15	98.00	1078.50	47.77	46.78	46.34	46.73
07/10/2019	12:20	89.00	689.52	50.06	49.10	48.55	49.15
07/10/2019	12:25	47.00	460.20	46.97	45.99	45.55	45.96
07/10/2019	12:30	30.00	305.17	40.68	39.66	39.21	39.25
07/10/2019	12:35	29.00	299.10	35.60	34.85	34.48	34.40
07/10/2019	12:40	36.00	318.43	32.40	31.84	31.53	31.55
07/10/2019	12:45	34.00	297.53	31.39	30.83	30.64	30.71
07/10/2019	12:50	42.00	355.03	30.81	30.31	30.12	30.33
07/10/2019	12:55	74.00	635.62	32.21	31.80	31.73	32.18
07/10/2019	13:00	52.00	472.70	35.51	34.87	34.77	35.32

Figure 71 - Raw data temperature sensors correlation.

Thus, to improve the system and remedy the problem it is necessary to add an algorithm that compares the temperature values in order to detect large mean deviations, which may affect the calculation of the PR. This modification should be done in the verification step of the raw data after the automatic import.

CONCLUSION

6 CONCLUSION

The inclusion of renewable energy sources in the global energy grid is becoming increasingly necessary due to the growing demand for energy and environmental concerns. In this sense, photovoltaic solar energy becomes an important alternative source of electricity generation, as it originates from a virtually inexhaustible source. It can be generated in a distributed way, that is, close to the point of consumption; can be modular in character, in order to allow the installation of low (W) to high power (MW) systems, do not generate noise during generation and have an expected operating life of approximately 20 years.

Through the initiative of some countries, notably Germany, Italy, the USA and Japan, the photovoltaic market has experienced great growth in the last decade, driven mainly by the creation of governmental tax incentive programs that required the purchase of electricity by utilities. These investments have caused component costs to fall due to scale gains, helping the PV industry to get consolidate.

The sizing of a grid-connected photovoltaic system must take into account the location and orientation, so that the sun's potentialities are better exploited. Thus, the different levels of irradiation registered in the world are determining factors for a correct dimensioning, in other words, for each location the PV system will have a performance proportional to the registered irradiation level. The temperature also must be considered in order to correct the forecast of the system production. But a well-developed solar plant not only needs to take radiation and temperature into account. There are several losses in the system, both in the absorption of radiation, as in the generation and transport of the energy. The electrical system of the power plant, despite being simple and easy to scale, must be thoroughly developed to limit the involved losses. The dimensioning of the power produced by the modules, inverters and transformers must be correctly scaled, allowing the system to work in harmony without capacity bottlenecks, which could produce overload and overheating. The accurate cabling thickness estimation and its losses. A well-sized earth grounding that encompass all components of the system and protect people and equipment from possible electrical discharges. A simple yet effective module mounting structure that withstands all possible weather conditions, and a stable monitoring system that capture all needed data autonomously for remote evaluation and performance ratio calculation. All these factors when properly evaluated, can eliminate or control the power debt, allowing for an energy production more stable and in line with the Yield Forecast.

In conclusion, the internship in a high quality company in Germany gave the author an outstanding gain of knowledge in the development and in the performance analysis of PV power plants in different countries. A software to assist the company process of calculating the PR was successfully concluded, making it completely automatic and eliminating 95% of errors during the raw data analysis and 90% of improvement in the time spent with the task.

6.1 FUTURE WORK

While the efficiency of a solar plant is determined by comparing its PR with the Yield Forecast, there are occasional situations where such equalization may not be true to reality. It has been realized that the incidence of radiation and temperatures are not in line with the last 10 years records used to produce the Yield Forecast.

This factor induces, in most cases, the PR of the power plant to be lower than estimated. Numerous environmental factors such as ambient temperature and the duration and intensity of the seasons of the year are decreasing the modules energy production. Despite being a very recent recurrence, it is a situation that can already be noticed in the total production of the last 18 months. The causes are yet to be determined, but there may be connection with recent climate change and global warming.

Therefore, future research should be conducted in more realistic settings by recalculating the Yield Forecast, based on the real weather data obtained from the irradiance and temperature sensors installed in each solar park. This would make possible the comparison of the PR with the Yield Forecast according to the actual climatic conditions of the plants, resulting in a more accurate examination of each site, and also in determining the main climatic factor that is most impacting the energy production nowadays.

**BIBLIOGRAPHY AND OTHER
SOURCES OF INFORMATION**

7 BIBLIOGRAPHY AND OTHER SOURCES OF INFORMATION

- [1] Jonathan G. Price, LLC, 2210 Andromeda Way, Reno, Nevada 89509, USA. Available on: <http://www.geosociety.org/gsatoday/archive/26/1/pdf/i1052-5173-26-14.pdf>
- [2] M. A. Islam et al., "Global Renewable Energy-Based Electricity Generation and Smart Grid System for Energy Security," *Sci. World J.* 2014, 197136 (2014).
- [3] IBC Solar, [Online]. Available on: <https://www.ibt-solar.de>.
- [4] CEMIG – Companhia Energetica de Minas Gerais. Alternativas Energéticas: Uma visão Cemig. Belo Horizonte: CEMIG, 2012.
- [5] CEPEL – Centro de Pesquisas de Energia Eletricas. As energias solar e eólica no Brasil. 2013. Available on: http://cresesb.cepel.br/download/casasolar/casasolar_2013.pdf
- [6] CEPEL – Centro de Pesquisas de Energia Eletrica; CRESESB – Centro de referencia para Energia Solar e Eolica Sergio Brito. Manual de Engenharia para Sistemas Fotovoltaicos. Rio de Janeiro, RJ: Especial 2014.
- [7] R. Gold, "Global Investment in Wind and Solar Energy Is Outshining Fossil Fuels," *Wall Street Journal*, 11 Jun 18.
- [8] J. Pinho and M. Galdino, Manual de Engenharia para Sistemas Fotovoltaicos, Rio de Janeiro: CEPEL - CRESESB, 2014.
- [9] IEA, "Report IEA PVPS T1-32:2017: Trends 2017 in Photovoltaic Applications," St. Ursen, 2017.
- [10] A. Mofiz, "Understanding solar tracking systems for PV power plants", India: Jakson – June 29, 2018 – Available on: <https://www.jakson.com/blog/understanding-solar-tracking-systems-for-pv-power-plants/>
- [11] M. R. Maghami, H. Hizam, C. Gomes, M. A. Radzi, M. I. Rezadad, S. Hajighorbani, "Power loss due to soiling on solar panel: A review", *Renewable and Sustainable Energy Reviews*. Volume 59, June 2016, Pages 1307-1316
- [12] A. Haque, Zaheeruddin, "Research on Solar Photovoltaic (PV) energy conversion system: An overview", Mumbai – India, Conference Oct. 2013, IEEE Xplore Digital Library, available on: <https://ieeexplore.ieee.org/document/6950937>
- [13] H. P. Ikkurti and S. Saha, A Comprehensive techno-economic review of microinverters for Bulding Integrated Photovoltaics (BIPV), *Science Direct*, available on: https://www.sciencedirect.com/science/article/pii/S1364032115_002348
- [14] SMA, Technology Brochure 7 – OptiTrac, MPP Tracking – the Search for the Optimum Operating Point, Germany. Available on: http://files.sma.de/dl/3491/_TECHOPTITRAC-AEN082412.pdf
- [15] SMA, Technical Information, Performance ratio – Quality factor for the PV plant, Germany. Available on: <http://files.sma.de/dl/7680/Perfratio-TI-en-11.pdf>

- [16] P. Deshpande, B. Bodkhe, Photovoltaic Module Interconnection Modified to Improve Efficiency & Robustness, International Journal of Applied Engineering Research ISSN 0973-4562 Volume 12, Number 24 (2017) pp. 15560-15563 , Research India Publications. Available on: https://www.ripublication.com/ijaer17_/ijaerv12n24_225.pdf
- [17] K. Zipp, "Why array oversizing makes financial sense", Solar Power World, ABB – February 12, 2018. Available on: https://new.abb.com/docs/libraries/provider117_/default-document-library/solar-inverters/solar_power_world-article.pdf?sfvrsn_=80a7614_4
- [18] S. Ekici, M. A. Kopru, "Investigation of PV System Cable Losses", International Journal of Renewable Energy Research, Article 7(2):807-815, Vol.7, No.2, 2017. Available on: https://www.researchgate.net/publication/317701311_Investigation_of_PV_System_Cable_Losses
- [19] IEC – International Standard, Photovoltaic system performance – Part 1: Monitoring, IEC 61724-1 Edition 1.0 2017-03. Available on: <https://www.sis.se/api/document/preview/8025333/>
- [20] Solar Power Europe, Operation & Maintenance – Best Practices Guidelines / Version 3.0, 2018 Edition. Available on: <http://www.solarpowereurope.org/wp-content/uploads/2018/12/OM-Best-Practices-Guidelines-V3.0.pdf>
- [21] Siemens, Transformers for Solar Power Solutions, Transformers for solar power plants, Article No. E50001-G640-A217-V2-4A00, Germany, 2015. Available on: [https://assets.new.siemens.com/siemens/assets/public.1541967491.963ed8b088184fd8f2c47d044701db831f8268f1.siemens-transformers-for-solar-power-solutions.pdf](https://assets.new.siemens.com/siemens/assets/public/1541967491.963ed8b088184fd8f2c47d044701db831f8268f1.siemens-transformers-for-solar-power-solutions.pdf)
- [22] Fraunhofer Institute for Solar Energy Systems, ISE, Freiburg, 14 March 2019. Available on: <https://www.ise.fraunhofer.de/content/dam/ise/de/documents/publications/studies/Photovoltaics-Report.pdf>
- [23] University of Minnesota, Mechanical Engineering, Appendix D: Solar Radiation. Available on: <http://www.me.umn.edu/courses/me4131/LabManual/AppDSolarRadiation.pdf>
- [24] Perovskites and Perovskite Solar Cells: An Introduction. Resource & Support. Ossila – Enabling Materials Science, June 2018. <https://www.ossila.com/>

APPENDIX

8 APPENDIX A - Datasheets

8.1 IBC PolySol 275 CS5 Module Datasheet

Smart Systems
for Solar Power





**EEEEASILY
MORE.**

Excellent. Efficient. Expert.



The Value-Added Modules of the IBC SOLAR Line.
IBC PolySol 275 CS5
 First-class solar modules made of polycrystalline silicon



-  25 year linear power and 15 year product warranty¹
-  Positive power tolerance (-0/+5 Wp)
-  Increased mechanical stability (5400 Pa)²
-  German warrantor
-  100% tested quality
-  Maximum transparent ARC glass

IBC SOLAR – your partner for energy solutions

IBC SOLAR AG has had a successful presence in the photovoltaic market for **more than 35 years** and is one of the leading international energy companies, providing high-performance system solutions in every size and for every application with intelligent photovoltaic systems. The **economic strength and financial independence** is confirmed by globally recognised rating agencies.

Smart Systems for Solar Power thanks to perfectly matched components. **More than 1,000 highly qualified partners** around the world, as well as **more than 3,000 megawatts of installed power**, which supply **around 2 million people with solar power**, underline the high level of expertise of IBC SOLAR.

IBC SOLAR – leading PV system integrator from Germany since 1982!






Engineered in GERMANY

The ideal solution for:





8.2 Sunrow SG49k5J String Inverter Datasheet



SG49K5J

String Inverter For Japan



High Yield

- Max. efficiency 98.9 % European efficiency 98.5 %
- Full power operation without derating at 50 °C
- Up to 4 MPP trackers

Easy O&M

- Integrated IV curve scan function for fast trouble shooting
- Plug-in design of fan and SPD, easy for on-site maintenance.

Saved Investment

- Max. DC/AC ratio up to 1.5
- Capacity less than 50 kW plant only need one inverter
- Can be installed horizontally, saving installation cost!

Grid Support

- Compliance with Japan utility grid standards
- Fault ride through (FRT) 2017
- Remote active power control

Circuit Diagram



Efficiency Curve



Normalized Output Power	VCC-FRT (%)	VCC-MPPT (%)	VCC-ESS (%)
0%	92%	92%	92%
10%	96%	96%	96%
20%	97.5%	97.5%	97.5%
30%	98.2%	98.2%	98.2%
40%	98.5%	98.5%	98.5%
50%	98.7%	98.7%	98.7%
60%	98.8%	98.8%	98.8%
70%	98.9%	98.9%	98.9%
80%	98.9%	98.9%	98.9%
90%	98.9%	98.9%	98.9%
100%	98.9%	98.9%	98.9%

© 2017 Sunrow Power Supply Co., Ltd. All rights reserved.
Subject to change without notice. Version#1.0

32




Input (DC)	SG49K5J
Max. PV input voltage	1000 V
Min. PV input voltage / Startup input voltage	200 V / 250 V
Nominal input voltage	660 V
MPP voltage range	200 - 950 V
MPP voltage range for nominal power	490 - 850 V
No. of independent MPP inputs	4
Max. number of PV strings per MPPT	3
Max. PV input current	112A (28 A / 28 A / 28 A / 28 A)
Max. current for input connector	12 A
Max. DC short-circuit current	140 A (35 A / 35 A / 35 A / 35 A)
Output (AC)	
Nominal AC power (at 50 °C)	49500 W
Max. AC output at PF=1 (at 50 °C)	49500 W
Max. AC apparent power (at 50 °C)	49500 VA(default), 55000 VA(settable)
Max. AC output current	80 A
Nominal AC voltage	3 / PE, 420 V / 440 V
AC voltage range	374 - 506 V
Nominal grid frequency / Grid frequency range	50 Hz / 45 - 55 Hz, 60 Hz / 55 - 65 Hz
THD	< 3 % (at nominal power)
DC current injection	< 0.5 % In
Power factor at nominal power / Adjustable power factor	> 0.99 / 0.8 leading - 0.8 lagging
Feed-in phases / Connection phases	3 / 3
Efficiency	
Max. efficiency / Euro. efficiency	98.9 % / 98.5 %
Protection	
DC reverse connection protection	Yes
AC short-circuit protection	Yes
Leakage current protection	Yes
Grid monitoring	Yes
DC switch / AC switch	Yes / Yes
DC fuse	Yes (positive, 15A)
PV string current monitoring	Yes
Anti-PID function	Optional
Overvoltage protection	DC Type II / AC Type II
General Data	
Dimensions (W*H*D)	677*962*282.5 mm 26.7**37.9**11.1"
Weight	70 kg 154.3 lb
Isolation method	Transformerless
Degree of protection	IP65
Night power consumption	< 2 W
Operating ambient temperature range	-25 to 60 °C (> 50 °C derating) -13 to 140 °F (> 122 °F derating)
Allowable relative humidity range (non-condensing)	0 - 100 %
Cooling method	Smart forced air cooling
Max. operating altitude	4000 m (> 3000 m derating) 13123 ft (> 9843 ft derating)
Display / Communication	Graphic LCD / RS485
DC connection type	OT terminal (Max. 6 mm ²)
AC connection type	OT terminal (Max. 70 mm ²)
Grid support	FRT 2017, active & reactive power control and power ramp rate control
Type designation	SG49K5J-10



9 APPENDIX B – Automatic PR Calculation Software

The tool developed to perform the automatic calculation of PR allowed to significantly reduce the time needed to compute the PR value. Understanding this represents a valuable advantage for the company where this work was produced, the source code was considered confidential.

Nevertheless, some information, as well as the flowchart, are provided below.

Programming tool: Visual Basic 2017

Programming language: C/C++

Database: Microsoft Office Excel 2017 + VBA (Macro)

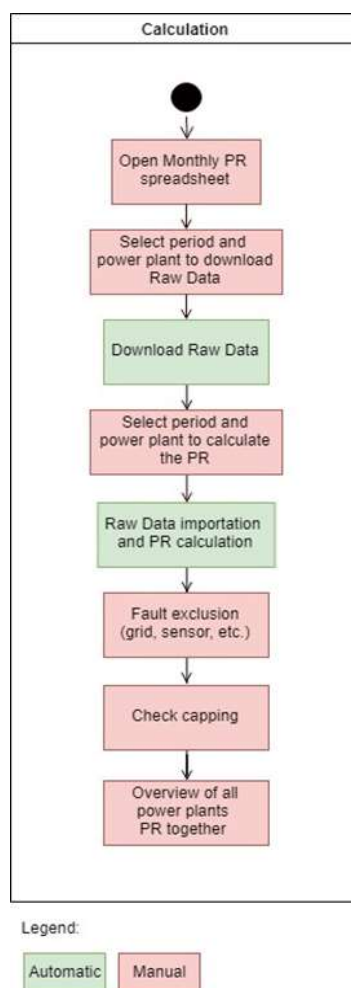


Figure 72 – Flowchart of the tool developed to perform the automatic calculation of PR.

For more information about the developed software, source-code and libraries contact the author.